

Research Paper

# The Dawes Review 13: A New Look at The Dynamic Radio Sky

Tara Murphy<sup>1,3</sup> and David L. Kaplan<sup>2,3</sup>

<sup>1</sup>Sydney Institute for Astronomy, School of Physics, The University of Sydney, New South Wales 2006, Australia

<sup>2</sup>Department of Physics, University of Wisconsin-Milwaukee, P.O. Box 413, Milwaukee, WI 53201, USA

<sup>3</sup>ARC Centre of Excellence for Gravitational Wave Discovery (OzGrav), Hawthorn, VIC 3122, Australia

arXiv:2511.10785v2 [astro-ph.SR] 24 Jan 2026

## Abstract

Astronomical objects that change rapidly give us insight into extreme environments, allowing us to identify new phenomena, test fundamental physics, and probe the Universe on all scales. Transient and variable radio sources range from the cosmological, such as gamma-ray bursts, to much more local events, such as massive flares from stars in our Galactic neighbourhood. The capability to observe the sky repeatedly, over many frequencies and timescales, has allowed us to explore and understand dynamic phenomena in a way that has not been previously possible. In the past decade, there have been great strides forward as we prepared for the revolution in time domain radio astronomy that is being enabled by the SKA Observatory telescopes, the SKAO pathfinders and precursors, and other ‘next generation’ radio telescopes. Hence it is timely to review the current status of the field, and summarise the developments that have happened to get to our current point. This review focuses on image domain (or ‘slow’) transients, on timescales of seconds to years. We discuss the physical mechanisms that cause radio variability, and the classes of radio transients that result. We then outline what an ideal image domain radio transients survey would look like, and summarise the history of the field, from targeted observations to surveys with existing radio telescopes. We discuss methods and approaches for transient discovery and classification, and identify some of the challenges in scaling up current methods for future telescopes. Finally, we present our current understanding of the dynamic radio sky, in terms of source populations and transient rates, and look at what we can expect from surveys on future radio telescopes.

**Keywords:** radio astronomy, radio transient sources, sky surveys, transient detection

(Received xx xx xxxx; revised xx xx xxxx; accepted xx xx xxxx)

## 1. Introduction

Transient radio emission is a signature of some of the most energetic and interesting events in our Universe: from stellar explosions (Weiler et al. 2002) and compact object mergers (Hallinan et al. 2017) to tidal disruption and accretion around supermassive black holes (Zauderer et al. 2011). These dynamic events happen in extreme physical conditions and hence let us test fundamental physics such as mechanisms for magnetic field generation, particle acceleration, the strong-field gravity regime (Kramer et al. 2021) and the cosmological star formation history (Tanvir et al. 2009; Chandra et al. 2010). They also act as probes of the interplanetary (Jokipii 1973), interstellar (Rickett 1990) and intergalactic media (Zhou et al. 2014), giving us insight into the structure and composition of the Universe on all scales.

Transient events have played an important role in astronomy since its early days. For example, there are numerous records of ‘guest stars’ by Chinese astronomers in the first century of the Common Era (Stephenson & Green 2002), some of which were later established to be historical supernovae. In Europe, Tycho Brahe’s detailed observations of SN 1572 were an important step forward in challenging the Aristotelian/Ptolemaic paradigm of the ‘unchanging heavens’ (Hinse et al. 2023). In the present era,

targeted monitoring and surveys of optical transients have led to major discoveries: perhaps most notably the discovery of the accelerating expansion of the Universe through observations of distant supernovae (Riess et al. 1998; Perlmutter et al. 1999), which won the 2011 Nobel Prize for Physics. Most recently, the detection of a gravitational wave transient, a binary black hole merger (Abbott et al. 2016), led to the 2017 Nobel Prize for Physics and opened up the field of multi-messenger transients (Abbott et al. 2017b).

In contrast to optical and X-ray wavebands, the dynamic radio sky had been relatively unexplored (beyond targeted observations). The notable exception to this was pulsars, the discovery (Hewish et al. 1968) and study (Hulse & Taylor 1975) of which have led to two Nobel Prizes, in 1974 and 1993 respectively. Looking beyond pulsars, the general lack of large-scale time domain studies at radio frequencies (until recent times — see Section 4.3) has been largely due to observational limitations: widefield, sensitive surveys with multiple epochs were difficult and time consuming to conduct.

We now know the radio sky is variable on all timescales, from nanoseconds (Hankins et al. 2003) through to months and years (Chandra & Frail 2012; Zauderer et al. 2013). The past decade has seen many advances in our understanding of radio transients, from the detection of radio emission from a binary neutron star merger (Hallinan et al. 2017), to the real-time detection of an extreme scattering event (Bannister et al. 2016) and the discovery of a new class of long period transients (Hurley-Walker et al. 2022b). This review is being written as we prepare for the wave

**Author for correspondence:** Tara Murphy, Email: tara.murphy@sydney.edu.au and David Kaplan, Email: kaplan@uwm.edu

**Cite this article:** Murphy T and Kaplan D.L., A New Look at The Dynamic Radio Sky *Publications of the Astronomical Society of Australia* **00**, 1–12. <https://doi.org/10.1017/pasa.xxxx.xx>

of discoveries that will come in the era of the SKA Observatory (SKAO; Dewdney et al. 2022), which is expected to begin science verification observations in 2027 and 2029 for the SKA-Low and SKA-Mid telescopes, respectively<sup>a</sup>.

### 1.1. The context for this review

There have been a number of reviews of radio transient surveys, mostly written in anticipation of the advent of the ‘next-generation’ radio telescopes that would enable large-scale time-domain imaging surveys on the path to the SKAO. The first of these is Cordes et al. (2004) who defined a phase space for the exploration of radio transients (we show an updated version of it in Figure 1), and proposed a metric for the optimisation of radio transients surveys (we discuss and expand on this in Section 4.1), as well as discussing some of the key science cases for the SKAO. When Fender & Bell (2011) reviewed the field, they considered the time domain radio sky was still relatively unexplored. They highlighted the great potential of the major surveys about to commence on MeerKAT (Jonas et al. 2016), the Australian SKA Pathfinder (ASKAP; Hotan et al. 2021), and other SKAO pathfinder and precursor telescopes, with a particular emphasis on the Low-Frequency Array (LOFAR; van Haarlem et al. 2013). However, their predictions were based primarily on the transient rates reported by Bower et al. (2007), most of which were later shown to be spurious (Frail et al. 2012, see Section 4.3.4).

The next review paper was the product of the ‘*Advancing Astrophysics with the Square Kilometre Array*’ meeting in Italy in 2014 (Braun et al. 2015). Fender et al. (2015a) discuss the advantages of radio observations for understanding transient objects and present updated limits on radio transient rates from the untargeted transient surveys available at the time; these rates and limits were crude, owing to the lack of robust large-scale samples and reliable real-time identification of transients. Although not formally a review paper, Mooley et al. (2016) presents the most comprehensive recent compilation of radio transient surveys and detection rates. The online table<sup>b</sup> has been updated to 2025, and hence serves as a very useful summary of work in this area. We draw on this in our review of the history of radio transient surveys presented in Section 4.3.

Just over twenty years on from Cordes et al. (2004) there are several major radio transient surveys well underway, with the capability to detect significant numbers of transient sources across the full range of their stated scientific goals. The SKAO will be operational within  $\sim 5 - 8$  years, and planning is underway for other future instruments including the next-generation Very Large Array (ngVLA; Murphy 2018) and Deep Synoptic Array (DSA-2000; Hallinan et al. 2019). Hence, it is timely to do a comprehensive review of this area. We hope it will be useful as a milestone in capturing the state of the field as we enter an era of transformational surveys.

The structure of the paper is as follows. In the rest of this section we outline the scope of the review and define some key terminology. In Section 2 we discuss the key emission mechanisms that cause radio variability and in Section 3 we describe each of the main classes of radio transients. In Section 4 we discuss the motivation for untargeted surveys, and present a history of radio transient surveys. In Section 5 we discuss the main detection methods and approaches for radio transients. In Section 6 we

discuss the metrics used to measure variability, and how we characterise the time variable sky. In Section 7 we discuss SKAO-era telescopes and how we can incorporate what we have learned from previous work. Finally, in Section 8 we present the future outlook for the field of radio transients.

### 1.2. The scope of this review

In this review we will focus on results from interferometers in a synthesis imaging mode (i.e. not single dish or coherent beam-forming, although we do discuss those separately), often referred to as ‘image domain’ or ‘slow’ transients<sup>c</sup> or similar (also see Section 1.3). Early observations of slow transients using single-dish telescopes (e.g. Spangler et al. 1974a), made detections that were difficult to verify and distinguish from interference (Davis et al. 1978). Most recent studies use interferometric imaging at frequencies  $< 30$  GHz, although very large single-dish telescopes can offer advantages (e.g. Route & Wolszczan 2013; Route 2019). At higher frequencies bolometric imaging arrays are the best option for millimetre surveys (Whitehorn et al. 2016; Naess et al. 2021).

For both scientific and technical reasons, this review focuses on astronomical phenomena that show variability at radio wavelengths on timescales of seconds to years. We will discuss the physical processes that cause this variability and summarise the main classes of objects that are detected as variable radio sources. We will also cover radio transients surveys, detection methods and population rates.

To define a clear scope for the paper, we will *not* discuss the following topics:

- **Solar, heliospheric, and ionospheric science:** The Sun is the brightest radio source in the sky, and was first detected in the early days of radio astronomy (Hey 1946). The proximity of the Sun to Earth means we are able to study its radio variability in great detail. Solar radio astronomy typically uses different observational approaches and techniques from the radio transients community. In fact, almost all continuum imaging observations (whether targeted, or untargeted surveys) deliberately avoid the Sun due to the impact on data quality. The main exceptions to this are recent programs that use interplanetary scintillation (IPS) caused by the solar wind (discovered by Clarke 1964, and reported by Hewish et al. 1964), for example Morgan et al. (2018), to both study the solar wind and to select the most compact extragalactic sources (e.g. Chhetri et al. 2018). Likewise, ionospheric variability is both interesting in its own right (e.g. Loi et al. 2015a) and due to its impact on studying radio variability at low frequencies (e.g. Loi et al. 2015b). However, for both scientific and methodological reasons we will not include solar, heliospheric and ionospheric radio astronomy in this review. For a review of this research area in the context of the SKAO, see Nindos et al. (2019).
- **Solar System objects:** the planets in our own Solar System are detectable at radio wavelengths. The five magnetised planets (Earth, Jupiter, Saturn, Uranus and Neptune) all show auroral radio emission (Zarka 1998) and emission from their radiation belts (Mauk & Fox 2010). The non-magnetised planets show radio emission from thermal heating of the planet by incident solar radiation (Kellermann 1966). Many radio studies of solar system planets have been done with both ground-based

<sup>a</sup><https://www.skao.int/en/science-users/timeline-science>

<sup>b</sup><http://www.tauceti.caltech.edu/kunal/radio-transient-surveys>

<sup>c</sup>The term ‘slow transients’ is widely, but not universally, used in the research community. It is defined in Section 1.3.

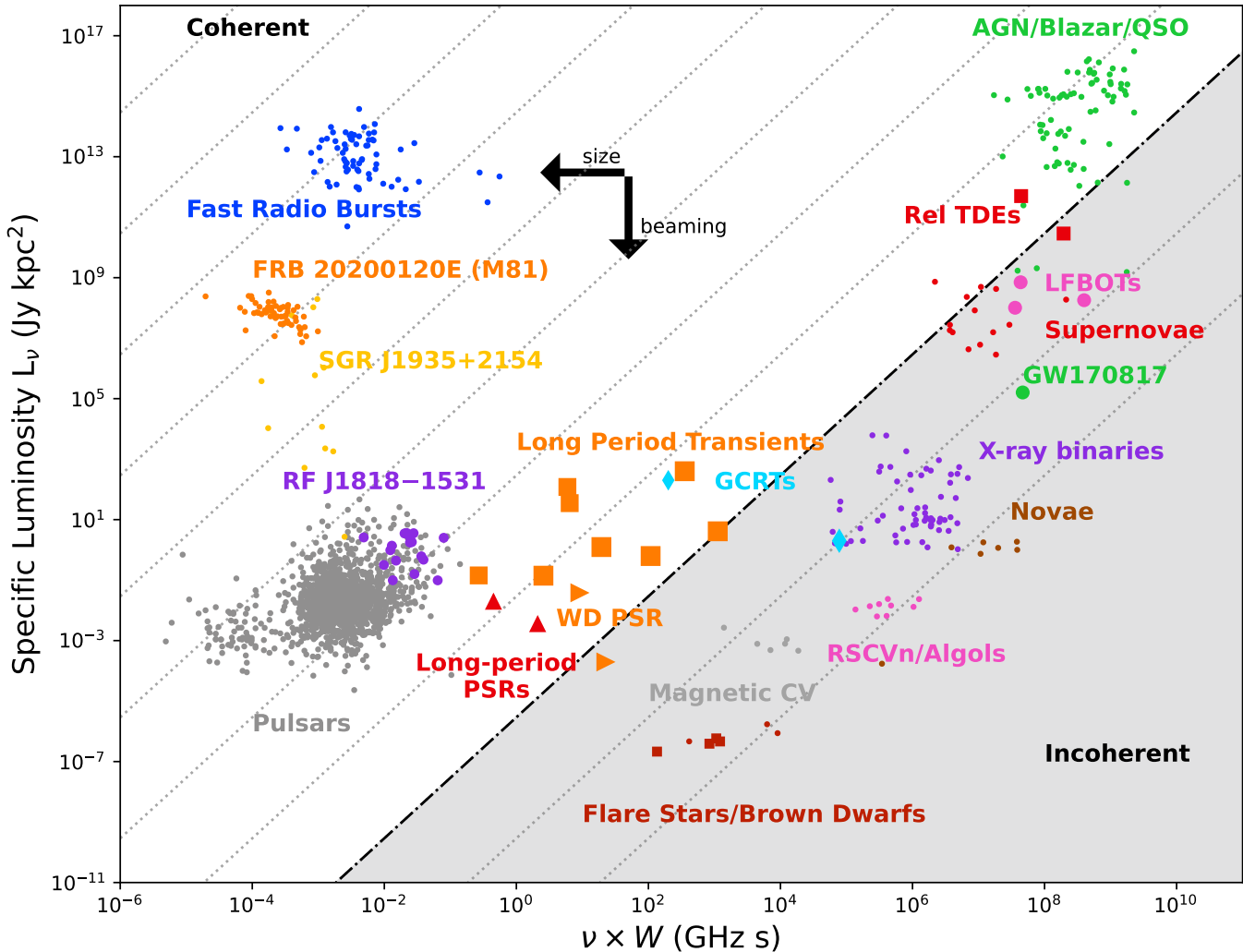


**Figure 1.** Transient phase space showing radio luminosity versus the product of timescale and observing frequency for different transient source classes, following Cordes et al. (2004). Note that the luminosity assumes sources are beamed into only 1 sr and no relativistic beaming, which may or may not be appropriate for individual objects, while the timescales are just the observed variability timescales and ignore more constraining limits such as the finite sizes of e.g. stellar sources. For sources with relativistic beaming the true brightness temperature could be significantly higher (e.g. Readhead 1994), while for some stellar sources the true brightness temperature could be significantly higher, as suggested by the arrows. The diagonal lines show contours of brightness temperature, with coherent emitters having  $T_B > 10^{12}$  K. Adapted from Pietka et al. (2015) and Nimmo et al. (2022), with select sources added: the binary neutron star merger GW170817 (Mooley et al. 2018c); LFBOTs (Ho et al. 2019; Coppejans et al. 2020; Ho et al. 2020); relativistic TDEs (Mimica et al. 2015; Andreoni et al. 2022); flare stars/brown dwarfs (Hallinan et al. 2007; Rose et al. 2023; Route & Wolszczan 2016; Zic et al. 2019); long-period radio pulsars (Caleb et al. 2022; Wang et al. 2025d); Galactic Centre radio transients (Hyman et al. 2005; Wang et al. 2021b); white dwarf pulsars (Pelinoli et al. 2023; de Ruiter et al. 2025) and long-period transients (Wang et al. 2025c; Lee et al. 2025; Wang et al. 2021b; Caleb et al. 2024; Hurley-Walker et al. 2024, 2023, 2022b; Dong et al. 2025b). In particular we highlight the range of sources from Table 2 that are filling out the centre of this space, straddling the coherent/incoherent divide: long-period radio pulsars are upward-pointing triangles, GCRTs are diamonds, pulsing white dwarf binaries are right-pointing triangles, and long period transients (LPTs) are squares.

telescopes and spacecraft (e.g. the Voyager 1 and 2 missions; Warwick et al. 1979). Because of their rapid movement across the sky, it is common to detect Solar System planets (in particular Jupiter) in widefield radio imaging surveys (e.g. Table 2; Lenc et al. 2018). Lessons learned from our solar system apply directly to exoplanetary systems (e.g., Kao et al. 2023 reported the first detection of radiation belts around an ultracool dwarf star). However, planets (and the Moon) are typically excluded in the process of searching for Galactic and extragalactic transients and we will not cover them in this review.

• **Asteroids and meteors:** When an asteroid (or material from an asteroid) enters the Earth's atmosphere it vaporises, and can be seen as a streak of light across the sky. These large meteors are often called ‘fireballs’, and there are regular monitoring

programs to detect them, such as the NASA All-sky Fireball Network<sup>d</sup>, due to their potential impact on orbiting spacecraft (e.g. Cooke & Moser 2012). Very low frequency (10–88 MHz) observations with the Long Wavelength Array (Taylor et al. 2012) established a correlation between low frequency transients and fireball trails, suggesting that the trails radiate at low radio frequencies (Obenberger et al. 2014; Varghese et al. 2024). In addition, meteor trails are known to reflect low frequency radio transmissions (e.g. Helmboldt et al. 2014). This makes asteroids a foreground source of radio transient bursts that need to be considered at low frequencies. However, since our focus is

<sup>d</sup><https://fireballs.ndc.nasa.gov>

on Galactic and extragalactic transients we will not discuss them further in this review.

- **Searches for extraterrestrial intelligence:** SETI has been an active area of research in radio astronomy since the early 1960s. Searching for extraterrestrial communications or other technosignatures requires many of the same approaches as searching for astronomical transients, and the history of SETI is interwoven with the history of radio transients. In some cases SETI projects have piggybacked on astronomy observations, or searched existing archival data. In other cases they have involved dedicated programs. Substantial funding for radio telescopes and instrumentation has also come from SETI-motivated philanthropy, for example the Allen Telescope Array (ATA; Welch et al. 2009) and Breakthrough Listen (Worden et al. 2017). However, since the focus of this review is variable astronomical phenomena, we will not discuss SETI further. For reviews of SETI research, see Tarter (2001) and Ekers et al. (2002). For a more recent discussion of approaches to detecting technosignatures, see Wright et al. (2022).
- **Radio frequency interference:** RFI is an ever-present challenge for radio transient detection. Avoiding RFI was perhaps the most important factor in determining the scientific quality of sites for the SKAO telescopes (Schilizzi et al. 2024). Often appearing as extreme bursts of emission localised in frequency or time, RFI can mimic the astronomical signals we are trying to detect. This has resulted in false detections, such as the so-called ‘perytons,’ which were later identified as RFI from microwaves ovens (Petroff et al. 2015). At longer timescales, RFI generally has less impact on transient detection as it is averaged out in the process of synthesis imaging. However, it can still have a significant impact on image quality. Reflection of low frequency radio signals off satellites in low Earth orbits can create transient objects in images, and is an increasing problem (Prabu et al. 2020). A very recent discovery is that of nanosecond electrostatic discharges from satellites (James et al. 2025). In this review we will only touch on RFI in the context of its impact on transient detection approaches, in Section 5. For an overview of RFI mitigation methods see Fridman & Baan (2001) and Offringa et al. (2010). Lourenço et al. (2024) and Sihlangu et al. (2022) provide recent analyses of the RFI environment on the ASKAP and MeerKAT sites, respectively.
- **Fast radio bursts:** FRBs are astronomical radio flashes with durations of milliseconds (Lorimer et al. 2007). Their physical origin is as-yet unknown, although there are likely to be multiple classes of objects that cause FRBs (Pleunis et al. 2021). While they are extremely interesting, and may be related to other types of radio transients (e.g., Bochenek et al. 2020b; Law et al. 2022), fast radio bursts themselves are beyond the scope of this review. This is partly for technical reasons (FRBs are most often discovered with different instrumentation and survey methods than the slower transients below, for instance using single dish telescopes or interferometric voltage beams) and partly for practical reasons (the huge amount of new science on FRBs and rapid developments necessitate their own reviews). For these reasons we point the reader to recent reviews such as Cordes & Chatterjee (2019), Petroff et al. (2022), or Zhang (2023).

A final note: in the sections discussing survey strategy and the history of radio transients surveys, our focus will be on wide-field imaging surveys. Hence we will not discuss, for example, large targeted monitoring programs such as those for interstellar scintillation (Lovell et al. 2003), follow-up of sources detected

in other wavebands, for example gamma-ray bursts (GRBs; Frail et al. 2003) and large triggered follow-up programs (e.g. Staley et al. 2013). When discussing what we know about different variable source classes, we will of course incorporate all sources of information.

### 1.3. Some notes on terminology

As the field of radio transients has evolved over the past few decades, there have been several important terms that are either (a) specific to this research area; (b) have been used in different ways in the community; or (c) have seen their usage evolve over this period. To avoid confusion we discuss and define them here.

- **‘Fast’ and ‘slow’ transients:** these terms are generally used to mean variability on timescales faster than and slower than the telescope correlator integration time. Fast transient searches need to use data at a pre-correlator stage, and for most radio telescopes this is of the order of seconds. For example, the ASKAP integration time is 10 seconds (Hotan et al. 2021) and MeerKAT is 2–8 seconds (Jonas et al. 2016). For the VLA the default integration times for each configuration are between 2–5 seconds<sup>e</sup>. Due to the completely different data processing and analysis approaches (for example dedispersion is usually required in fast transient searches) it makes sense to consider these two domains separately. As a result, most of the major survey projects on SKAO pathfinder and precursor telescopes have split along these lines. For example, on ASKAP, the Commensal Real-time ASKAP Fast Transients Survey (CRAFT; Macquart et al. 2010) focuses on fast transients (also see Wang et al. 2025b) and the Variables and Slow Transients (VAST; Murphy et al. 2013) survey focuses on slow transients. Likewise on MeerKAT, the Transients and Pulsars with MeerKAT (TRAPUM; Stappers & Kramer 2016) project focused on fast transients and the ThunderKAT project (Fender et al. 2016) focused on slow transients. Conveniently, the behaviour of most astrophysical phenomena also fall into one of these two regimes (see Figure 1), although some such as pulsars can show variability on both millisecond timescales and much slower timescales of minutes to hours, and new discoveries (e.g. Section 3.9) are further blurring the lines. This review will focus on slow transients.
- **Transients and variables:** as the era of large-scale imaging surveys started, there was considerable debate about how the terms ‘transient’ versus ‘variable’ should be used. When considering the underlying astronomical objects themselves, it is possible to make a distinction between persistent objects that show variable behaviour (e.g. flaring stars) and explosive events that appear, then fade and ultimately disappear (e.g. gamma-ray bursts). However, observationally this distinction is less clear, since the time morphology of a particular dynamic event is highly dependent on the sensitivity limit and time sampling of the observations. For example, radio bursts from a star that has quiescent emission below the sensitivity limit of the image will appear as transient events. Hence in this review, as in much of the literature, we use the terms transient and highly variable, relatively interchangeably (see, for example, comments in Section 5 of Mooley et al. 2016).
- **Commensal and piggyback observations:** The term ‘piggyback’ refers to the situation in which observations that are

<sup>e</sup><https://science.nrao.edu/facilities/vla/docs/manuals/oss/performance/tim-re>

taken for a particular scientific purpose can be used for a different purpose, without affecting the original observing schedule and specifications. In radio astronomy, this strategy has been extensively used by SETI; for example the SERENDIP project in which data collected by all science projects on Arecibo was analysed independently for narrowband radio signals (Werthimer et al. 2001). The word ‘commensal’ has its origins in biology. The Oxford Concise Medical Dictionary defines it as: ‘*an organism that lives in close association with another of a different species without either harming or benefiting it*’. It was introduced into the radio astronomy literature in the context of the plans for the Allen Telescope Array, to imply a more active form of piggybacking in which both parties had some influence over the observational strategy (DeBoer 2006). The usage of commensal became more widespread in the literature after 2010, in the context of a number of new radio surveys being designed (e.g. Macquart et al. 2010; Wayth et al. 2011). In the current literature commensal and piggyback observations are often used interchangeably. Note that readers outside this area of research can be confused by this technical meaning.

- **‘Blind’ and untargeted surveys:** The terms blind and untargeted are used interchangeably in the literature, to refer to a survey that has been designed without targeting specific objects, and with as few prior assumptions as possible. We prefer the term *untargeted survey* as it is more accurate and more inclusive.

## 2. Radio emission mechanisms and causes of variability

Astronomical objects that emit radio waves (from nearby planets and stars, to distant galaxies and active galactic nuclei; e.g. Kellermann & Verschuur 1988) have a wide variety of emission types. In this section we focus on those types that produce transient and variable radio emission, either intrinsically, or as a result of propagation through an inhomogeneous ionised medium or other external causes. In general the emission will come from plasma where the particles (primarily electrons) are in local thermodynamic equilibrium (Condon & Ransom 2016), leading to *thermal* emission, or are not in equilibrium, leading to *non-thermal* emission (note, though, that some authors restrict thermal emission to only blackbody or thermal bremsstrahlung radiation). In most cases the sources of radio emission considered here arise from non-thermal plasmas.

For all of these objects we can consider the *brightness temperature* of the emission (Rybicki & Lightman 1985; Condon & Ransom 2016), which is the temperature of a hypothetical optically-thick thermal plasma that would emit at the same intensity. Note that this definition can be used even when the assumptions (like thermal emission) are not valid, as it is still a useful quantity for comparison. The brightness temperature is defined as:

$$T_B(\nu) \equiv \frac{I_\nu c^2}{2k_B \nu^2} \quad (1)$$

where  $I_\nu$  is the specific intensity (measured in  $\text{erg s}^{-1} \text{cm}^{-2} \text{Hz}^{-1} \text{sr}^{-1}$  or equivalent), the frequency is  $\nu$ ,  $k_B$  is Boltzmann’s constant, and  $c$  is the speed of light. For a source with flux density  $S_\nu$  and solid angle  $\Omega$ , we have  $I_\nu = S_\nu / \Omega$ . Note that this form assumes radiation is in the Rayleigh-Jeans limit, with  $h\nu \ll k_B T$ , even if that is not actually true. For non-thermal sources the brightness temperature,  $T_B$ , is different from the actual electron temperature  $T_e$ , and typically  $T_B \gg T_e$ .

We should also distinguish between *incoherent* and *coherent* emission (Melrose 2017). Most radiation sources are incoherent, such that each electron radiates independently and the total emission is found by summing over a distribution of electrons. For an incoherent source,  $T_B$  is limited by two mechanisms:  $k_B T_B$  should be less than the energy of the emitting electrons, and  $T_B$  should be  $< 10^{12} \text{ K}$  because above this point radiation by inverse Compton scattering will increase significantly, leading to rapid energy loss and cooling back down to  $10^{12} \text{ K}$  (Kellermann & Pauliny-Toth 1969). Note that the upper limit on  $T_b$  could be even lower if set by equipartition between magnetic and particle energies (Readhead 1994). In general it can be difficult to directly measure or constrain  $T_B$ . However, sources that vary on a timescale  $\tau$ , have their angular size limited to  $\theta < c\tau/d$  at a distance  $d$ , which limits the solid angle to  $\Omega < (c\tau/d)^2$ . This then implies for the brightness temperature (e.g. Readhead 1994; Cordes et al. 2004; Miller-Jones et al. 2008; Bell et al. 2019):

$$T_B \gtrsim \frac{S_\nu d^2}{2k_B \nu^2 \tau^2} \quad (2)$$

with flux density  $S_\nu$ , ignoring relativistic beaming or cosmological effects. While the latter can be easily estimated for a source with a known redshift, relativistic beaming is an important contributor to sources having apparent brightness temperatures much higher than their intrinsic values (Readhead 1994): depending on the speed of the relativistic motion and the geometry, the luminosity can be boosted by the Doppler factor to some power (depending on the intrinsic spectrum) which can be 10 or more, with the inferred brightness temperature from variability boosted by the Doppler factor cubed since the timescale is also modified (Readhead 1994; Lähteenmäki & Valtaoja 1999), so the overall boost can exceed a factor of 1000.

When beaming is not a factor, or when corrections have been done, the intrinsic (excluding variability caused by propagation, discussed in Section 2.5.1) brightness temperature can then be estimated. For brighter sources (large  $S_\nu$ ) and faster variability (small  $\tau$ ), sources can have  $T_B > 10^{12} \text{ K}$ , sometimes by many orders of magnitude, requiring an alternate mechanism for the emission (Cordes et al. 2004). These coherent mechanisms, where the contributions of individual particles can add up in-phase, relate to plasma instabilities or ‘collective plasma radiation processes’ (Melrose 1991, 2017), where the emission from  $N$  particles is  $\propto N^2$  rather than  $\propto N$  for incoherent emission. A full description of these mechanisms is beyond the scope of this review, and we point the reader to helpful reviews such as Melrose (2017). In this review we will discuss each briefly and associate the mechanisms with the sources where they operate.

### 2.1. Synchrotron emission

The majority of the extragalactic radio sources that are bright enough for us to observe, are either active galactic nuclei (AGN, both ‘radio-loud’ and ‘radio-quiet’; Kellermann et al. 1989) or star-forming galaxies, with the former dominating at higher flux densities (Condon et al. 2002; Matthews et al. 2021). For AGN the emission is primarily via *synchrotron radiation* (Rybicki & Lightman 1985), a (typically) non-thermal, incoherent process, from a combination of their cores/nuclei and jets (Fanaroff & Riley 1974) produced by accretion onto central supermassive black holes (Blandford et al. 2019). For star-forming galaxies the emission is a combination of synchrotron emission from supernova remnants (SNRs) and diffuse gas as well as thermal emission

from H II regions (Helou et al. 1985; Chevalier 1982). Since sources like SNRs and H II regions are usually too extended to show variability we will not consider them further, although in some cases young SNRs can show secular evolution (e.g. Sukumar & Allen 1989), and their study can connect back to supernovae (Milisavljević & Fesen 2017).

Synchrotron emission is the result of relativistic electrons spiralling around magnetic field lines (Rybicki & Lightman 1985; Condon & Ransom 2016). The emission from a single electron depends on its energy, the magnetic field strength, and the angle between the electron's motion and the magnetic field, with a spectrum peaking near the critical frequency which is the gyrofrequency (depending on the magnetic field strength) modified by the electron's Lorentz factor. But for a power-law distribution of electron energies, the summed emission results in a power-law with spectral index  $\alpha$ , defined as:

$$S_v \propto v^\alpha \quad (3)$$

depending on the underlying distribution of the electrons (note that some authors define the spectral index with the opposite sign,  $S_v \propto v^{-\alpha}$ , and care must be taken to correctly interpret values).

Most synchrotron sources have a steep spectrum ( $\alpha < 0$ ) with  $\alpha \approx -0.7$  (Sabater et al. 2019; Franzen et al. 2021, and indeed most non-thermal sources have negative spectral indices in general). At lower frequencies, the brightness temperature approaches the effective temperature of the relativistic electrons and this emission is modified by synchrotron self-absorption, which causes the steep spectrum to turn over into one with  $\alpha \approx 2.5$ .

Synchrotron radiation is ubiquitous in radio astronomy, and most sources are steady emitters. However, there are two physical scenarios that can lead to transient or variable emission: changes in accretion rate and jet launching in accreting compact objects on different mass scales; and explosions interacting with the surrounding medium.

### 2.1.1. Accretion and jet ejection

The process of disk accretion and jet ejection is ubiquitous across astrophysics (e.g. de Gouveia Dal Pino 2005), and where compact objects are involved those jets are typically relativistic (e.g. Bromberg et al. 2011b) with similar characteristics that depend primarily on the accretor mass, accretion rate, and ejection velocity. In the context of radio transients, we focus on relativistic jets from AGN and X-ray binaries (XRBs), which we discuss below.

AGN dominate the radio sky at flux densities above a few millijanskys (at centimetre wavelengths), and most show little variability (Hovatta et al. 2007; Hodge et al. 2013; Stewart et al. 2016; Mooley et al. 2016; Bell et al. 2019; Murphy et al. 2021), although fluctuations of a few to few tens of percent are not uncommon (e.g. Falcke et al. 2001; Mundell et al. 2009) and variations are both more significant and faster at higher radio frequencies (e.g. Ackermann et al. 2011; Hovatta et al. 2007), especially for sub-classes of AGN such as blazars (Max-Moerbeck et al. 2012; Richards et al. 2011a; Max-Moerbeck et al. 2014).

Aside from extrinsic causes (see Section 2.5.1) most of these changes are thought to be due to modest changes in the jets (e.g. Nyland et al. 2020), such as the propagation of shocks along the jets (Marscher & Gear 1985; Hughes et al. 1989), disk instabilities (Czerny et al. 2009; Janiuk & Czerny 2011), or changes in accretion power (Koay et al. 2016; Wołowska et al. 2017). These effects can be magnified by the jet orientation, with jets directed close to the line of sight having larger variability on shorter timescales due to relativistic effects (Lister 2001): changes in orientation

can therefore dominate any intrinsic changes in their effects on variability.

However, a subset of these sources show higher variability (e.g. Barvainis et al. 2005). This may be due to large-scale changes in the jet orientation from accretion instabilities or interaction within a binary super massive black hole (Palenzuela et al. 2010; An et al. 2013), or large-scale changes in the jet power from changes in the accretion flow (Mooley et al. 2016; Nyland et al. 2020). These sources apparently transition from radio-quiet (often undetectable) to radio-loud (although the distinction may not be so simple, e.g. Kellermann et al. 2016), with the radio luminosity apparently increasing by more than an order of magnitude over several decades, potentially as a result of newly-launched jets.

Such changes in the jet behaviour can be replicated on much smaller scales (both physical and mass) through accreting X-ray binaries hosting neutron stars or black holes (Fender et al. 2004a, 2006; Fender 2016). Here, small-scale changes in the jet power during the hard state correspond to normal AGN variability, while significant launching of superluminal jet components in the transition between hard and soft states correspond to the radio-quiet to radio-loud transitions of AGN.

### 2.1.2. Explosions and shocks

In contrast to the scenarios above, where accretion leads to jets that can vary as the accretion rate or direction varies, the radio emission from transient events such as classical novae (Chomiuk et al. 2021a,b), supernovae (Weiler et al. 2002), long and short gamma-ray bursts (Piran 2004; Berger 2014), magnetars (Frail et al. 1999a), neutron star mergers (Hallinan et al. 2017), tidal disruption events (Levan et al. 2011; Bloom et al. 2011) and similar phenomena lead more naturally to variable radio emission. These sorts of explosions/ejections have been among the most anticipated targets for large-area radio surveys (e.g. Metzger et al. 2015b). Note that even though some of these sources, like gamma-ray bursts, may be powered by very short-lived relativistic jets, we discuss them separately from Section 2.1.1 as the jets themselves are not seen at radio wavelengths, but only their impact on the surrounding medium.

The basic scenario here is where an explosion leads to a rapid ejection of material. This outflow can be Newtonian or relativistic, and it can be collimated or spherical. Eventually the ejecta will impact the surrounding medium (typically circumstellar or interstellar material) leading to shock waves that amplify any magnetic fields present and accelerate electrons to relativistic energies, leading to synchrotron emission (Chevalier 1982). This so-called ‘afterglow’ model is present in many variants in many different physical scenarios, where the mass, velocity, and angular profile of the ejecta and the radial profile of the surrounding medium can all change (Sari et al. 1998; Chevalier & Li 2000; Chandra & Frail 2012; Mooley et al. 2018a,c; Troja et al. 2018; Lazzati et al. 2018).

Normally, for very energetic events like gamma-ray bursts the ejecta are observed to be ultrarelativistic and jetted (Rhoads 1997; Mészáros & Rees 1997), such that the initial afterglow emission is beamed into a solid angle of  $\sim 1/\Gamma^2$  (where  $\Gamma$  is the bulk Lorentz factor) centred on the jet axis, which is also where the  $\gamma$ -rays themselves are visible. At later times the Lorentz factor will decrease so the solid angle will increase, leading to increasing visibility of the late-time afterglow emission. Eventually, when  $1/\Gamma$  approaches the intrinsic jet size the entire jet will be visible. This tends to happen at the same time as the jet material will begin to expand sideways (Sari et al. 1999). Together these lead to an

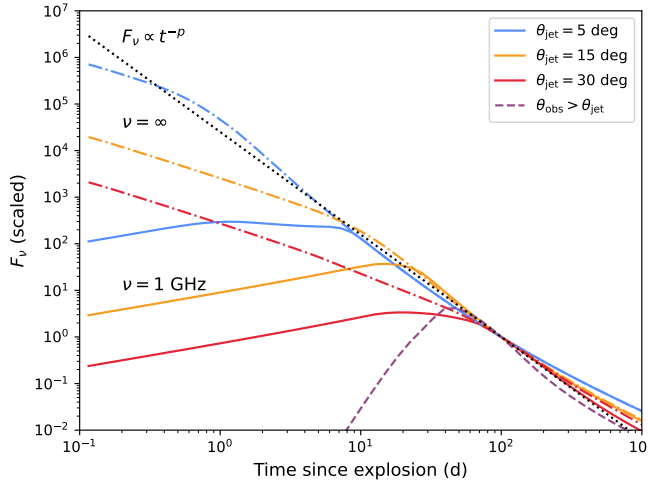


**Figure 2.** Model GRB lightcurves, computed using Ryan et al. (2020) and inspired by Piran (2004). These models use the simplest possible model for a relativistic jet. The top dash-dotted curves are for infinite frequency (ignoring any effects of self-absorption), while the lower solid curves are for a frequency of 1 GHz. All curves are normalised at 10 d. For both frequencies, we show jet opening angles of  $\theta_{\text{jet}} = 5$  deg (blue), 15 deg (orange), and 30 deg (green) with an on-axis observer ( $\theta_{\text{obs}} = 0$ ). The infinite frequency models show jet breaks when the jet has decelerated to a bulk Lorentz factor of  $1/\theta_{\text{jet}}$ , after which they have a similar power-law behaviour with  $F_v \propto v^{-p}$  (black dotted line), where  $p$  is the power-law index of the electron distribution. We also show a jet seen by an off-axis observer, potentially an ‘orphan afterglow’, since the observer would miss any high-energy emission (red dashed curve). This has similar late-time behaviour but is much fainter at early times.

achromatic ‘jet break’ in the lightcurve (Sari et al. 1999; Rhoads 1999). Measurement of jet breaks can then be used to infer the jet size and hence intrinsic energetics of collimated explosions (Frail et al. 2001).

This also gives rise to the concept of an ‘orphan afterglow’, where only the late-time radio emission is visible from our line of sight (Rhoads 2003; Ghirlanda et al. 2014). Such an event would have a steeper and shorter rise than an on-axis GRB, but merge onto the same power-law in the decline (see Figure 2).

The general behaviour for all of these afterglows is a series of power-law increases and declines (Sari et al. 1998), where the increase reflects the expanding shock front as well as the changing level of self-absorption. This increase happens first at higher frequencies because the self-absorption is less significant there. Eventually the entire afterglow becomes optically thin, at which point it transitions into a decline phase as the ejecta expand and slow down. During this phase a standard non-thermal steep spectrum is present (Weiler et al. 2002). This is illustrated in Figure 2, which shows lightcurves with and without the effect of self-absorption. If absorption is not an issue, the peak on-axis flux density is expected to occur when the shock has swept up a mass comparable to its own material and starts to decelerate, and it will scale with the energy of the explosion (Nakar & Piran 2011; Metzger et al. 2015b). The time until the peak will scale with the energy of the explosion to the  $\frac{1}{3}$  power (neglecting cosmological effects).

We can also see in Figure 2 the lightcurve from a potential orphan afterglow. One clear difficulty with all of these lightcurves is that they have the same late-time behaviour, so without a lucky early detection or robust limits on prompt high-energy emission (complicated when the explosion time is also weakly constrained), many different phenomena can be fit with the same data.

## 2.2. Free-free emission

A small fraction of variable sources emit primarily via free-free (or bremsstrahlung) emission (Condon & Ransom 2016; Osterbrock & Ferland 2006), typically in a thermal plasma. This is produced by electrons accelerated electrostatically around ions. At higher frequencies the emission typically has  $\alpha \approx -0.1$  (Condon & Ransom 2016; Chomiuk et al. 2021b), which then turns over into an opaque source with  $\alpha \approx 2$  once it becomes self-absorbed at lower frequencies.

The primary sources of variable free-free emission are classical novae (CNe; Chomiuk et al. 2021b,a), where a thermonuclear explosion on an accreting white dwarf has expelled material into the interstellar medium. These are frequently detected through optical and infrared time-domain surveys<sup>f</sup> although their emission spans the electromagnetic spectrum. At radio wavelengths, the traditional emission from CNe is free-free emission from a slowly expanding sphere of ionised ejecta (Hjellming et al. 1979; Seaquist & Palimaka 1977), which evolves over timescales of weeks–years as the emission first increases due to decreasing self-absorption and then declines due to decreasing density (since emission is proportional to the square of the electron density). While more complex sources are now observed to have non-thermal synchrotron emission from interactions between the ejecta and the surrounding medium (Krauss et al. 2011; Weston et al. 2016a,b; Finzell et al. 2018, and see Section 2.1.2), even the thermal emission itself can be more complex both spatially and temporally (Nelson et al. 2014; Chomiuk et al. 2014, 2021b).

## 2.3. Stellar emission: gyrosynchrotron, plasma, and electron cyclotron maser emission

In a number of stellar systems, especially for cooler, later-type stars we can detect **gyrosynchrotron emission**, which is an incoherent, (usually) non-thermal process related to synchrotron emission (Dulk 1985; Güdel 2002). Here, however, the electrons are only mildly relativistic. This leads to broad-band emission that has significant (but not 100%) circular polarisation at higher frequencies, where it is optically thin. At lower frequencies we see a typical optically-thick spectral index of  $\alpha = +2.5$  and a steep spectrum on the higher frequency side, with the power-law index depending on the underlying distribution of electron energies.

In contrast, **plasma emission** is a *coherent* process (Melrose 2017) observed in stellar flares (Güdel 2002; Bastian 1990), converting plasma turbulence into radiation via non-linear plasma processes. It can account for brightness temperatures up to  $10^{18}$  K, with emission at the fundamental or harmonic of the plasma frequency (determined by the local electron density), typically at lower radio frequencies ( $\lesssim 1$  GHz): at higher frequencies the emission suffers from free-free absorption.

Finally, **electron cyclotron maser emission** (ECME) is also a coherent process observed in stellar flares (Dulk 1985; Güdel 2002). Instead of the plasma frequency, the emission is at the fundamental or (low) harmonic of the cyclotron frequency (determined by the local magnetic field). ECME dominates over plasma emission in diffuse highly-magnetised plasma such that the plasma frequency is much less than the cyclotron frequency (Treumann 2006), so measurement of frequency structure or cutoffs can be used to constrain the magnetic field strength. It can result in brightness temperatures up to  $10^{20}$  K and circular polarisation of up to

<sup>f</sup><https://asd.gsfc.nasa.gov/Koji.Mukai/novae.html>

100%. The emission can also be elliptically polarised, with a combination of linear and circular polarisation. This is typically only seen in pulsars (Melrose 2017) and planets (Zarka 1998), although it has been seen in a small number of late-type stars (Spangler et al. 1974b; Lynch et al. 2017; Villadsen & Hallinan 2019).

#### 2.4. Pulsar-related variability

Pulsar radio emission as seen from Earth is inherently variable, with regular modulation on the timescale of the rotational period (although see Basu et al. 2011). Despite decades of study the pulsar emission mechanism still eludes detailed understanding (Melrose 2017; Lorimer & Kramer 2012; Philippov & Kramer 2022), but it can achieve extremely high brightness temperatures of above  $10^{20}$  K. Typically the emission has a steep spectral index ( $\alpha \approx -1.5$ ; Bates et al. 2013; Jankowski et al. 2018; Anumarlapudi et al. 2023; Karastergiou et al. 2024), although some highly-magnetised pulsars known as magnetars can have much flatter spectra (Camilo et al. 2006). It can be highly polarised — both linear and circular — with rotations of the linear position angle and sign changes of the circular polarisation occurring during the pulse.

However, these properties do not explain why pulsars (especially millisecond pulsars) can be identified in traditional image domain transient and variable searches. The rotational modulation, on timescales of 1 ms to 10's of seconds, is typically far too fast to appear as a variable source for an imaging survey (although this is now changing with short timescale imaging — see Sections 3.9 and 5.4). In addition to extrinsic modulations that can be very significant for pulsars (Section 2.5.1), there are a number of intrinsic mechanisms that can lead to variability on longer timescales. These range from ‘nulling’ (Backer 1970), where the pulsar turns off for tens to hundreds of pulses, to intermittency (Kramer et al. 2006), where the pulsar turns off for days to months, to eclipses where the pulses or even the continuum emission disappear for part of a binary orbit (timescales of minutes to hours; Fruchter et al. 1988; Broderick et al. 2016; Polzin et al. 2020). It is also possible that rather than distinct variable sub-classes, there may be a continuum of variability across the population (Lower et al. 2025; Keith et al. 2024) with ties between the rotational, pulse profile, and flux density variations that can be seen broadly with sufficient precision. Like the underlying emission mechanism, the theoretical basis for these changes is also not well understood.

Finally, for magnetars (Kaspi & Beloborodov 2017), presumed reconfiguration of their magnetic fields during bursts or giant flares can lead to the sudden appearance of pulsed radio emission (Camilo et al. 2006), in addition to the ejection of relativistic plasma leading to synchrotron afterglows discussed in Section 2.1.2. This pulsed emission can have different spectral properties to typical pulsars, and fades on timescales of months.

#### 2.5. Extrinsic variability

##### 2.5.1. Diffractive and refractive scintillation

When the radio waves from a source propagate through an inhomogeneous ionised medium, the waves can bend and diffract to form spatial variations in the wavefront. If the observer is moving relative to the wavefront, this can result in temporal variability known as *scintillation* (Rickett 1990; Narayan 1992). Such scintillation has been observed coming from the heliosphere and interplanetary medium (IPS; Hewish et al. 1964) as well as the

interstellar medium (interstellar scintillation or ISS; Scheuer 1968; Rickett 1969). Interstellar scintillation is only detectable for the most compact radio sources, such as compact cores of AGN (Lovell et al. 2003), distance relativistic explosions (Goodman 1997; Frail et al. 1997), or pulsars and fast radio bursts. Moreover, scintillation can have a range of properties depending on the source size and observing frequency.

Relevant for scintillation is the Fresnel scale,  $r_F \equiv \sqrt{\frac{\lambda d}{2\pi}}$ , for a source at distance  $d$  observed at wavelength  $\lambda$ . Also relevant is the diffraction scale  $r_d$  over which the phase variance is 1 rad. The ratio of these then defines the scintillation strength,  $r_F/r_d$ . At higher frequencies and for closer sources the scintillation is typically in the ‘weak’ regime ( $r_F/r_d \ll 1$ ), with small ( $\ll 1$ ) rms phase perturbations on the Fresnel scale (Rickett 1990; Cordes & Lazio 1991; Narayan 1992; Hancock et al. 2019), leading to fractional variability  $\ll 1$ .

More interesting is the ‘strong’ regime ( $r_F/r_d \gg 1$ ), where the phase fluctuations over the Fresnel scale are large. In this regime we can observe both diffractive (Scheuer 1968) and refractive (Sieber 1982; Rickett et al. 1984) effects.

Diffractive scintillation results from multipath propagation (Goodman et al. 1987) from many independent patches which can add constructively or destructively, leading to large intensity fluctuations in a frequency-dependent manner. The patches each scatter radiation into an angle  $\theta_r = r_r/d$ , with the refractive scale  $r_r \equiv r_F^2/r_d$ . This phenomenon requires very small sources, with angular sizes  $\theta_d \equiv r_d/d \ll \theta_r$ , and so is usually limited to pulsars, although compact relativistic explosions like GRBs can also scintillate diffractively in their early phases (Goodman 1997). For diffractive scintillation, the timescale and bandwidth both increase with observing frequency, and the modulation can saturate at  $\sim 100\%$  although it can also appear to be lower when averaging over multiple ‘scintles’ (time-frequency maxima).

Refractive scintillation, on the other hand, is due to large scale focusing and defocusing over scales  $r_r$ , and where the sources need to be compact compared to  $\theta_r$ . Refractive scintillation corresponds to lower modulation over longer timescales and wider bandwidths.

##### 2.5.2. Extreme scattering events

Beyond the stochastic variations caused by the turbulent interstellar medium discussed above, systematic monitoring of compact extragalactic radio sources discovered discrete high-amplitude changes in source brightness with a characteristic shape, called ‘extreme scattering events’ (ESEs; Fiedler et al. 1987). Subsequently also seen in Galactic pulsars (Cognard et al. 1993), ESEs are believed to be due to coherent lensing structures within the interstellar medium (ISM) (Fiedler et al. 1994). However, significant questions remain regarding the natures of those structures that seem much denser and with higher pressure than the average ISM (Clegg et al. 1998). Whether the structures are one dimensional (filaments), two dimensional (sheets), or three dimensional is still debated (Romani et al. 1987; Pen & King 2012; Henriksen & Widrow 1995; Walker & Wardle 1998), as the models need to reproduce the temporal and frequency structure of ESEs (Walker 2007; Vedantham 2018).

There is considerable work ongoing to improve real-time detection of ESEs (Bannister et al. 2016), which would lead to better observations of their environments. At the same time there are studies of the models of the structures that cause ESEs (Jow et al. 2024; Dong et al. 2018; Rogers & Er 2019), as well as attempts

to identify the underlying causes of the ISM inhomogeneities (Walker et al. 2017).

### 2.5.3. Gravitational lensing

Separate from variability induced by scintillation, extragalactic radio sources may exhibit variability induced by gravitational lensing along the line of sight. This has been predicted to appear in several ways. Radio sources that already showed multiple lensed images could have substructure lensed by small compact objects (typical masses  $\sim M_{\odot}$ ) within the lensing galaxy (Gopal-Krishna & Subramanian 1991; Koopmans & de Bruyn 2000; Biggs 2023), showing correlated but not identical variations between the separate images on timescales of days. However, this can be hard to distinguish from scintillation (Koopmans et al. 2003; Biggs 2021) — indeed there have been many reports of microlensing in the radio that have been difficult to verify (Koopmans & de Bruyn 2000; Vernardos et al. 2024). While gravitational lensing should be achromatic, and hence show different behaviour from scintillation, the varying size of the radio emission region — assumed to be a knot of synchrotron-emitting material within a Doppler-boosted relativistic jet — with frequency can cause apparent frequency dependence.

A related phenomenon could be seen with larger lensing masses. In this case (Vedantham et al. 2017; Peirson et al. 2022) the lens masses would be  $10^{3-6} M_{\odot}$ , causing achromatic variability on timescales of months–years in the lightcurve of a single source (the lensed images are not separable). This would be similar to lensing observed from high-energy blazars in  $\gamma$ -rays (e.g. Barnacka et al. 2011), although the details of the lensed sources are likely different (Spingola et al. 2016).

## 3. Classes of radio transients

Now we have presented the main physical mechanisms that cause radio variability, in this section we discuss each of the main classes of radio transient and variable objects. Our focus is on intrinsic variability (propagation effects were covered in Section 2.5) and what we can learn from radio observations. We also make the case for why radio transient surveys are important, in addition to targeted observations of individual objects. Since there is a limit to the amount of detail we can go into in this paper, where possible we point the reader to relevant review papers. The following subsections are roughly ordered from highly energetic extragalactic objects, through to stars, binaries with compact objects, and Galactic transients. We summarise the different variability timescales for the different classes of transients in Figure 3.

### 3.1. Gamma-ray bursts

Detecting radio afterglows from gamma-ray bursts (GRBs), unbiased by higher frequency detections, was a major motivation for widefield radio transient surveys (as discussed in Section 4.1). Because of their particular importance in this context, we give a brief background to radio observations of GRBs, before summarising our current understanding of their physics.

#### 3.1.1. Radio detection of gamma-ray bursts

The detection of gamma-ray bursts was first reported by Klebesadel et al. (1973), and their origin remained the subject of debate for over two decades. Observations from the Burst

And Transient Source Experiment provided a key breakthrough, showing that the sky distribution of GRBs was isotropic (Meegan et al. 1992; Briggs et al. 1996); and hence ruling out progenitors such as Galactic neutron stars. The focus then shifted to identifying a counterpart at other wavelengths so that a distance scale could be established. The detection of a counterpart, now called an ‘afterglow’, to GRB 970228 in X-ray (Costa et al. 1997) and optical (van Paradijs et al. 1997) wavebands, in a host galaxy at  $z = 0.695$ , established that GRBs were cosmological. A review of early gamma-ray burst afterglow observations, and our derived understanding, is given by van Paradijs et al. (2000).

The first GRB for which a radio afterglow was detected was GRB 970508 (Frail et al. 1997). High variability was observed in the first month after the explosion, which was attributed to diffractive scintillation. Since diffractive scintillation occurs only when the source is smaller than a characteristic size, the transition from the diffractive to refractive regime could be used to measure the angular size of the fireball, determining that it was a relativistically expanding explosion. The subsequent monitoring of this event in radio (Frail et al. 2000b) demonstrated the utility of radio observations in measuring the calorimetric properties of GRBs.

The next decade and a half of radio follow-up campaigns is summarised by Chandra & Frail (2012). They collate observations of 304 afterglows at frequencies between 0.6 GHz and 660 GHz. Of the 306 GRBs with radio follow-up observations, 95 were detected in radio (31%). Of these, 65 had radio lightcurves (three or more detections in the same band). A key issue is that if a source was not detected early in a follow-up program, it was generally not observed subsequently. This is one factor motivating untargeted searches for GRB afterglows.

In the rest of this section we discuss our current understanding of long and short GRBs, and the connection between short GRBs and neutron star mergers.

#### 3.1.2. Long gamma-ray bursts

Once GRB studies became more fruitful with the launch of dedicated satellites, it was quickly determined (Kouveliotou et al. 1993) that there appeared to be two separate populations of GRBs delineated mostly by burst duration but also somewhat by spectral characteristics, short-hard GRBs (SGRBs) with durations  $< 2$  s and long GRBs (LGRBs) with longer durations, although there are other subtleties as well (e.g. low-luminosity long GRBs, GRBs with extended emission; Campana et al. 2006; Norris & Bonnell 2006). Long GRBs are generally understood in the ‘collapsar’ model (Woosley 1993; Paczyński 1998; MacFadyen & Woosley 1999; Piran 2004). In this model the GRB originates from the collapse of a massive star (confirmed through observations of associated supernovae; Galama et al. 1998), leading to a jetted, relativistic outflow and then an afterglow when the jet hits the surrounding interstellar medium and/or the remains of the progenitor’s winds (Section 2.1.2).

Early radio observations made important contributions to the studies of relativistic expansion (Frail et al. 1997; Taylor et al. 2004), the nature of the progenitors (Li & Chevalier 2001; Frail et al. 2000a), the effects of viewing geometry on observables (Mészáros et al. 1998), the structure of the jet (van der Horst et al. 2005; Panaiteescu et al. 1998), the passage of the reverse shock (Kulkarni et al. 1999), and the basic energetics of GRBs (Frail et al. 2001, 2003, 2005).

More recent observations and larger samples have refined and complicated this picture, providing constraints on the environment

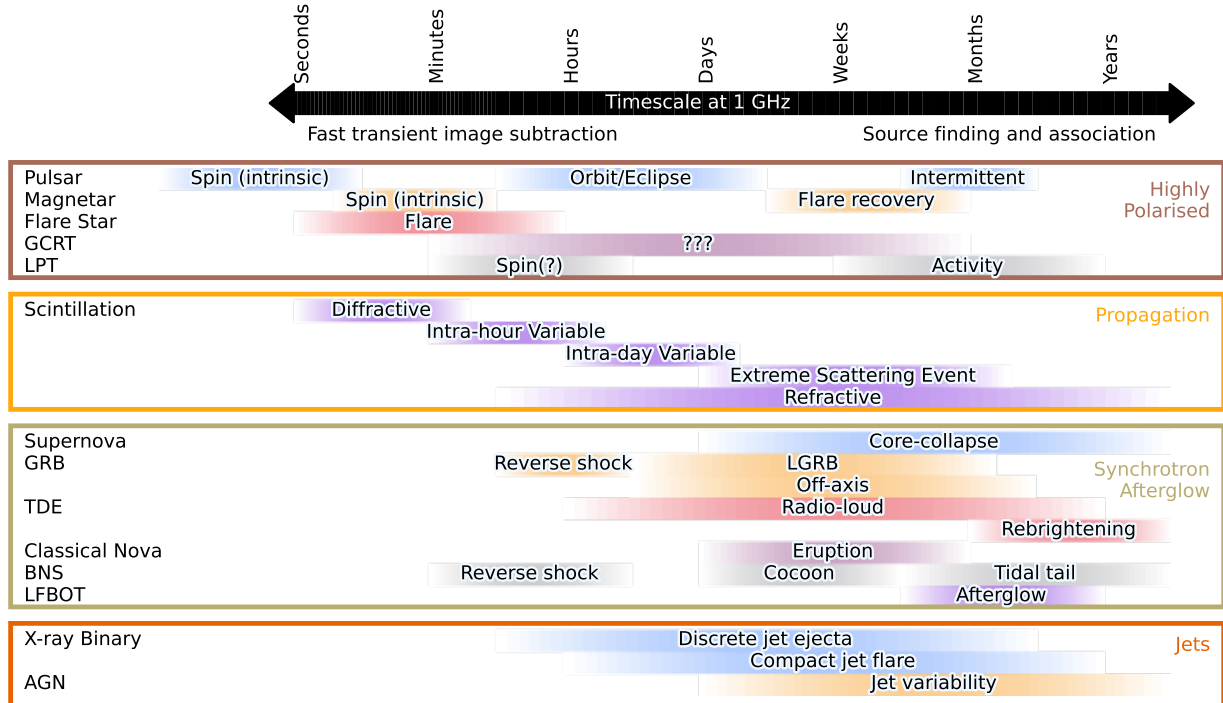


**Figure 3.** Plot showing the relevant timescales of different classes of radio transients. Approximate limits of variability timescales are shown for different sources and different mechanisms. We also separate the highly-polarised largely coherent transients in the top box from the synchrotron afterglow (Section 2.1.2) in the bottom two boxes. We roughly delineate the timescales for traditional transient searches that find sources individually in each epoch and associate them across epochs ( $\gtrsim$  hours, e.g. Swinbank et al. 2015; Rowlinson et al. 2019; Pintaldi et al. 2022) and those that use image-subtraction or related techniques to find shorter-timescale variability at a reduced computational cost ( $\lesssim$  hours, e.g. Wang et al. 2023; Fijma et al. 2024; Smirnov et al. 2025a).

and related selection effects at multiple wavelengths (Schroeder et al. 2022; Osborne et al. 2021); information on the shock structure (Horesh et al. 2015; Laskar et al. 2016; McMahon et al. 2006) and the nature of the central engine (Li et al. 2015); and revealing a diversity in progenitors (Lloyd-Ronning & Fryer 2017). See van Paradijs et al. (2000) and Piran (2004) for early reviews of GRBs, and Chandra (2016), Resmi (2017) and Anderson et al. (2018) for more recent discussions focusing on radio observations.

Current sensitive, wide-band, surveys have enabled searches for larger samples of afterglows at later times, building on earlier results like Seaton & Partridge (2001) to move beyond the biases present in other studies. For instance, Peters et al. (2019) did a dedicated search for late-time radio emission from three supernovae associated with GRBs, while Leung et al. (2021) used ASKAP data to do a similar search. This approach helps explore late-time afterglow behaviour, which is affected by the progenitor's wind output many years before the explosion.

However, those searches still targeted GRBs known from high-energy triggers. One of the longstanding goals of radio surveys (e.g. Murphy et al. 2013; Metzger et al. 2015b; Mooley et al. 2016; Lacy et al. 2020) is understanding the true rate of cosmic explosions through the detection of orphan afterglows, which are not viewed along the jet axis. While early results were encouraging (e.g. Levinson et al. 2002), they were hard to validate as the candidates were discovered many years after the putative events, making followup impossible. More recent surveys have come some way to rectifying this, with much better candidates that are amenable to followup (Law et al. 2018b; Mooley et al. 2022) or robust limits (Leung et al. 2023), although the numbers are still small and it can

be hard to definitively determine the cause of a synchrotron transient due to their similarity across many source types (e.g. tidal disruption events and supernovae).

### 3.1.3. Short gamma-ray bursts

Neutron star mergers have long been believed to be the origin of short gamma-ray bursts (Eichler et al. 1989; Kochanek & Piran 1993; although it can be more complicated, as in Troja et al. 2022b; Rastinejad et al. 2022). Like with long GRBs there is a collimated, relativistic jet that impacts the surrounding medium, and so many of the phenomena related to long GRBs could also take place in short GRBs (Granot & van der Horst 2014; Berger 2014).

This means that we expect similar relativistic afterglows for short GRBs (Section 2.1.2). However, in contrast to long GRBs, the radio emission is considerably fainter (Panaiteanu et al. 2001) and hence the first detections were not made until years later (Berger et al. 2005; Soderberg et al. 2006c). This is due to both the difference in the energetics of the GRBs themselves, as well as considerably lower circumburst medium densities (Berger 2014; Fong et al. 2015; O'Connor et al. 2020; with the flux density scaling as the density to the 0.5 power). This environmental difference likely relates to the different underlying model (merger of compact objects instead of an exploding massive star) as well as the resulting change in delay time between formation and burst, which can be much longer in the cases of short GRBs (Gyr vs. Myr; Zevin et al. 2022). For a full review, see Granot & van der Horst (2014) and Berger (2014).

After years of meagre (but important) returns at radio wavelengths (e.g. Fong et al. 2015), the advent of more sensitive radio instruments and surveys has improved the prospects for radio detections of short GRBs (Schroeder et al. 2025). Combined with X-ray observations, radio afterglow measurements constrain the energetics, geometry, and environment of short GRBs (e.g. Jin et al. 2018; Dichiara et al. 2020; Rouco Escorial et al. 2023). Radio observations are especially important for measuring jet collimation (Fong et al. 2014; Troja et al. 2016), and deviations from a simple shock model that could indicate prolonged energy injection and/or passage of the reverse shock (e.g. Lloyd-Ronning 2018; Lamb et al. 2019; Troja et al. 2019; Schroeder et al. 2024; Anderson et al. 2024).

In the future, observations with more sensitive instruments (Lloyd-Ronning & Murphy 2017) and untargeted surveys should detect a larger number of sources in a wider range of environments, exploring whether the conclusions drawn so far are biased and how they may relate to the related populations of Galactic neutron star binaries and extragalactic neutron star mergers (e.g. Chattopadhyay et al. 2020; Gaspari et al. 2024).

### 3.1.4. Neutron star mergers

While short GRBs have been studied with the understanding that they are most likely the result of neutron star mergers, this was largely untested empirically until the first (and so far still only) multi-messenger detection of a neutron star merger, GW170817/GRB170817A (Abbott et al. 2017a,b). In this case a mildly relativistic off-axis afterglow was detected at radio wavelengths (Hallinan et al. 2017) after first being detected at X-ray wavelengths (Troja et al. 2017; Margutti et al. 2017). The proximity of this event allowed detailed study (e.g. Mooley et al. 2018a; Alexander et al. 2017b; Dobie et al. 2018; Troja et al. 2018; Corsi et al. 2018; Mooley et al. 2018c) giving constraints on the structure, opening-angle, and viewing geometry (e.g. Lazzati et al. 2018). Further observations, including very long baseline interferometry (VLBI) astrometry, allowed more robust constraints on the geometry (Mooley et al. 2018b; Ghirlanda et al. 2019) that in turn allowed direct constraints on the Hubble parameter (Hotokezaka et al. 2019).

While a burst of gamma-rays was seen from GW170817/GRB170817A (Goldstein et al. 2017), it was considerably lower luminosity than that from most GRBs. The distinction is that the observer needs to be on-axis to see a GRB, while the more general neutron star merger phenomena could be observed off-axis, as was the case with GW170817/GRB170817A. Most subsequent searches for neutron star mergers at radio wavelengths still rely on multi-messenger triggers. Given the uncertain nature of many of those triggers and the wide sky areas they point to (e.g. Petrov et al. 2022), even triggered searches still retain some aspects of wide-field radio surveys, with many sources to consider and tight control over false positives required. With these triggered searches, non-detections can still be used to constrain the geometry, energetics, and environments of neutron star mergers (Gulati et al. 2025). But even without such a trigger, the collimated afterglow from a SGRB/neutron star merger could still be detectable by wide-field radio surveys (Metzger et al. 2015b; Hotokezaka et al. 2016; Lin & Totani 2020), although as with many similar events it may be a challenge to distinguish them from other related synchrotron transients. Nonetheless, they are promising targets to understand the diversity in jet launching and how neutron star mergers are tied to their environments. If

detected, followup observations including astrometry and searches for scintillation can then be used to determine the jet geometry and energetics (Dobie et al. 2020), especially with next-generation radio facilities (Dobie et al. 2021; Corsi et al. 2024).

Beyond the collimated, relativistic ejecta there are also predictions for an additional component, with mildly-relativistic dynamical ejecta interacting with the surrounding medium and causing a second afterglow-like component (Nakar & Piran 2011; Piran et al. 2013; Hotokezaka & Piran 2015; Hotokezaka et al. 2018). Unlike the jet launching discussed above, detecting this dynamical ejecta could allow studies of the neutron star equation of state and merger dynamics. So far there has not been a definitive radio detection of this emission from GW170817/GRB170817A (Hajela et al. 2019b; Balasubramanian et al. 2022), and while there have been claims of a second emission component at X-ray wavelengths (Hajela et al. 2022), this is currently a subject of debate (Troja et al. 2022a; Ryan et al. 2024; Katira et al. 2025). Nonetheless, for future events these transients should be detectable by wide-field radio surveys (Metzger et al. 2015b; Hotokezaka et al. 2016; Corsi et al. 2024; Bartos et al. 2019).

Finally, there are models of neutron star mergers where the gravitational wave signal is expected to be accompanied by a coherent burst of low-frequency radio waves, potentially even before the gravitational wave signal (e.g. Usov & Katz 2000; Totani 2013; Zhang 2020b; Yamasaki et al. 2018; Wang et al. 2018; Cooper et al. 2023, and for candidate detections see Moroianu et al. 2023; Rowlinson et al. 2024). Identification of prompt emission would aid in prompt localisation of the gravitational wave event (thus aiding further electromagnetic followup), potentially provide a dispersion measure-based distance (e.g. Palmer 1993), and help understand the physical conditions at the site of the merger. These signals would not generally be detectable by most of the imaging surveys discussed here, but could be identified by beam-forming surveys, especially wide-area/all-sky surveys (Section 7.5).

## 3.2. Supernovae

Core-collapse supernovae (SNe) represent the end point in the evolution of massive stars. They are responsible for injecting mass, energy and enriched material into the ISM (Alsabti & Murdin 2017). The many different observational classifications/manifestations of SNe come from differences in the evolutionary state and mass-loss history of the progenitor (Alsabti & Murdin 2017; Smith 2014). Radio emission from SNe largely comes from interaction between the SN ejecta and the circumstellar material (Chevalier 1981, 1982, 1998; see Weiler et al. 2002). Observing the evolution of the radio emission allows one to unwind the mass-loss history of the progenitor, allowing studies of the latest stages of mass-loss right before explosion (which are unconstrained empirically; Chandra 2018). This can then be used to study the peculiarities of mass-loss for individual SNe (e.g. Sfaradi et al. 2024b) and for large samples (Bietenholz et al. 2021; Sfaradi et al. 2025), which can then be correlated with the optical classification.

The simple picture of steady spherical mass-loss is, in many cases, contradicted by detailed radio observations. This has been studied in detail in the case of SN 1987A in the Large Magellanic Cloud (Staveley-Smith et al. 1993; McCray & Fransson 2016; Petruk et al. 2023), through multi-wavelength modeling of the evolving morphology and spectrum, but usually this level of detail is not possible. Instead observations can usually only constrain the

flux density, and in small numbers of cases the size and rough shape (with very long baseline interferometry; e.g. DeMarchi et al. 2022). But even the basic lightcurve information is complex, and can show multiple radio peaks (Anderson et al. 2017; Palliyaguru et al. 2021; Rose et al. 2024) indicating episodic mass-loss, or broadened peaks (Soderberg et al. 2005; Sfaradi et al. 2024b) showing aspherical ejecta. In particular, we highlight the use of unbiased surveys (Stroh et al. 2021; Rose et al. 2024) in systematically probing for unexpected emission of a large, diverse sample of SNe, and further searching for (likely) SNe that were not identified previously (Gal-Yam et al. 2006; Dong et al. 2021).

Beyond the simple blast-wave model, sub-classes of SNe such as the stripped-envelope types Ibc or Ic-BL can probe additional particle acceleration and/or central engines that may be present in some SNe (Corsi et al. 2023; Soderberg et al. 2010, 2006b). Studying the radio emission properties of these SNe can help constrain the energetics and geometries of relativistic jets (Shankar et al. 2021; Barnes et al. 2018). Some type Ic-BL supernovae also show long GRBs (Woosley & Bloom 2006; Cano et al. 2017), presumably from a jet associated with a central engine. Other observational manifestations can arise from partially successful jets that either lead to Ic-BL SNe without GRBs or with low-luminosity GRBs (Eisenberg et al. 2022; Bromberg et al. 2011a; Pais et al. 2023; Piran et al. 2019).

Aside from core-collapse SNe, thermonuclear SNe (Type Ia; Blondin 2024) are of considerable interest for their elemental enrichment patterns (Dwek 2016) and their use in cosmology (Riess et al. 1998; Perlmutter et al. 1999), but the underlying natures of their progenitors are still poorly understood (Maoz et al. 2014; Liu et al. 2023). Radio observations can in principle distinguish between progenitor scenarios (Horesh et al. 2012; Pérez-Torres et al. 2014), constraining the presence of a non-degenerate companion. However, despite considerable investment of observational resources (e.g. Panagia et al. 2006; Hancock et al. 2011; Chomiuk et al. 2012; Margutti et al. 2012; Horesh et al. 2012; Pérez-Torres et al. 2014) no type Ia SNe were detected for many years. This changed with the detection of SN2020eyj by Kool et al. (2023), whose radio properties show signs of interaction between a blast wave and the circumstellar medium (CSM), suggesting a non-degenerate companion. However, the optical/infrared signature of this SN is also somewhat unusual, showing signs of CSM interaction (Type Ia-CSM; Silverman et al. 2013), so it remains to be seen whether this signature is borne out by future observations of a larger sample of Ia SNe.

### 3.2.1. Luminous fast blue optical transients

Sitting at the intersection of core-collapse SNe and GRBs, there are expected to be a variety of relativistic explosions that would lack high-energy emission (e.g. Mészáros & Waxman 2001). Such sources have begun to be discovered in increasing numbers by large optical surveys. The first of these from an emerging new class is AT2018cow (Prentice et al. 2018; Perley et al. 2019; Ho et al. 2019; Margutti et al. 2019; Nayana & Chandra 2021), which was notable for having bright, fast, blue optical emission along with very bright and long-lasting (sub)millimetre emission transitioning, along with quickly declining centimetre emission whose properties are not easily reconciled with the millimetre emission (Margutti et al. 2019; Ho et al. 2019, 2022) in the usual way for synchrotron explosions. These sources are called ‘(luminous) fast blue optical transients’ or (L)FBOTs, with LFBOTs those with the highest peak luminosities ( $10^{44}$  erg s $^{-1}$ ) that are achieved in the

shortest times (few days), although FBOTs can span a range of lower luminosities and slower timescales (e.g. Drout et al. 2014).

While the model for these sources is not clear (e.g. Kuin et al. 2019; Lyutikov & Toonen 2019; Lyutikov 2022; Mohan et al. 2020; Pellegrino et al. 2022; Chen & Shen 2022; Pasham et al. 2021; Vurm & Metzger 2021), with models including tidal disruptions of white dwarfs, ongoing central engines, accretion, and circumstellar interactions in unusual environments, many observations suggest that they are related to relativistic explosions from massive stars although this is far from certain (Metzger 2022; Migliori et al. 2024). Increasing numbers of LFBOTs are being identified through optical surveys (e.g. Ho et al. 2023b), which are now able to optimise their selection procedures (Bright et al. 2022; Ho et al. 2020; Coppejans et al. 2020; Perley et al. 2021; Ofek et al. 2021; Ho et al. 2023a; Yao et al. 2022; Chrimis et al. 2024a), and radio followup is playing a crucial role in understanding their properties and hence progenitor models. What is still lacking, though, are discoveries beginning with radio or millimetre wavelengths, although this may change with the next generation of millimetre surveys (Eftekhari et al. 2022). Like the supernova cases above, such discoveries can help understand the biases in the optical selection functions and what the true underlying rates are.

### 3.3. Active galactic nuclei

As discussed in Section 2.1.1, AGN are the dominant radio source by number in most widefield surveys to date<sup>g</sup> (Condon et al. 2002), and also the dominant source of variability (e.g. Falcke et al. 2001; Mundell et al. 2009). Some of this is extrinsic (Section 2.5.1) but much of the variability is due to intrinsic changes in the sources themselves. For most variable sources this manifests as modest stochastic variability at the few percent to few tens of percent level on timescales from days to years. This low-level intrinsic variability is typically ascribed to changes in the accretion rate onto the central super-massive black hole, propagation of shocks along the jets, or similar phenomena (e.g. Bignall et al. 2015; Marscher & Gear 1985).

However, there are also examples with much more extreme variability, exceeding 100% (Barvainis et al. 2005). Causes for this can include reorientation of AGN jets, potentially from a binary supermassive black hole (Palenzuela et al. 2010; An et al. 2013), or dramatic changes in the accretion rate (Kunert-Bajraszewska et al. 2020; Wołowska et al. 2021; Nyland et al. 2020). Both of these are of considerable interest. Binary supermassive black holes are likely related to the model for hierarchical growth of these black holes through mergers (Volonteri 2010), and contribute to the low-frequency gravitational wave background (Agazie et al. 2023b) detected through pulsar timing experiments (Agazie et al. 2023a; EPTA Collaboration et al. 2023; Miles et al. 2025; Reardon et al. 2023; Xu et al. 2023) and potentially the expected signal at higher frequencies that would be detected through forthcoming space-based interferometers (Huang et al. 2024). In contrast, significant changes in jet activity and accretion rate may give clues to the duty cycle and intermittency of AGN activity, which is important for understanding black hole growth (Volonteri 2010) as well as feedback processes in galactic environments (e.g. Czerny et al. 2009).

<sup>g</sup>Narrower, deeper surveys show that star forming galaxies dominate at lower flux densities (see Padovani 2016).

### 3.4. Tidal disruption events

Tidal disruption events (TDEs; Hills 1975; Rees 1988; Komossa 2015; see Gezari 2021 for a recent review) occur when a star is disrupted while passing within the tidal radius of a supermassive black hole (note that other TDE scenarios involving compact objects and lower-mass black holes have been proposed, e.g. Krolik & Piran 2011). This leads to emission potentially across the electromagnetic spectrum, including at radio wavelengths (van Velzen et al. 2011; Giannios & Metzger 2011; see Alexander et al. 2020 for a recent review).

The best studied cases of TDE emission in the radio are where relativistic jets are launched as in Swift J1644+57 (Bloom et al. 2011; Zauderer et al. 2011; Levan et al. 2011). However, there is a large diversity in the radio properties of TDEs, with many lacking relativistic jets and only 20–30% with detectable prompt (within the first few months after an optical/UV/X-ray transient) radio emission that instead originates from synchrotron emission from fast but sub-relativistic outflows and a wide range in luminosity (Alexander et al. 2020). There are a number of proposed models for this radio emission, ranging from debris streams or winds from the accretion disk interacting with the surrounding medium, to self-interaction within debris streams (Bower et al. 2013; Krolik et al. 2016; Alexander et al. 2016; Pasham & van Velzen 2018).

Perhaps even more interesting are the recent discoveries of significantly-delayed radio emission (Horesh et al. 2021a,b; Cendes et al. 2022), years after the original event. The origin of this — either a delay in mass ejection (Cendes et al. 2022) or a viewing angle effect (Sfaradi et al. 2024a) — is still debated, but it seems to be relatively common (30–40%) among TDEs discovered at other wavelengths (Horesh et al. 2021b; Cendes et al. 2024; Anumarlapudi et al. 2024). This points to a further diversity in TDE properties, based on the nature of the disrupted star, the characteristics of the surrounding medium, the mass/spin of the black hole, or additional factors. Understanding the underlying cause of this full range of manifestations can help with studies of accretion and the environments of supermassive black holes.

The results above are from TDEs discovered at (primarily) optical wavelengths and then followed up in the radio. However, new radio surveys have led to discoveries of TDEs (and TDE candidates) starting with their radio emission (Anderson et al. 2020; Ravi et al. 2022b; Somalwar et al. 2023, 2025a,b; Dykaar et al. 2024). Such discoveries, along with those at infrared wavelengths (e.g. Mattila et al. 2018), have the potential to more robustly probe the radio properties of TDEs without the underlying biases in optical surveys, such as being able to determine a rate independent of any host obscuration (Bower 2011). This is echoed by the use of unbiased surveys to reveal unexpected flares in late-time emission (Ravi et al. 2022b; Anumarlapudi et al. 2024).

We show a compilation of a diverse set of synchrotron transient lightcurves in Figure 4. This highlights the extreme range in luminosity (at least 6 orders of magnitude for the peak) and timescale ( $> 3$  orders of magnitude). Such empirical analyses are often helpful when classifying new events (e.g. Coppejans et al. 2020; Ho et al. 2020).

### 3.5. Stars

Radio emission has been detected from stars at all stages of their evolution (Güdel 2002): pre-main sequence and main sequence stars; ultracool dwarfs and supergiants; and a range of unusual stellar types such as magnetically chemically peculiar stars, RS CVn

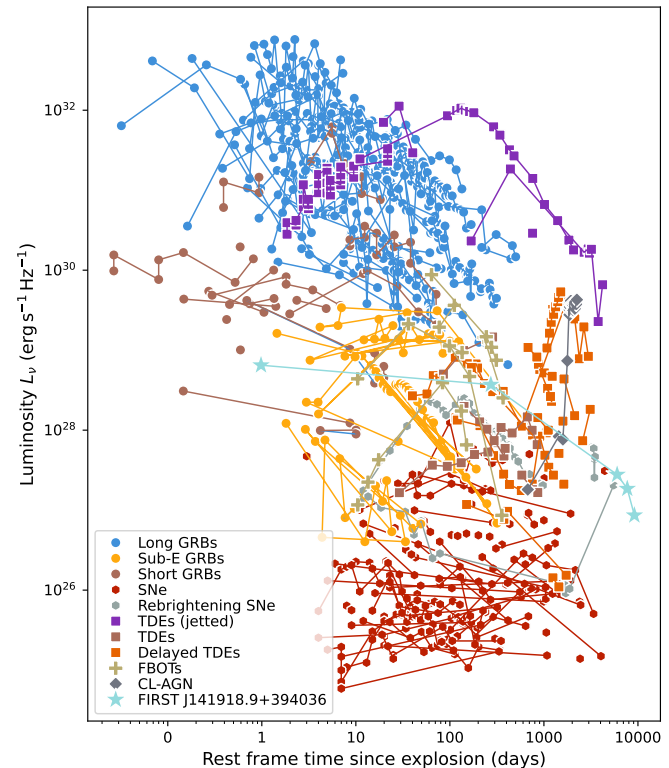


**Figure 4.** Radio lightcurves of a diverse set of synchrotron transients, following examples like Ho et al. (2020) and Coppejans et al. (2020). The sources include: long GRBs, sub-energetic GRBs, and short GRBs (circles; Section 3.1), supernovae (hexagons; Section 3.2), TDE (squares; Section 3.4), FBOTs (pluses; Section 3.2.1), changing-look AGN (diamonds; Section 3.3), and the potential orphan afterglow FIRST J141918.9+394036. Data are primarily at 7–10 GHz, except FIRST J141918.9+394036 (1.4 GHz, but which was scaled following Mooley et al. 2022), a few GRBs at 5 GHz, and a few TDEs at 15 GHz; in those cases no spectral correction or  $K$ -correction has been applied. Data were compiled by A. Gulati and are from Alexander et al. (2016, 2017a); Anderson et al. (2024); Andreoni et al. (2022); Berger et al. (2001b,c, 2000, 2003, 2005); Bietenholz et al. (2021); Bright et al. (2022); Brown et al. (2017); Cendes et al. (2022, 2021, 2024); Cenko et al. (2011, 2006, 2012); Chandra et al. (2008, 2010); Chrimes et al. (2024b); Coppejans et al. (2020); Djorgovski et al. (2001); Eftekhari et al. (2018); Fong et al. (2014, 2015); Fong et al. (2021); Frail et al. (2000b, 2003, 2005, 2006, 2000c, 1999b); Galama et al. (2000, 2003); Goodwin et al. (2023); Goodwin et al. (2025); Greiner et al. (2013); Hajela et al. (2025); Hancock et al. (2012b); Harrison et al. (2001, 1999); Ho et al. (2019, 2020); Horesh et al. (2021b,a, 2015); Kulkarni et al. (1998); Lamb et al. (2019); Laskar et al. (2023, 2016, 2018); Laskar et al. (2022); Law et al. (2018b); Leung et al. (2021); Levan et al. (2024); Margutti et al. (2019, 2013); Mattila et al. (2018); Meyer et al. (2025); Moin et al. (2013); Mooley et al. (2022); O'Connor et al. (2023); Pasham et al. (2015); Perley et al. (2014, 2008); Price et al. (2002); Rhodes et al. (2024); Rol et al. (2007); Rose et al. (2024); Schroeder et al. (2025, 2024); Sfaradi et al. (2024a); Soderberg et al. (2006c, 2004b,a, 2006a); Stein et al. (2021); Taylor et al. (1998); van der Horst et al. (2008); Zauderer et al. (2013). See [https://github.com/ashnagulati/Transient\\_Comparison\\_Plots](https://github.com/ashnagulati/Transient_Comparison_Plots)

binaries and Wolf-Rayet stars. Figure 5 (adapted from Driessen et al. 2024) demonstrates this diversity, showing the radio luminosity of a sample of known radio stars, spanning the entire colour-magnitude diagram, including the supergiant and white dwarf branches.

Radio emission gives us insight into a range of stellar phenomena that can not be fully understood with observations in other wavebands. This includes questions about: (i) stellar mass loss throughout the different stages of stellar evolution; (ii) how young stars and planets evolve in their common disk environment; (iii)

the magnetic field structure of stars; and (iv) how the flaring activity of stars affects the habitability of planets they host (Matthews 2019).

However, radio emission has only been detected from a tiny fraction of stars. Of the  $\sim 1.8$  billion stars detected by Gaia (Gaia Collaboration et al. 2023), fewer than 1 500 have been detected at radio frequencies. Widefield radio transient surveys (and circular polarisation surveys), notably with ASKAP and LOFAR, are now transforming this area of research, with the number of known radio stars increased substantially from the well-established Wendker (1987, 1995) catalogue, which contains 228 radio stars detected at  $< 3$  GHz (and which was last updated in 2001), to the Sydney Radio Stars Catalogue which contains confirmed detections of 839 unique stars (Driessen et al. 2024).

Radio stars exhibit a wide range of variability behaviours, driven by a range of emission mechanisms (see Section 2.3). Transient and highly variable radio emission is an indication of strong magnetic fields, shocks, or interactions between stars in binary systems. In this section we can only briefly summarise our current understanding of stellar radio emission (with a focus on variability), and point the reader to suitable review papers on each stellar class. We have summarised the key characteristics of each class in Table 1. Binary systems involving a compact object are addressed separately in Sections 3.6 and 3.7. The following subsections are presented in (roughly) decreasing order of temperature.

### 3.5.1. O & B type main sequence stars

The dominant source of radio emission from hot ( $\sim 10\,000$  K to  $> 50\,000$  K), massive ( $> 10 M_{\odot}$ ), OB stars is their stellar winds (Güdel 2002). As the stars shed their strongly ionised winds, they produce thermal (free-free) radio emission (Section 2.2); and indeed radio observations are a well-established way of measuring stellar mass loss rates in OB stars (Leitherer et al. 1995; Scuderi et al. 1998). The associated radio emission is predicted to have a positive spectral index ( $\alpha \sim +0.6$ ) and not be variable (Wright & Barlow 1975). However, these theoretical models assume a steady, spherically symmetric wind. In cases where the wind is inhomogeneous, filaments and clumps in the wind can cause variations in the radio flux density. This has been observed in, for example, P Cygni, a luminous blue variable star, and the first OB star detected in radio (Wendker et al. 1973). VLBI observations by Skinner et al. (1997) and Exter et al. (2002) demonstrated that the stellar wind of P Cyg is highly inhomogeneous and as a result its integrated flux density changes on timescales of days.

Both blue and red supergiants (the highly evolved counterparts of massive OB stars) exhibit thermal radio emission from their stellar atmospheres, and where present, their stellar winds, via the same mechanisms as main sequence OB stars (Scuderi et al. 1998). See, for example, radio studies of  $\alpha$  Ori (Betelgeuse) (Lim et al. 1998; O’Gorman et al. 2020).

Up to 25 – 40% of radio-detected OB stars have been found to have signatures of non-thermal radio emission (Bieging et al. 1989), and in some cases this dominates the thermal component (Abbott et al. 1984). This emission, due to synchrotron radiation (Section 2.1), has a characteristic flat or negative spectral index, and can be variable on short timescales (e.g. Bieging et al. 1989; Persi et al. 1990). Synchrotron emission implies the presence of strong magnetic fields and shocks. Initially there were a range of hypotheses for the source of non-thermal emission, considering both single stars and binary systems. However, it is now

established that most (if not all) OB stars that show non-thermal emission are binary systems (see Table 2 in De Becker 2007). The emission is caused by shocks in the colliding-wind region of binary OB systems, where the winds from both stars in the binary interact (see also Section 3.5.6). This has been demonstrated in a number of systems through the observed periodicity of the radio variability (see the series of papers studying stars in the Cyg OB association for examples Blomme et al. 2005; van Loo et al. 2008; Blomme et al. 2010). A review of non-thermal radio emission in massive stars is given by De Becker (2007).

### 3.5.2. Wolf-Rayet stars

Wolf-Rayet (W-R) stars are the helium-burning remnants of massive OB stars. They are highly evolved, having lost their hydrogen-rich outer layers through the processes of Roche lobe overflow to a companion (in close binaries), mass loss by a strong stellar wind (in single stars), or a combination of both (Crowther 2007). W-R stars have extremely hot, dense stellar winds, and so exhibit strong thermal radio emission, via the same mechanisms as OB stars, and are some of the most luminous stellar radio sources (Abbott et al. 1986). As with OB stars, this radio emission can also be used to measure stellar mass loss rates, which, for W-R stars, are very high (Nugis & Lamers 2000).

A subset of W-R stars exhibit non-thermal synchrotron radiation, and as with OB stars, most (if not all) of these are in binary systems (see Table 1 in De Becker 2007). The archetypal example is WR 140, a W-R+O star binary, with a 7.9 year orbit. Extensive monitoring with the VLA by White & Becker (1995) showed variability in the non-thermal emission, clearly correlated with the orbital phase. Further work by Dougherty et al. (2005) showed that the spectral index is also correlated with the orbital phase, suggesting that the relative importance of emission, absorption and plasma processes changes with stellar separation (and hence electron and ion density) throughout the orbit. For more information we refer the reader to the review of non-thermal radio emission in massive stars (including W-R stars) by De Becker (2007).

### 3.5.3. A & early F type main sequence stars

A and early F-type stars ( $\sim 6\,500$  K to  $< 10\,000$  K) have neither the strong ionised stellar winds of OB type stars, nor the dynamo-generated magnetic fields of later type stars (Güdel 2002, and see below). Hence they are generally expected to have weak thermal emission from their atmospheres, and mostly not be detectable at radio wavelengths (Brown et al. 1990). A small number of nearby objects have been detected in radio, for example Sirius A (A0/1; White et al. 2018, 2019) and Procyon (F5; Drake et al. 1993). For Procyon, the observed quiescent emission is thermal (free-free) chromospheric emission from the entire stellar disk. The variable emission is potentially due to either (a) active regions on the corona, analogous to our Sun; or (b) flares or bursts due to localised magnetic fields, again analogous to our Sun. See also the discussion of thermal radio emission detected from the late F9 star  $\eta$  Cas A by Villadsen et al. (2014).

A subset of A-type (and B-type) stars that do show strong radio emission are the magnetic chemically peculiar (Ap and Bp type) stars. We discuss these separately in Section 3.5.4.

### 3.5.4. Magnetic chemically peculiar stars

Magnetic chemically peculiar stars (MCPs, also referred to as Ap and Bp type stars), are a subset of main sequence stars that have strong (kilogauss), organised magnetic fields, and unusual

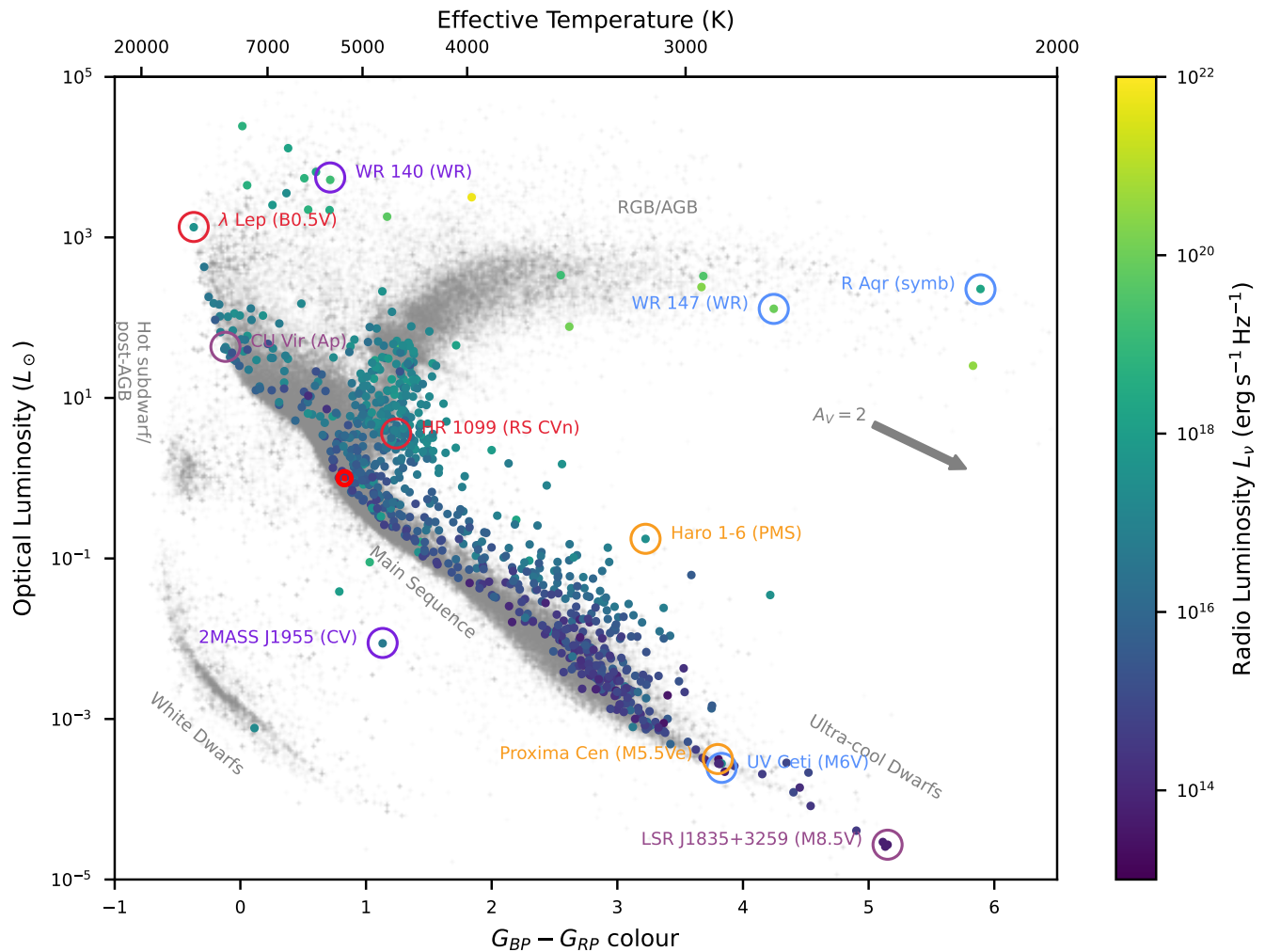


**Figure 5.** Gaia DR3 colour-magnitude diagram showing the stars in an updated version of the Sydney Radio Stars Catalogue. The colour scale shows the radio luminosity based on the maximum flux density of each star in the SRSC and the Gaia  $r_{\text{geo}}$  distance. The grey background points show the Gaia DR2 CMD for reference (Pedersen et al. 2019), and we annotate some of the major features. The Sun is indicated by the red  $\odot$  symbol. Individual stars are indicated by the coloured circles and are labeled with their types. We show a rough translation between Gaia  $G_{\text{BP}} - G_{\text{RP}}$  colour and effective temperature determined from synthetic photometry (based on STScI Development Team 2013) and an extinction vector (Zhang & Yuan 2023). Even cooler sources such as brown dwarfs are located off the right edge of the figure, and are not included as they do not have Gaia measurements. Figure is adapted from Driessen et al. (2024).

chemical abundances on their surfaces (Preston 1974; Landstreet 1992).

There were many searches for radio emission from these stars, carried out over several decades (e.g. Trasco et al. 1970; Turner 1985), until Drake et al. (1987) successfully detected five systems with the VLA:  $\sigma$  Ori E, HR 1890, and  $\delta$  Ori C, IQ Aur, and Babcock's star (HD 215441). Subsequent work by Linsky et al. (1992) showed the radio emission was consistent with gyrosynchrotron radiation from particles in the magnetosphere, accelerated due to interactions with the stellar wind.

The geometry of magnetic fields in MCP stars is generally dipolar, with the magnetic axis inclined with respect to the rotational axis. Hence the observed magnetic field of the star is modulated by its rotational period (Landstreet 1992). Consistent with this, Leone & Umana (1993) showed that the observed radio emission of two MCPs (HD 37017 and  $\sigma$  Ori E) was periodic, and varied with the rotational period of the star.

However, the gyrosynchrotron mechanism can not explain the observed radio emission of all MCPs. Observations of CU Vir

by Trigilio et al. (2000) detected bright, highly directional, and highly circularly polarised emission, that required a coherent mechanism to explain it. They showed this was consistent with electron cyclotron maser emission, a result supported by long-term monitoring observations of CU Vir (e.g. Trigilio et al. 2008; Ravi et al. 2010; Lo et al. 2012).

The current generation of radio telescopes (and in particular widefield radio surveys) has enabled the detection of an increased number of magnetic chemically peculiar stars, including at lower radio frequencies. See Hajduk et al. (2022), Das et al. (2022) and Das et al. (2025) for recent results from LOFAR, GMRT (the Giant Metrewave Radio Telescope), and ASKAP respectively.

### 3.5.5. Late F, G & K type main sequence stars

Late F-type to early K-type main sequence stars are often referred to as ‘solar-type’ stars, as they are broadly similar to our Sun in terms of temperature, mass, and other physical processes. The Sun is extremely well-studied in radio: see Dulk (1985) and Bastian et al. (1998) for earlier reviews of solar radio emission, and

Benz & Güdel (2010) for a more recent review of solar flares across the electromagnetic spectrum. Kowalski (2024) provides an equivalent review of stellar flares.

Like our Sun, F, G and K-type stars are observed to have quiescent thermal radio emission (Villadsen et al. 2014). If the Sun’s thermal radio emission was scaled to the distance of stars in our local neighbourhood, it would only reach  $\mu\text{Jy}$  levels, which until recently was below the detection threshold of most radio telescopes. Hence the stars detected to date tend to be more luminous than the Sun.

F to K-type stars (and many other main sequence stars) have a magnetic corona like our Sun, and hence have magnetic fields generated by a dynamo at the interface between the radiative core and the convective envelope. They therefore show stellar flares, with both thermal and non-thermal components (e.g. Güdel 1992; Lim & White 1995; Budding et al. 2002).

Solar-type stars have also been observed to flare with much higher energies than our own Sun (so-called ‘superflares’; Maehara et al. 2012). Superflares are caused by magnetic reconnection, and often linked to starspot activity. Superflares have not been definitively detected at radio wavelengths to date.

Finally, some F, G & K stars exhibit coherent bursts from a range of mechanisms (e.g. Matthews 2025) — although in general the stellar equivalents of solar radio bursts have been primarily studied on K & M dwarfs due to their extremely strong magnetic fields, since these result in stronger and more frequent flare activity (see Section 3.5.7).

### 3.5.6. RS CVn and Algol binaries

RS Canum Venaticorum (RS CVn) and Algol stars are two subtypes of chromospherically active binary star systems.

RS CVn binaries consist of a subgiant or giant star of spectral type F–K with a companion main sequence star of spectral type G–M. They have typical orbital periods of 1–30 days, and typical separations of  $\sim R_\odot$  (Hall 1976). They have active chromospheres, high rotational velocities and strong magnetic fields.

Algol binaries consist of two semi-detached stars, in which one is a hot (B or A-type) main sequence star, and the second is a more evolved (G or K-type) giant or subgiant. They have typical orbital periods of 1–20 days and typical separations of  $\sim 10 - 40 R_\odot$  (Giuricin et al. 1983).

At gigahertz frequencies, these stellar systems exhibit quiescent emission, due to mildly relativistic electrons radiating gyrosynchrotron emission in magnetic fields (Güdel 2002). Both RS CVn and Algol-type binaries also show variability in this gyrosynchrotron emission, on timescales of minutes to hours. This activity can be present for a significant fraction ( $\sim 30\%$ ) of the time (Lefevre et al. 1994). In addition, they show significant radio flaring activity (Drake et al. 1989; Lefevre et al. 1994; Umana et al. 1998).

At low radio frequencies, coherent emission mechanisms dominate in RS CVn binaries. Toet et al. (2021) propose that this electron cyclotron maser emission could be generated by enhanced chromospheric flaring due to tidal forces or the interaction between the two binary stars, analogous to the Jupiter-Io interaction.

Two well-studied active binary systems are the RS CVn binary HR 1099 (e.g. Owen et al. 1976; Feldman et al. 1978; Osten et al. 2004; Slee et al. 2008) and the canonical Algol binary,  $\beta$  Persei (Mutel et al. 1985, 1998).

### 3.5.7. M dwarf and ultracool dwarf stars

M-dwarfs are very low mass (typically  $0.1 - 0.6 M_\odot$ ), cool ( $T < 3800$  K) stars. They are long lived, and extremely abundant, accounting for roughly 75% of the stars in our local neighbourhood (Winters et al. 2019). M-dwarfs show bright radio bursts across all wavebands, associated with their extremely strong (up to kilogauss; Shulyak et al. 2017) magnetic fields.

The observed radio emission comes from a range of different emission mechanisms. Intense and highly polarised electron cyclotron maser emission often dominates (e.g. Hallinan et al. 2008; Lynch et al. 2017; Villadsen & Hallinan 2019). This likely originates both from magnetic active regions, and from auroral emission (e.g. Hallinan et al. 2015), analogous to solar system planets (Zarka 1998). M-dwarfs also show quiescent and flaring emission due to gyrosynchrotron radiation (e.g. Berger et al. 2001a; Lynch et al. 2016).

Ultracool dwarfs (later than M7-type) are the coolest ( $T < 2900$  K) stellar and substellar objects. Only ten L & T-type dwarfs have been detected in radio to date (see Table 2 in Rose et al. 2023, and in addition the recently published detection by Guirado et al. 2025), but these observations have provided evidence for kilogauss magnetic fields even in the coolest of substellar objects (Kao et al. 2018). Given that ultracool dwarfs are fully convective (without a radiative core), this requires an alternative dynamo mechanism (e.g. Browning 2008).

Like M-dwarfs, ultracool dwarfs can show quiescent, flaring and auroral radio emission (e.g. Route & Wolszczan 2012; Kao et al. 2016). Because radio observations allow us to probe the magnetic field strength, they are critical for understanding energy generation in ultracool stars and substellar objects.

Radio observations complement X-ray and optical observations by providing direct measurements of the magnetic field strengths and plasma densities associated with stellar activity (Benz & Güdel 2010). Because coherent emission mechanisms often dominate, many M-dwarf and ultracool dwarf stars do not fit the empirically established (over 10 orders of magnitude) Güdel-Benz relation between quiescent gyrosynchrotron radio and soft X-ray luminosity.

Untargeted searches with current telescopes are enabling detection of larger samples of M dwarf and ultracool dwarf stars than were previously available (e.g. Callingham et al. 2021). They also enable searches that are unbiased by the properties of the stars in other wavebands (previous samples were often selected on the basis of their known chromospheric activity (e.g. Lynch et al. 2017; Crosley & Osten 2018).

### 3.5.8. Star-planet interactions and exoplanetary systems

Radio emission is expected from exoplanetary systems, in analogy to what we observe from the magnetised planets in our own solar system (Zarka 2007). This predicted emission originates from several different mechanisms: (i) auroral emission from the interaction between the host stellar wind and the exoplanetary magnetosphere, as seen in magnetised planets in our solar system (Zarka 1998; Farrell et al. 1999); (ii) electron cyclotron maser emission from the magnetic interaction between a so-called ‘hot Jupiter’ and its host star (referred to as star-planet interactions, or SPI; Zarka 2007); (iii) emission from the interaction between an exoplanet and its exomoon/s, analogous to the Jupiter-Io system (Noyola et al. 2014).

There has been substantial theoretical and empirical work in predicting the flux densities expected (e.g. Lazio et al. 2004;

Grießmeier et al. 2007; Hess & Zarka 2011; Lynch et al. 2018). For (i) the radio emission has a cutoff frequency determined by the strength of the exoplanetary magnetic field, and hence is only likely to be detectable at low radio frequencies (< 300 MHz). For (ii), the emission frequency can be higher (up to gigahertz), as it is determined by the magnetic field strength of the host star rather than the planet.

Over the past two decades there have been many searches for radio emission from exoplanetary systems, from targeted observations of individual exoplanets considered likely to be detectable (e.g. Bastian et al. 2000; Lazio & Farrell 2007; Vidotto et al. 2012) to large-scale searches for emission from known exoplanetary systems in both targeted (e.g. Ortiz Ceballos et al. 2024) and untargeted radio surveys (e.g. Murphy et al. 2015). In recent years there have been a number of tentative detections (e.g. Vedantham et al. 2020; Turner et al. 2021), although none have yet been definitively confirmed as originating from star-planet interactions.

The improved sensitivity of current and future telescopes, and the capability of widefield surveys to target many systems at once means detecting exoplanetary systems at radio wavelengths is increasingly likely (see Zarka et al. 2015, for a discussion of SKAO capabilities). However, a significant observational challenge is that the emission is beamed, and dependent on the orbital period of the planet. Although beaming can make the emission brighter, the high directionality reduces the probability of detection. In addition, once radio emission has been detected from an exoplanetary system, it is challenging to distinguish between an exoplanet-related cause, and emission from the host star (see, for example, the discussion in Pineda & Villadsen 2023). See Callingham et al. (2024) for a recent review of radio emission from star planet interactions and space weather in exoplanetary systems.

### 3.6. Classical novae

Classical and recurrent novae — forms of cataclysmic variables (highly-variable binary systems involving a white dwarf), with the distinction between classical and recurrent novae coming from comparing the recurrence time to observational spans — are thermonuclear explosions on the surfaces of white dwarfs in binary systems (Gallagher & Starrfield 1978; Bode et al. 1987; for a recent review see Chomiuk et al. 2021a). A thin layer of accreted material undergoes unstable nuclear burning, driving off a modest amount of mass (more or less than the accreted amount) at a speed of hundreds to thousands of  $\text{km s}^{-1}$ . These are among the most common explosions in the Milky Way, although the number of detections (largely from wide-field optical surveys) is limited by available monitoring and dust obscuration. While classical novae (CNe) are common, and broadly understood, further studies of CNe can help probe binary interactions, chemical enrichment, shocks, and high-energy acceleration (Chomiuk et al. 2021a).

The traditional view of radio emission from CNe (Sequist & Palimaka 1977; Hjellming et al. 1979; and see Chomiuk et al. 2021b for a recent synthesis of radio emission properties) is where an expanding sphere of ionised gas emits via free-free radiation, with the temporal/spectral evolution depending on the expansion of the gas and the changes in the emission measure and self-absorption that result. Even in this simple model, measurements of the free-free emission can help constrain the distances to CNe, the masses of ejected material, and their energetics (Bode et al. 1987; Gulati et al. 2023).

As more observations accumulated, the picture grew more complex. Suggestions that the brightness temperature required

non-thermal emission (Snijders et al. 1987; Taylor et al. 1987; Krauss et al. 2011; Weston et al. 2016a,b) emerged as radio observations sampled more CNe at earlier times. This emission — presumably synchrotron emission from shocks between the ejecta and surrounding material — may tie to the GeV  $\gamma$ -ray emission (Ackermann et al. 2014) that may have other signatures across the electromagnetic spectrum (Chomiuk et al. 2021a). Even the thermal emission itself may be more complex, with evidence for multiple, aspherical components (Chomiuk et al. 2014) or prolonged/delayed ejection (Nelson et al. 2014), which can best be probed through detailed radio followup of a wide range of CNe.

Finally, while the vast majority of novae discovered come from optical surveys, these will miss many sources that are obscured by dust in the Milky Way (Chomiuk et al. 2021a). The advent of near-infrared (Lucas et al. 2020) surveys offers a new opportunity to discover obscured novae deep in the Galactic plane. Even more than that, radio surveys with sufficient sampling can identify new nova candidates on their own, probing a different aspect of the eruption process (tied more to ejecta mass and velocity than bolometric luminosity).

### 3.7. X-ray binaries

Low-mass X-ray binaries, where neutron stars or black holes accrete from stellar-mass companions, are highly variable sources seen across the electromagnetic spectrum (Fender & Gallo 2014; van den Eijnden et al. 2021; Fender 2006). The jets produced by these systems inject energy into the surrounding medium (Gallo et al. 2005), regulating star formation and ionising the surrounding gas (Fender et al. 2005), and can be used to study the formation of jets and accretion across many orders of magnitude in accretor mass (from stellar-mass systems to supermassive black holes; Gallo et al. 2003, 2014; van den Eijnden et al. 2021), giving insight into the fundamental mechanisms of jet launching (McClintock et al. 2014) and synchrotron-emitting regions (e.g. Chauhan et al. 2021). Detailed imaging of the radio jets can also show direct evidence for relativistic jet launching and superluminal motion (Mirabel & Rodríguez 1994; Fender et al. 2004b).

Radio emission from X-ray binaries depends on the jet type, which can change over time. Discrete blobs of ejected material have steeper radio spectra ( $\alpha \approx -0.7$ ), emitting as they move away from the compact object. In contrast, steady jets have much flatter spectra coming from a superposition of regions at different radii dominating at different frequencies.

Observing such systems over time and across wavelengths, there is evidence for correlation between the radio and X-ray luminosities that extends across many orders of magnitude in mass (Merloni et al. 2003; Migliari & Fender 2006; Gallo et al. 2003) when the X-ray emission is in the ‘hard’ state, but which may also break into multiple tracks with different levels of radio emission (Soleri & Fender 2011) whose origin and significance are not understood (Gallo et al. 2018). However, when the X-ray emission is in other spectral states (‘intermediate’ or ‘soft’; Belloni 2010) this correlation disappears as steady jet emission stops and discrete blobs may be ejected (Fender et al. 2004a). The transitions between these states likely represent disc instabilities changing the rate at which material moves from the disc onto the compact object (Coriat et al. 2012). Such transitions can give rise to transient radio jets, either going from the ‘soft’ X-ray state to the ‘hard’ or the other way, when newly-launched jets can impact the material from previous ejection cycles (Koljonen et al. 2013).

**Table 1.** Key characteristics of radio emission from different stellar types. For each type we give a couple of key example objects, and the associated references. The types are roughly ordered in decreasing temperature, following the subsections in the main text.

Stellar type	Emission mechanisms	Key features	Example sources	Citations
Main seq. O & B	(i) Thermal free-free emission from ionized stellar winds	Low variability; unpolarised; $\alpha + 0.6$	$\zeta$ Pup, P Cyg	<a href="#">1, 2, 3</a>
	(ii) Non-thermal synchrotron emission in binaries	Variable; $\alpha \leq 0.0$		
Wolf-Rayet Stars	(i) Thermal free-free emission from ionized stellar winds	Strong, some of the most luminous radio stars; low variability	WR140, WR147	<a href="#">4, 5, 6</a>
	(ii) Non-thermal synchrotron emission in binaries	Variable in flux and spectral index; can be aligned with orbital phase		
Main seq. A & early-F	(i) Thermal free-free emission from the chromosphere	Weak, rarely detected; quiescent emission	Sirius A, Procyon	<a href="#">7, 8</a>
	(ii) Thermal free-free emission from the corona	Low variability; weak flares or bursts		
Magnetic chemically peculiar (Ap & Bp)	(i) Gyrosynchrotron radiation from the interaction between stellar wind and magnetosphere	Quiescent; sometimes variable with rotation period; moderately to highly polarised	CU Vir, $\sigma$ Ori E	<a href="#">9, 10, 11</a>
	(ii) Coherent auroral emission (ECMI)	Variable and periodic; moderately to highly polarised		
Main seq. late-F, G & K	(i) Thermal free-free emission from the corona	Low variability; weak; unpolarised	$\alpha$ Centauri, AB Dor	<a href="#">12, 13, 14</a>
	(ii) Gyrosynchrotron (and thermal) radiation from stellar flares	Variable; can be periodic; can be polarised		
	(iii) Coherent bursts	Variable; highly polarised		
RS CVn and Algol binaries	(i) Gyrosynchrotron radiation (quiescent and flaring)	Both quiescent and variable	HR 1099, $\beta$ Persei	<a href="#">15, 16, 17</a>
	(ii) Electron cyclotron maser emission	Short strong bursts; highly polarised		
M dwarfs & ultracool dwarfs	(i) Electron cyclotron maser emission and coherent auroral emission	Strong, highly polarised, highly variable, can be periodic	Proxima Cen; LP944-20; WISE J062309-045624	<a href="#">18, 19, 20</a>
	(ii) Gyrosynchrotron radiation (quiescent and flaring)			

Citations: 1 — Wendker et al. (1973); 2 — Morton & Wright (1978); 3 — Bieging et al. (1989); 4 — Dougherty et al. (2005); 5 — Churchwell et al. (1992); 6 — Abbott et al. (1986); 7 — White et al. (2019); 8 — (Drake et al. 1993) 9 — Leto et al. (2006); 10 — Leone & Umana (1993); 11 — Drake et al. (1987); 12 — Gudel (1992) 13 — Trigilio et al. (2018) 14 — Lim et al. (1992) 15 — Feldman et al. (1978); 16 — Mutel et al. (1998); 17 — Drake et al. (1989); 18 — Zic et al. (2020); 19 — Berger et al. (2001a); 20 — Rose et al. (2023);

Historically, most radio observations of X-ray binaries have been triggered by state transitions observed at X-ray wavelengths (e.g. Plotkin et al. 2017; Russell et al. 2014), where the prevalence of all-sky X-ray monitors (e.g. Barthelmy et al. 2005; Matsuoka et al. 2009) allows for easy identification of sources requiring follow-up (although see e.g. Miller-Jones et al. 2004). However, this leads to time-lags between when X-ray behaviour occurs and radio monitoring commences, and may overlook radio variability that is less tied to X-ray state changes (e.g. Wilms et al. 2007). Moreover, X-ray sources can be subject to significant absorption by intervening Galactic material. Therefore future radio monitoring of the Galactic plane can be used to identify transient/variable X-ray binary sources across a much wider range of radio luminosity, potentially independent of high-energy behaviour, to help understand if the standard paradigm actually holds in all cases (e.g. Corbel et al. 2015).

### 3.8. Pulsars and magnetars

Rotation-powered pulsars (spinning, highly-magnetised neutron stars; Lorimer & Kramer 2012) and magnetars (neutron stars powered by decay of ultra-strong magnetic fields; Kaspi & Beloborodov 2017) are most commonly identified by single-dish

radio surveys and X-ray surveys, respectively. They are of broad astrophysical interest as probes of matter at extreme densities (e.g. Demorest et al. 2010; Miller et al. 2021) and magnetic fields (Kaspi & Beloborodov 2017; Philippov & Kramer 2022), as well as related topics like how supernova asymmetries lead to high kick velocities (e.g. Cordes et al. 1993), searches for planets (Wolszczan & Frail 1992), and tests of gravity (e.g. Archibald et al. 2018); networks of pulsars can also be used to search for low-frequency gravitational waves (Agazie et al. 2023a; Reardon et al. 2023; EPTA Collaboration et al. 2023; Xu et al. 2023; Miles et al. 2025).

Intrinsically, individual pulses from pulsars are highly variable (magnetospheric ‘weather’, in the language of Philippov & Kramer 2022), but they tend to add together to form highly-stable averages (magnetospheric ‘climate’; Philippov & Kramer 2022; also see Lorimer & Kramer 2012) with stable flux densities (Kumamoto et al. 2021). Hence, there must be some specific reason for pulsars to appear variable, and be detectable in image domain transient surveys; these mechanisms are discussed in Section 2.4.

Many cases of variability are due to extrinsic effects, such as diffractive or refractive scintillation (Section 2.5.1) or interactions in tight binary systems. The former results from the fact

that neutron stars are extremely compact and hence are among the very few sources to show diffractive scintillation. The latter can be either periodic, with eclipses and modulations during the orbits of so-called ‘spider’ pulsars (pulsars with low-mass non-degenerate companions in tight orbits; Roberts 2013), or secular, with radio variability and optical state changes caused by the transition from an accretion-powered low-mass X-ray binary phase to a rotation-powered millisecond pulsar (Archibald et al. 2009). Both of these can cause pulsars to appear and disappear (e.g. Bond et al. 2002; Zic et al. 2024) during imaging observations, depending on the timescale of those observations compared to the orbital period and eclipse duration (for spiders) or state changes. In all cases these effects can be exploited to discover new pulsars (Backer et al. 1982; Dai et al. 2016, 2017), while scintillation itself can help understand the properties of the turbulent interstellar medium (e.g. Kumamoto et al. 2021), the pulsar velocity distribution (e.g. Cordes & Rickett 1998), and the origin of extreme scattering events (Zhu et al. 2023).

However, some types of pulsars also show intrinsic variability. In some cases, the time between seeing individual pulses is sufficiently long compared to the observation duration that normal pulse-to-pulse variations show up as significant variability between images. This can occur when the rotation period is very long (say  $\gtrsim 10$  min; e.g. Hurley-Walker et al. 2022b, 2023) although it is not yet clear if these objects are indeed neutron stars (see Section 3.9) or when the neutron stars do not emit a pulse every rotation period, as with rotating radio transients (RRATs; McLaughlin et al. 2006), where pulses are only detected once per hundreds or thousands of rotation periods. In fact, the RRAT phenomenon appears to be at least partly based on observational limitations, where the sources likely form a continuum of behaviour between pulsars that emit every pulse; pulsars that show short-term nulling behaviour (Backer 1970); intermittent pulsars (Kramer et al. 2006); and those that only emit sporadically (Keane & McLaughlin 2011; Keane et al. 2011). Broadly, this is likely to be related to the dynamics of the pulsar magnetosphere as pulsar emission weakens and then (in most cases) ceases, moving toward the so-called ‘death line’ (Philippov & Kramer 2022).

Finally, larger-scale magnetospheric changes can also lead to changes in the radio properties of magnetars (Kaspi & Beloborodov 2017), which are powered not by rotation like most pulsars but by an overall magnetic energy store. Most magnetars do not emit radio pulses, but following outbursts there can be radio emission lasting months (Camilo et al. 2006) to years (Liu et al. 2021), although emission can also turn on absent any high-energy transient (Levin et al. 2010, 2019; Dai et al. 2019). While in some ways this emission is pulsar-like, the spectral and polarisation properties can differ from those of most pulsars, with flatter spectra (Camilo et al. 2006; Torne et al. 2015) and higher polarisation fractions (Camilo et al. 2007; Philippov & Kramer 2022).

As with the extrinsic effects, these intrinsic variations can be used to identify new pulsars through imaging surveys (Wang et al. 2022b; McSweeney et al. 2025b) or new activations of known sources (e.g. Driessen et al. 2023), as well as gather robust statistics of nulling and intermittency.

Beyond these phenomena, which relate to the pulsed emission from the neutron star, there are several related phenomena that likely tie to the birth and energetics of pulsars. We discuss these below.

### 3.8.1. Nascent pulsar/magnetar wind nebulae

When a supernova leaves behind a compact object, the luminosity of this object (both particle and electromagnetic) can power a new pulsar wind nebula (PWN; Gaensler & Slane 2006; Olmi & Bucciantini 2023) or magnetar wind nebula, depending on the nature of the compact object. This represents a transition from the supernova stage to a supernova remnant, a phase that may span a decade or so and is poorly probed observationally (e.g. Milisavljevic et al. 2018; Milisavljevic & Fesen 2017) but can help constrain the population of newly formed compact objects and tie them to the properties of their parent supernovae (e.g. Metzger et al. 2015a; Fransson et al. 2024). This is especially relevant for sub-classes of supernovae (including Type Ic-BL and superluminous supernovae) that may be powered by ongoing emission from a central engine, often thought to be a magnetar (Thompson et al. 2004; Kasen & Bildsten 2010; Dessart 2024).

So far, direct radio searches for transitional sources have been mixed. Broad and targeted radio surveys of supernovae (e.g. Law et al. 2019; Eftekhari et al. 2019) have only yielded a few detections of new wind nebula candidates. Results from untargeted radio surveys have also only discovered a small number of sources (Dong & Hallinan 2023; Marcote et al. 2019), and the interpretation of these discoveries is often unclear (Mooley et al. 2022) since the nature of the synchrotron emission is degenerate between many classes. Nonetheless, continued deep radio observations of large samples of supernovae from diverse classes, whether done as targeted searches or just parts of broad surveys, will help to further resolve this question and establish links between different supernova types and potential central engines.

### 3.8.2. Fast radio burst persistent radio sources

While we are not in general discussing FRBs in this review, we will briefly discuss the related phenomenon of ‘persistent radio sources’ (PRSs). First identified following the first FRB localisation (Chatterjee et al. 2017), PRSs are long-lived compact ( $\sim$ mas; Marcote et al. 2017; Bhandari et al. 2023) non-thermal radio sources that are co-located with (so far) repeating FRBs (Chatterjee et al. 2017; Marcote et al. 2017; Niu et al. 2022; Bruni et al. 2024b,a). They are spatially offset from the nuclei of their host galaxies and have properties inconsistent with star-formation such as very high degrees of magnetisation (Michilli et al. 2018; Niu et al. 2022) that appears to be tied to their luminosities (Yang et al. 2020). This suggests a common origin with FRBs and perhaps an interpretation as a magnetar-powered nebula (Margalit & Metzger 2018), although other models are possible (e.g. Zhang 2020a; Sridhar & Metzger 2022, Ibik et al. 2024 and references therein). If confirmed, this interpretation would allow persistent radio sources to be used as FRB calorimeters and place constraints on the origin and evolution of FRBs and their progenitors.

Note that, while called ‘persistent’, PRSs do in fact have significant changes in both their Faraday rotation measure (Michilli et al. 2018; Niu et al. 2022) and in their flux densities (Rhodes et al. 2023; Zhang et al. 2023), likely from intrinsic causes. This then open an avenue for discovery of new PRSs: searching for compact, non-thermal, potentially variable radio sources either associated with known FRBs (Ibik et al. 2024; Eftekhari et al. 2018) or not (Ofek 2017; Dong & Hallinan 2023). Such searches can help constrain the rate and lifetimes of repeating FRBs and PRSs, although care must be taken to not be confused by galactic nuclei, chance alignments, or thermal radio emission (e.g. Ravi et al. 2022a; Dong et al. 2024).

### 3.9. Long period transients and Galactic Centre Radio Transients

Imaging surveys with the latest generation of radio telescopes have begun to discover apparently periodic radio sources that lie at or well beyond the traditional pulsar ‘death line’ where radio emission is expected to stop (Figure 6). Called long-period transients (LPTs), their periods range from minutes (Hurley-Walker et al. 2022b, 2023; Caleb et al. 2024; Dong et al. 2025b; Wang et al. 2025c) to hours (Hurley-Walker et al. 2024; Lee et al. 2025). We summarise the properties of the currently known LPTs in Table 2.

LPTs emit very bright, highly polarised radio pulses that last for several minutes (exhibiting peak flux densities of up to tens of Jy), with polarisation position-angle swings like those observed in pulsars or FRBs (McKinven et al. 2025), but on timescales hundreds of times longer (Dobie et al. 2024; Men et al. 2025). By using sub-structure within the pulse, we can determine a dispersion measure (DM) and infer the distance using a Galactic model (Cordes & Lazio 2002; Yao et al. 2017); most LPTs appear to be at several kpc and largely within the plane of the Galaxy (which may be an observational bias). Some sources are only radio-loud for a few weeks to months, while others remain radio-loud for decades (Hurley-Walker et al. 2023). Many show a range of different emission ‘modes’ reminiscent of pulsar behaviour (Caleb et al. 2024), while others show ‘interpulses’, again much like pulsars (Lee et al. 2025). Even among those that do not show discrete modes, there is extremely large variability in the intensity and morphology of individual pulses (Lee et al. 2025). However, unlike other populations of very intermittent radio sources (McLaughlin et al. 2006; Surnis et al. 2023; Anna-Thomas et al. 2024), LPT energetics computed from spin-down limits suggest that these sources *cannot* be rotation-powered neutron stars (Hurley-Walker et al. 2022b; Wang et al. 2025c), unlike some of the long-period radio pulsars also discovered recently (e.g. Wang et al. 2025d).

These sources were discovered only once it became possible to explore widefield radio surveys with short-timescale imaging (sometimes called ‘fast imaging’). Prior to that, objects with periods of this length were largely overlooked by both pulsar surveys (often only sensitive to signals with periods  $< 10$  s, although there are some exceptions often related to detection of individual pulses rather than periodicity, such as Caleb et al. 2022) and radio transient imaging surveys. They are therefore filling in an under-populated area in the transient phase space (Figure 1). Short-timescale imaging approaches are discussed more in Section 5.4.

The initial discoveries lacked any detections at optical/IR or X-ray wavelengths, despite some extensive searching (e.g. Rea et al. 2022; Lee et al. 2025), although given their locations in the Galactic plane with significant extinction/absorption, not all of the upper limits were equally constraining. We also note that many of those searches were not contemporaneous with periods when the radio source was active, raising questions about variability. Nonetheless, recent discoveries have uncovered sources with a wider range of multi-wavelength properties that include binary systems containing a white dwarf and late-type star (Hurley-Walker et al. 2024; Rodriguez 2025; de Ruiter et al. 2025) where it is clear that the radio periodicity is tied to the orbit, instead of the spin. These sources were discovered as radio transients like the other LPTs, but may represent a different underlying population (see below). Even more intriguing is ASKAP J1832–0911, which was serendipitously detected in soft X-rays by *Chandra* (Wang et al. 2025c). The X-ray luminosity exceeds the radio luminosity

by a factor of  $\sim 10$ , making the standard pulsar energetic argument even more challenging, and the X-ray flux is seen to pulse on the radio period and then vary secularly together with the radio flux. This likely points to a shared magnetospheric origin (not accretion or intra-binary shocks), but detailed models are still lacking.

The characteristics of LPTs were immediately reminiscent of the so-called Galactic Centre Radio Transients (GCRTs) that had been discovered two decades earlier (Hyman et al. 2002, 2005; also see Davies et al. 1976; Zhao et al. 1992). The most well known of these is GCRT J1745–3009, the so-called ‘cosmic burper,’ which showed bursts of up to 1 Jy every 77 min, but then long spans in which it was undetectable. Long-term follow-up (e.g. Hyman et al. 2006, 2007; Roy et al. 2010) showed intermittent behaviour (which contributes to the difficulty of monitoring these sources) and different burst properties (flux density, spectral index, burst duration and periodicity). Additional GCRT sources have been discovered (Wang et al. 2021b, 2022a) recently, although it is unclear if they resemble the periodic emission of GCRT J1745–3009, and if their location near the Galactic centre is a selection effect.

LPTs also share some radio properties with radio pulsating white dwarf binary systems (that consist of a white dwarf star with an M-dwarf companion)<sup>h</sup>. There have been potentially six such systems detected to date: AR Sco, with a radio period of  $\sim 1.95$  min in a 3.5 h orbit (Marsh et al. 2016); J1912–4410, with a radio period of  $\sim 5.3$  min in a 4 h orbit (Pelisoli et al. 2023); ILT J1101+5521, with a much longer period of 2.1 h, matching the orbital period (de Ruiter et al. 2024); GLEAM-X J0704–37, with a period of 2.9 h (again matching the orbit; Hurley-Walker et al. 2024; Rodriguez 2025); SDSS J230641.47+244055.8 with pulsations at the 92 s WD spin period and a 3.5 h orbit (Castro Segura et al. 2025); and CHIME/ILT J163430+445010, with a 14 min radio period and a 0.6 or 1.2 h orbital period (Dong et al. 2025a; Bloot et al. 2025).

We summarise the properties of all the sources that fit into this broad category in Table 2<sup>i</sup>. It is highly likely there are multiple underlying source classes that produce the observed behaviour of long period transients: the two most promising being neutron stars and highly magnetised white dwarfs (either isolated or in binaries) (Rea et al. 2024; Qu & Zhang 2025). In this table we have roughly categorised them based on how the authors report them in the discovery papers and subsequent papers. There are further sources that have been recently discovered but not yet fully characterised, and which might align with any or none of these classes.

While the field is rapidly moving, at the time of writing the origin(s) of LPTs is unclear. LPTs may be old magnetars whose radio emission would ordinarily be expected to have ceased (Hurley-Walker et al. 2022b; Rea et al. 2022; Zhou et al. 2024), which were spun down to long periods through an initial ‘propeller’ accretion phase (Ronchi et al. 2022; Fan et al. 2024; also see Ho & Andersson 2017); this would explain the long periods and energetic emission. Fully explaining the radio emission and evolution are still a challenge (Cooper & Wadiasingh 2024; Suvorov & Melatos 2023), but work is ongoing.

However, other models such as isolated or binary (like some of the sources discussed above) white dwarf (WD) pulsars, or even other binaries, are all possible (Zhang & Gil 2005; Katz 2022;

<sup>h</sup>Although these are sometimes referred to in the literature as ‘white dwarf pulsars’, we find this terminology confusing as (a) it mixed both physical and phenomenological information, and (b) ‘pulsar’ is a well established term for neutron stars, which are not present in these systems.

<sup>i</sup>See <https://vast-survey.org/LPTs/> for an up-to-date version.

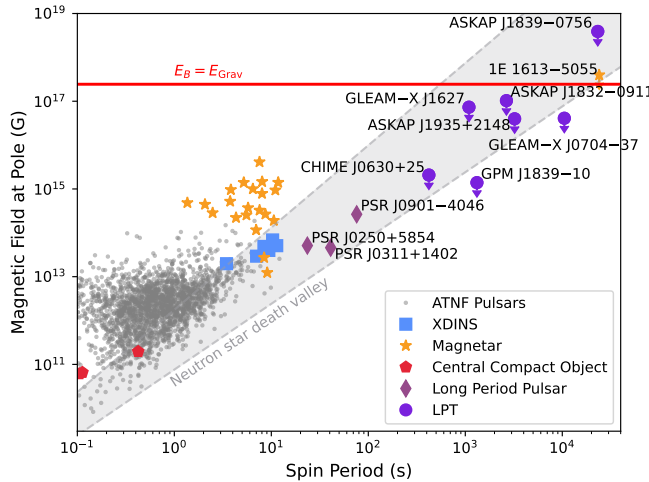


**Figure 6.** Pulse period versus polar magnetic field ( $6.4 \times 10^{19} \text{ G}\sqrt{P\dot{P}}$ ) diagram for pulsars, magnetars, LPTs, and related sources, following Rea et al. (2024). We show radio pulsars as well as magnetars (stars), X-ray dim isolated neutron stars (XDINS; squares), central compact objects (CCOs, also some times referred to as ‘anti-magnetars’; pentagons) and select long-period radio pulsars (diamonds) from Manchester et al. (2005, version 2.6.0). We also plot LPTs (large circles; Wang et al. 2025c; Lee et al. 2025; Wang et al. 2021b; Caleb et al. 2024; Hurley-Walker et al. 2024, 2023, 2022b; Dong et al. 2025b; Hurley-Walker et al. 2024), the radio pulsar J0311+1402 (Wang et al. 2025d), and the long-period magnetar 1E 1613-5055 (Esposito et al. 2011). In those cases we are assuming that the measured period is the spin period, and that the moment of inertia is that of a neutron star. We plot a range of possible ‘death lines’ for purely-dipolar (top) and highly-twisted (bottom) magnetospheres, based on Rea et al. (2024), which delineate a ‘death valley’ in which radio emission is expected to cease. Finally, we show the limit where the total magnetic energy is roughly the gravitational binding energy (solid red line).

Loeb & Maoz 2022; Rea et al. 2024; Tong 2023; Qu & Zhang 2025; Xiao & Shen 2024; Mao et al. 2025; Zhou et al. 2025), and may be relevant for a part of the population. For instance, Rodriguez (2025) suggest that the longer period sources ( $\gtrsim 1.2$  hr) are different classes, with the short period sources related to white dwarf or neutron star spins and the longer period sources related to (in at least some cases) orbits in cataclysmic variables, potentially magnetised systems like polars: disentangling orbital versus spin properties remains a challenge, especially in the absence of optical counterparts, but one that could also be solved by space-based gravitational wave observations (e.g. Suvorov et al. 2025). Recent long-term timing observations show that even among the ‘classical’ LPTs in Table 2 there may be connections to binary systems, may place a larger number of similar sources on a continuum of magnetic WD binaries, although evolutionary challenges still remain (Castro Segura et al. 2025).

Regardless of the specific model, both observationally and theoretically it appears that there is a significant underlying population of similar sources (Rea et al. 2024; Beniamini et al. 2023) which are only now being discovered. Hopefully through continued identification of new sources and longer-term studies of known ones (e.g. radio timing to determine the spin-down rate) the origin of these sources can be elucidated.

### 3.10. Unknown classes

Serendipity (the fact of finding interesting or valuable things by chance<sup>j</sup>) is a driving force in discovery-driven science. The importance of serendipity in astronomy has been discussed by many people, for example Harwit (1981) and Fabian (2009). One of the most well known examples of serendipity in time-domain astronomy is the discovery of gamma-ray bursts using data from the Vela nuclear test monitoring satellites (this history is summarised by Bonnell & Klebesadel 1996).

There have been many serendipitous discoveries in radio astronomy, as discussed in the proceedings of an 1983 workshop “*Serendipitous Discoveries in Radio Astronomy*” held at NRAO<sup>k</sup>. Serendipity was built into the science case for the Square Kilometre Array (Schilizzi et al. 2024) and has been considered in the design of widefield transients surveys on SKAO pathfinder and precursor instruments.

When new transient candidates are discovered in radio imaging surveys, there is usually an extensive process of identification. This typically involves using other radio data, archival multi-wavelength data, and conducting new follow-up observations in radio and other wavebands. See Ofek et al. (2010) and Wang et al. (2021b) for examples of this kind of analysis. It is often straightforward to identify the object as an already-catalogued object based on the available information. However, sometimes the source of the variable radio emission can not be identified.

In early surveys this was often due to poor time sampling in radio, a lack of multi-wavelength information, and the archival nature of the searches meaning that the transient was discovered long after the event occurred. An example of a well-investigated radio transient that remains unidentified is the one reported by Stewart et al. (2016). It is likely that this object will remain unidentified, but the improved specifications and availability of rapid multi-wavelength follow-up in current and future surveys will make the discovery of new classes of radio transients more likely. The most recent example of this is the emergence of a new class of long-period transients, as discussed in Section 3.9.

## 4. Radio transient surveys

In this section we outline the motivation for radio transient surveys (in contrast to triggered observations or targeted monitoring). We discuss the parameters of an ideal radio transient survey, and then give a brief history of how such surveys have evolved from the early days of radio astronomy to the present day.

### 4.1. Motivation for radio transient surveys

There are a relatively small number of classes of astronomical objects that have been discovered and detected primarily at radio frequencies. Some key examples are pulsars (e.g. Hewish et al. 1968), fast radio bursts (e.g. Lorimer et al. 2007), Galactic Centre radio transients (e.g. Hyman et al. 2005) and the newly emerging class of long period transients (e.g. Hurley-Walker et al. 2022b). We also observe radio variability caused by diffractive and refractive scintillation, that can either be observed as long-term stochastic behaviour in the case of scintillating quasars (e.g. Dent

<sup>j</sup>Definition from the Cambridge Dictionary <https://dictionary.cambridge.org/dictionary/>

<sup>k</sup>The full PDF is available online: <https://library.nrao.edu/public/collection/0200000000280.pdf>

**Table 2.** Properties of long period transients and related Galactic sources. The sources are broadly grouped according to how they are reported in the literature. We have only included published objects here, but we know of a number of new discoveries currently in preparation.

Source	Period	Duty	DM	<i>b</i>	Polarisation		Steep	Optical	X-ray	Comment	Citation
					Cycle	(pc/cm <sup>3</sup> )	Linear	Circular	Spectrum		
<b>GCRTs: .....</b>											
GCRT J1745–3009	77 min	13%	–	0.5°	No	Yes	Yes	No	No	“cosmic burper”	<a href="#">1, 2, 3, 4</a>
GCRT J1746–2757	–	–	–	0.4°	?	?	?	No	No		<a href="#">5</a>
GCRT J1742–3001	–	–	–	0.1°	?	?	Yes	No	No		<a href="#">6</a>
ASKAP J173608.2–321635	–	–	–	0.0°	Yes	Yes	Yes	No	No		<a href="#">7</a>
<b>Unclassified LPTs: .....</b>											
CHIME J0630+25	7 min	0.6%	23.0	7°	?	?	Yes	No	No	Glitch	<a href="#">8</a>
GLEAM-X J162759.5–423504.3	18 min	4%	57.0	3°	Yes	No	Yes	No	No		<a href="#">9, 10</a>
GPM J1839–10	21 min	10%	274.0	2°	Yes	No	Yes	No	No	$P_b = 8.8$ h	<a href="#">11</a>
ASKAP J1832–0911	44 min	6%	458.0	0.1°	Yes	Yes	Yes	No	Pulsed		<a href="#">12</a>
ASKAP J1935+2148	54 min	< 1%	146.0	0.7°	Yes	Yes	Yes	No	No	Mode switching	<a href="#">13</a>
ASKAP J175534.9–252749.1	70 min	2%	710.0	0.1°	Yes	Yes	Yes	No	No		<a href="#">14, 15</a>
ASKAP J1839–0756	6.5 h	2%	188.0	1°	Yes	Yes	Yes	No	No	Interpulse	<a href="#">16</a>
<b>Magnetic WD Binaries: .....</b>											
SDSS J230641.47+244055.8	1.5 min	?	–	32°	?	?	?	WD+M4	No	$P_b = 3.5$ h	<a href="#">17</a>
AR Sco	2 min	50%	–	19°	Weak	Yes	No	WD+M5	Pulsed	$P_b = 3.6$ h	<a href="#">18, 19</a>
J191213.72–441045.1	5 min	< 1%	–	22°	?	?	?	WD+M4.5	Pulsed	$P_b = 4.0$ h	<a href="#">20</a>
CHIME/ILT J163430+445010	14 min	1.2%	25.0	42°	Yes	Yes	?	WD+?	No	$P_b = 1.2$ h or 0.6 h; Spin-up	<a href="#">21, 22</a>
ASKAP J1448–6856	1.5 h	25%	–	8°	Yes	Yes	Yes	Hot	Yes		<a href="#">23</a>
ILT J1101+5521	2.1 h	2%	–	55°	Yes	No	Yes	WD+M4.5	No	$P_b = 2.1$ h	<a href="#">24</a>
GLEAM-X J0704–37	2.9 h	0.004%	36.0	13°	Yes	Yes	Yes	(WD?)+M3	No	Most likely interpretation	<a href="#">25, 26</a>
<b>Long-period Pulsars: .....</b>											
PSR J0311+1402	41 s	1%	19.9	37°	Weak	Weak	Yes	No	?	Neutron star	<a href="#">27</a>
PSR J0901–4046	1 min	1%	52.0	4°	Yes	Yes	Yes	No	No	Neutron star	<a href="#">28</a>

Periods given are the primary radio periods, but these may be a mix of rotation and orbital periods or even beat frequencies, depending on the source; where both orbital and rotation periods are known they are given separately. Many sources show multiple modes with differing pulse widths and polarisation properties, and are highly variable. Properties given as “?” could not be determined from the available information. An up-to-date version of this table is available at <https://vast-survey.org/LPTs>. Also see Dong et al. (2025b) and <https://lpt.mwa-image-plane.cloud.edu.au/published/tables/1> for related samples.

Citations: 1 — Hyman et al. (2005); 2 — Hyman et al. (2007); 3 — Roy et al. (2010); 4 — Kaplan et al. (2008); 5 — Hyman et al. (2002); 6 — Hyman et al. (2009); 7 — Wang et al. (2021b); 8 — Dong et al. (2025b); 9 — Hurley-Walker et al. (2022b); 10 — Rea et al. (2022); 11 — Hurley-Walker et al. (2023); 12 — Wang et al. (2025c); 13 — Caleb et al. (2024); 14 — Dobie et al. (2024); 15 — McSweeney et al. (2025a); 16 — Lee et al. (2025); 17 — Castro Segura et al. (2025); 18 — Marsh et al. (2016); 19 — Stanway et al. (2018); 20 — Pelisoli et al. (2023); 21 — Bloot et al. (2025); 22 — Dong et al. (2025a); 23 — Anumarlapudi et al. (2025); 24 — de Ruiter et al. (2025); 25 — Hurley-Walker et al. (2024); 26 — Rodriguez (2025); 27 — Wang et al. (2025d); 28 — Caleb et al. (2022).

1965), or discrete occurrences such as extreme scattering events (e.g. Fiedler et al. 1987).

Much of what we have learned about other transient and variable radio phenomena has come from monitoring individual objects with targeted observations, often triggered by a discovery event detected in other wavebands. This is the case for explosive phenomena including long gamma-ray bursts (e.g. Frail et al. 1997) short gamma-ray bursts (e.g. Berger et al. 2005), core-collapse radio supernovae (e.g. Gottesman et al. 1972) and recently, Type Ia supernovae (e.g. Kool et al. 2023).

For many classes of persistent radio variables, objects of interest have been selected for radio monitoring based on their variability at other wavebands. This is largely the case for radio stars (e.g. Lovell et al. 1963), X-ray binary systems (Andrew &

Purton 1968) and blazars (Hufnagel & Bregman 1992). This targeted radio follow-up and monitoring has led to significant physical insights into these source classes (see Section 3), but remains limited by the selection effects present at other wavebands. Hence there are still gaps in our understanding of the phenomena themselves and also the overall populations as observed in the radio band.

Perhaps the best case study to demonstrate both the value of targeted follow-up and the need for untargeted surveys is radio follow-up of gamma-ray burst afterglows. As discussed in Section 3.1, our knowledge of the radio properties of these objects (and the subsequent insights in their physical properties) comes from radio follow-up campaigns of individual objects, initially detected at higher energies.

However, there are still some unanswered questions to address, for which untargeted surveys are needed. For example, as mentioned in Section 3.1 gamma-ray telescopes can not detect GRBs for which the jets are beamed away from our line of sight (Rhoads 1997). In principle, widefield radio surveys allow us to detect such ‘orphan afterglows’ and hence constrain the beaming fraction of GRBs — a key quantity for understanding the true GRB event rate (Perna & Loeb 1998). They will also result in a significant increase in the number of radio afterglows detected, unbiased by selection criteria at other wavebands. These factors were key motivators in some of the early searches for radio transients in untargeted widefield surveys (e.g. Levinson et al. 2002; Gal-Yam et al. 2006) which we will discuss further in Section 4.3.

## 4.2. Ideal survey design

The exploration of the unknown was a critical driver from the beginning of the SKAO project (see the discussion in Schilizzi et al. 2024, which gives a detailed account of the history of the SKAO). Time domain science has always been one of the key science areas, and as the SKAO project progressed, discussions of what an ideal time domain imaging survey would look like were initiated.

### 4.2.1. A figure of merit for transient surveys

In this context, Cordes et al. (2004) proposed a figure of merit for transient detection surveys:

$$\text{FOM}_{\text{CLM}} \equiv A\Omega_{\text{epoch}} \left( \frac{T}{\Delta T} \right) \quad (4)$$

that should be maximised for a given survey (subject to various constraints regarding actual telescope designs etc.). In this figure of merit,  $A$  is the collecting area of the telescope,  $\Omega_{\text{epoch}}$  is the solid angle coverage in a single epoch (not an instantaneous field-of-view like the usage in a classical étendue),  $T$  is the total duration of the observation, and  $\Delta T$  is the time resolution. For continuum imaging surveys, the trade-off has typically been between sensitivity and area, spending a finite total time either on a smaller number of deeper pointings or a larger number of shallow ones (e.g. the LOFAR Two-metre Sky Survey (LoTSS) covering 20,000 deg<sup>2</sup> with a rms of 2000  $\mu\text{Jy beam}^{-1}$  vs. LoTSS Deep covering 30 deg<sup>2</sup> at 10  $\mu\text{Jy beam}^{-1}$  rms; Shimwell et al. 2017; Best et al. 2023).

For the figure of merit in Equation 4, increasing the collecting area,  $A$ , increases the instantaneous sensitivity of the observations, which means a fainter source population can be probed. Increasing the solid angle coverage,  $\Omega_{\text{epoch}}$ , means the sky can be covered more efficiently, increasing the survey speed. Increasing the total duration of the observation,  $T$ , increases the sensitivity to phenomena on the timescale of the observations, and increasing the time resolution,  $\Delta T$ , broadens the range of timescales that can be explored by the survey.

However, there are limitations to the metric in Equation 4, especially when comparing surveys with very different telescopes at very different frequencies over very different timescales.

Firstly,  $A$  is not an ideal way to fully parameterise the sensitivity of a telescope. Better would be  $A/T_{\text{sys}}$  (where  $T_{\text{sys}}$  is the system temperature, including both the receiver temperature and the sky temperature, and  $A$  could also include the antenna efficiency  $\eta_A$  to define the effective area  $A_{\text{eff}} \equiv \eta_A A$ ). Alternately, especially when considering surveys done at a range of timescales, more appropriate might be the delivered RMS noise  $\sigma$ , which

can include contributions from the system-equivalent flux density (related to  $A/T_{\text{sys}}$ ; e.g. Crane & Napier 1989; Wrobel & Walker 1999; Lorimer & Kramer 2012) but also things like confusion noise, and which will depend on the angular resolution and the timescale probed ( $\sigma(\Delta T) \propto \Delta T^{-1/2}$  typically, if not dominated by confusion). This can be further modified to account for varying sensitivity as a function of observing frequency. Since most of the sources considered here have non-thermal spectra (the overall population will have a median spectral index of  $\alpha \approx -0.7$  or lower) we will use  $\sigma(v/v_0)^{-\alpha}$  comparing to some reference frequency  $v_0$  (this is also done elsewhere, as in Best et al. 2023). And unlike  $A$  or  $A/T_{\text{eff}}$ , which we seek to maximise, smaller values of  $\sigma$  are better.

Secondly, the survey area is hard to compare between telescopes that have very different angular resolutions. For example, some low-frequency dipole arrays (e.g. the Long Wavelength Array) have essentially instantaneous fields-of-view of  $2\pi$  sr, but might have limited resolutions of a few arcmin or worse changed (which can lead to a higher confusion limit), while others (e.g. LOFAR) have intrinsic fields-of-view of  $2\pi$  sr but are limited by beam-formed to focus on smaller areas. This compares with traditional dish-based interferometers at higher frequencies (e.g. the VLA and the Australia Telescope Compact Array; ATCA) that have fields-of-view of arcmin<sup>2</sup> but resolutions of arcsec. Therefore instead of just  $\Omega_{\text{epoch}}$  we use  $\Omega_{\text{epoch}}/\theta^2$ , with  $\theta$  the angular resolution. This effectively normalises to the rough number of independent pixels (ignoring oversampling) or potential sources in a pointing. For a traditional interferometer this reduces to roughly  $B^2/D^2$ , where  $B$  is the maximum baseline and  $D$  the element diameter, but systems like phased-array feeds (Hotan et al. 2021) can increase this significantly.

Finally, rather than use  $T/\Delta T$  separately we just use the number of epochs,  $N_{\text{epochs}}$ , which has the same value. Putting these together we choose:

$$\text{FOM} \equiv N_{\text{epochs}}(\Delta T) \left( \frac{\Omega_{\text{epoch}}}{\theta^2} \right) \left( \frac{v}{v_0} \right)^\alpha \frac{1}{\sigma(\Delta T)} \quad (5)$$

as the figure-of-merit that a survey should maximise, where we retain the explicit dependence of  $N_{\text{epochs}}$  and  $\sigma$  on the time-scale probed since the same data can be processed in multiple ways, although this assumes that there are sufficient sources on the relevant timescales to make this reprocessing worthwhile. This functions like an effective survey volume, multiplying the number of epochs times the number of sources divided by the noise. It could in principle be further modified to account for the total physical volume probed and various source number density scalings (such as  $N(\geq S_v) \propto S_v^{-3/2}$  for standard candles in a Euclidean universe), which would adjust the relative importance of going wider versus deeper, but we do not do that here. Such explorations can be done, but are best tied to individual source types and do not generalise to the entire field as well.

Our figure of merit here expands on the commonly used survey speed metric (the number of square degrees per hour needed to achieve a given sensitivity; e.g. Johnston et al. 2007) which is more relevant for design of a telescope than a particular survey (indeed we revisit it in Section 7 when discussing future facilities). Firstly, we divide the survey speed by the synthesized beam solid angle  $\theta^2$  to allow comparison of widely different telescopes. Secondly, we do an explicit frequency correction assuming a spectral index  $\alpha$  to allow comparison of widely different frequencies. But most importantly we explicitly consider the number of individual epochs and

the timescale over which that sensitivity is achieved, to make sure that we probe variability on the timescales of interest.

#### 4.2.2. Comparing transient surveys

In the ideal case, a survey that optimised all of the parameters in Equation 5 would be suitable for detecting and monitoring radio time domain phenomena across all timescales (which, as Figure 1 shows, span many orders of magnitude). In practice, in any given survey to date, some aspects of this ideal were significantly compromised, limiting the effectiveness of the survey for particular phenomena. In addition, in many of the surveys conducted to date, it has not been possible to control the time sampling or integration times, because they relied on archival data (e.g. Levinson et al. 2002; Bower et al. 2007; Bannister et al. 2011).

Over the past two decades there have been a large number of radio transient surveys, which we discuss in Section 4.3. Figure 7 shows how the effective survey ‘volume’ has evolved over time, using the figure of merit in Equation 5. It is important to note that while this way of representing the surveys does distinguish between different sampling times  $\Delta T$ , it does not look at how sources vary over such timescales, as discussed below.

To compare the effectiveness of different surveys, a range of metrics have been used, most of which involve collapsing down the time dimension to form a ‘two-epoch equivalent’ source density parameter, introduced by Bower et al. (2007). For the two-epoch source density to provide a meaningful comparison, it requires the assumption that we do not know the characteristic timescale of variability of the underlying population/s, and hence a survey of 10 epochs spanning hours is equivalent to a survey of 10 epochs spanning months. Clearly this is not a valid assumption for any given, known source type: a survey with a total duration spanning hours would not be optimal for detecting gamma-ray bursts and supernovae, which evolve over months. However, the two-epoch source density has proved to be a useful tool in comparing surveys as the field has grown, from the four surveys listed by Bower et al. (2007) to the more than 50 that have been conducted to date, some of which are shown in Figure 7. In Section 4.3 we discuss the evolution of radio transient surveys over the past two decades.

#### 4.2.3. Other survey properties

Looking beyond the pure detection capabilities, survey design also affects the capacity for multi-wavelength follow-up, which is often critical for classification and identification of radio transients. A survey with two epochs separated by years (such as the NVSS versus FIRST comparison conducted by Levinson et al. 2002) can identify objects that have changed on those timescales, which is useful for estimating transient rates. However, confirming the nature of the individual objects (in that case, trying to distinguish between orphan afterglows, radio supernova and scintillating AGN) is made challenging by (a) the length of time after the transient event that the detection is made; (b) the lack of precision in identifying when the event occurred; and (c) the poor sampling of the event. So in addition to optimising the survey figure of merit, an ideal radio transients survey would also have:

- A radio reference survey at a similar, or better, sensitivity;
- Sampling of a wide range of timescales;
- Rapid data processing to enable rapid identification;
- Effective RFI and artefact rejection;
- Archival multi-wavelength survey data;
- Contemporaneous multi-wavelength observations;

- Capability to trigger follow-up with other telescopes.

Triggered follow-up is often important in identifying transients, particularly those identified at higher frequency wavebands (optical, X-ray) or with multi-messenger detectors. The most notable example of a comprehensive multi-wavelength follow-up campaign in recent years is that of the binary neutron star merger GW170817, detected in gravitational waves (Abbott et al. 2017a), with a counterpart identified in electromagnetic radiation (Abbott et al. 2017b) and followed up in all wavebands from gamma-rays to radio, providing an incredibly detailed picture of the event (Kasliwal et al. 2017).

For many phenomena discovered in radio, follow-up is complicated by the fact that radio emission arrives later than X-ray, optical and other higher frequency emission due to the nature of the underlying physical processes. Taking GW170817 as an example, gamma-rays were detected 1.7s after the gravitational wave event (Goldstein et al. 2017), optical/IR at 10.9 hours post-event (Coulter et al. 2017), X-ray after 9 days (Troja et al. 2017), and finally radio at 15 days after the event (Hallinan et al. 2017). Had the radio been detected first, say as an orphan afterglow, triggers at other wavelengths would most likely have been too late to detect the event itself, or the subsequent time evolution of the emission.

For more short-lived phenomena, such as flares or bursts from radio stars, triggering from radio is also problematic, as it is rare that the burst is detected in real time, due to the data processing times. Fender et al. (2015b) demonstrated that rapid triggering (in this case the Arcminute Microkelvin Imager Large Array (AMI-LA), operating at 15 GHz, responding to a Swift burst) can be successful in detecting stellar flares, but these examples are relatively uncommon. An ideal survey for detecting these phenomena would have simultaneous, or contemporaneous, multi-wavelength monitoring.

There have been a number of successful coordinated monitoring programs. For example, Osten et al. (2004) reports on a 4-year monitoring campaign of RS CVn system V711 Tau, spanning radio, ultraviolet, extreme ultraviolet, and X-ray; and MacGregor et al. (2021) reported an extreme flaring event on Proxima Centauri, detected during a joint monitoring campaign with radio, millimetre and optical telescopes. Of course several challenges of this approach are the resources required, and the difficulty of coordinating time availability on competitive-access telescopes. The ideal for future large scale projects would be dedicated facilities for conducting shadowing observations in other wavebands. A demonstrator of this approach is the MeerLICHT telescope (Bloemen et al. 2016) that was built to shadow MeerKAT observations, hence providing optical lightcurves once a radio transient is identified (e.g. Andersson et al. 2022).

### 4.3. A brief history of radio transient surveys

Time variable behaviour has been observed since the early days of radio astronomy (e.g. Hey et al. 1946; Ryle & Elsmore 1951). It was first observed in the closest, and brightest, radio sources: the Sun (see Wild et al. 1963, for a review of early results on solar bursts, and Sullivan 2009 for a more general history), Jupiter (Burke & Franklin 1955), and supernova remnant Cassiopeia A (Högbom & Shakeshaft 1961).

There were a number of attempts to monitor supernova remnants and radio galaxies for longer timescale variability in the late 1950s and early 1960s. However, most found either no significant variability, or were inconclusive, due to limited sensitivity

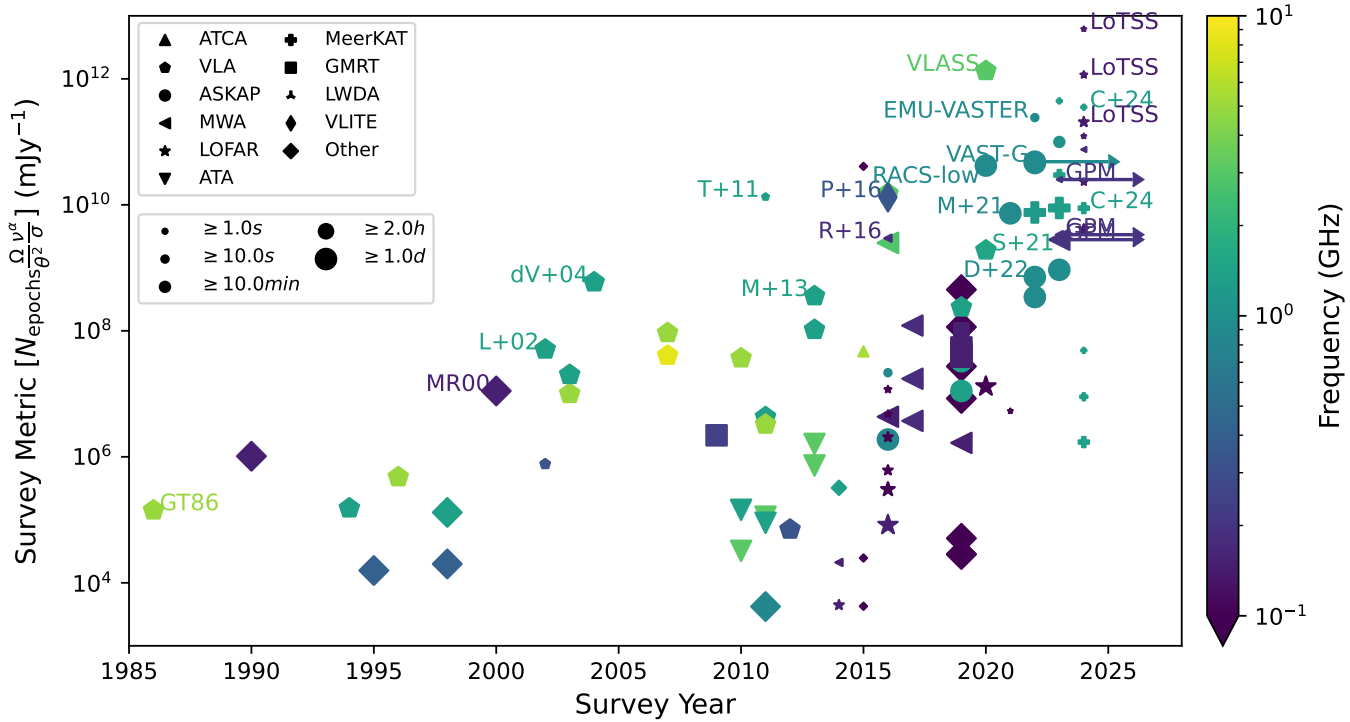


**Figure 7.** This plot shows how the effective survey volume, using the figure of merit in Equation 5 has evolved over time. Estimates are included for upcoming, but as yet unpublished, surveys. Some individual surveys of interest are labelled. The surveys are coloured by observing frequency, the shape corresponds to the telescope, and the size corresponds to the survey timescale (if multiple results are reported for a single survey on different timescales, it is plotted multiple times). Information has been updated from the survey compendium by Kunal Mooley and Deepika Yadav <http://www.tauceti.caltech.edu/kunal/radio-transient-surveys/index.html>. Labelled surveys include: GT86 (Gregory & Taylor 1986); MR90 (McGilchrist & Riley 1990; Riley 1993); MR00 (Minns & Riley 2000); L+02 (Levinson et al. 2002); dV+04 (de Vries et al. 2004); T+11 (Thyagarajan et al. 2011); M+13 (Mooley et al. 2013); R+16 (Rowlinson et al. 2016); P+16 (Polisensky et al. 2016); S+21 (Sarbadhicary et al. 2021); M+21 (Murphy et al. 2021); D+22 (Dobie et al. 2022); and C+24 (Chastain et al. 2025). Additional surveys from Table 4 are RACS-low, VAST-G (for VAST-Galactic), VLASS, LoTSS, and GPM, as well as a projection for using the VASTER fast-imaging pipeline (Wang et al. 2023) on the EMU survey (Hopkins et al. 2025).

or poor time sampling. Pauliny-Toth & Kellermann (1966) give a good summary of the research during this period. For example, the search for long period variability in radio ‘stars’ (as most discrete radio objects were thought to be, before the discovery/identification of radio galaxies, and then quasars), by Burke & Franklin (1955), found that none of  $\sim 100$  sources monitored showed variability of greater than 10% over 18 months. The discovery of quasars and the advent of synthesis imaging changed time domain radio astronomy significantly.

In this section we summarise the development of radio transient surveys in the image domain, as they evolved from discovery and monitoring of variable radio continuum sources, through to the current state of the field. In doing this we acknowledge the very useful compilation of survey specifications originally provided by Mooley et al. (2016) and updated since, which we draw on here. We present the summary in largely chronological order, with some survey types (i.e. low and high frequency surveys, Galactic plane surveys, and circular polarisation surveys) treated separately for clarity (see Sections 4.3.7 to 4.3.10).

#### 4.3.1. Targeted monitoring of stars and radio galaxies

Early radio observations were not expected to be sensitive enough to detect radio stars (and here we mean actual stars), on the assumption that the stars were similar in brightness to our own Sun (Lovell 1964). However, the discovery that flare stars (for which UV Ceti is the prototype) had flares several orders of magnitude greater than the Sun in optical (Luyten 1949) saw renewed

attempts to detect stellar radio emission. These attempts faced two main challenges: firstly the sensitivity of the telescopes, and secondly the difficulty of distinguishing flares from radio frequency interference (see, for example, the discussion of stellar flare rates by Lynch et al. 2017).

To unambiguously determine that observed flares were associated with a given star, combined optical and radio monitoring programs were carried out, resulting in simultaneous optical and radio flares detected on several stars including UV Ceti and V371 Ori (Slee et al. 1963; Lovell et al. 1963). Calculations from these observations implied a non-thermal emission mechanism, but the nature of this emission mechanism was not determined until much later. See Hjellming & Wade (1971) for a contemporaneous review of early radio star discoveries, and Dulk (1985) for a review of stellar emission mechanisms.

The first quasar to be discovered and confirmed as extragalactic (quasar 3C 273; Schmidt 1963) was also one of the first extragalactic radio sources to have its variability characterised through monitoring (Dent 1965). Over the next decade a number of teams conducted long-term repeated observations of radio galaxies and quasars from low to high radio frequencies (e.g. Pauliny-Toth & Kellermann 1966; Hunstead 1972; Schilizzi et al. 1975)

The 1960s also saw the discovery of, and further searches for, interplanetary scintillation (e.g. Hewish et al. 1964; Cohen et al. 1966), which ultimately led to the discovery of pulsars (Hewish et al. 1968). It was recognised from the start that IPS was a tool for measuring the angular size of extragalactic objects (e.g. Cohen et al. 1967).

In the 1980s, monitoring of extragalactic radio sources continued, including on shorter timescales (e.g. Heeschen et al. 1987) and lower frequencies (e.g. Slee & Siegman 1988). By the end of the decade it was a well established that a majority of the observed variability could be explained by interstellar scintillation (e.g. Blandford et al. 1986; Rickett 1990). In other words, it was a propagation effect extrinsic to the source itself (Section 2.5.1).

Later work identified annual cycles in the observed variability due to interstellar scintillation (e.g. Jauncey & Macquart 2001) caused by the relative velocity of the scintillation pattern as the Earth orbits the Sun. Eventually large surveys of compact extragalactic sources were conducted, most notably the Microarcsecond Scintillation-Induced Variability (MASIV; Lovell et al. 2003, 2008) survey. However, all of this work still involved targeted observations of individual objects.

#### 4.3.2. The first imaging surveys for radio variability

The advent of synthesis imaging meant it was possible to conduct untargeted surveys for variability, observing a (relatively) large sample of sources, with better flux stability and source localisation than what had previously been available.

The first radio transient detected in a synthesis image was the X-ray binary Cygnus X-3, which was found in a Westerbork search for radio counterparts to X-ray sources (Braes & Miley 1972) and which led to numerous followup studies (e.g. Hjellming et al. 1972; Hjellming & Balick 1972; Gregory et al. 1972; Seaquist et al. 1974; Molnar et al. 1984). About a decade later, in the 1980s, the first larger scale searches for radio transients and variability commenced.

At low frequencies, McGilchrist & Riley (1990), followed by Riley (1993) and Minns & Riley (2000) conducted a  $\sim 600 \text{ deg}^2$  survey over 10 years, at 151 MHz, with the Cambridge Low Frequency Synthesis Telescope. Riley & Green (1995, 1998) conducted a 100  $\text{deg}^2$  survey at 408 MHz with the Dominion Radio Astrophysical Observatory Synthesis Telescope. In both cases, the sampling was roughly yearly, and these projects found that only a very small percentage of radio sources ( $< 1 - 2\%$ ) were highly variable at low frequencies, although that percentage was much higher for steep spectrum sources.

The conclusions of these surveys were that most radio sources were not highly variable, and that most observed variability was consistent with scintillation. However, it is important to note that the sensitivity and limited time sampling meant that most timescales were not well explored.

#### 4.3.3. Widefield few-epoch searches

The possibility of detecting orphan afterglows from gamma-ray bursts motivated the next phase of radio transient searches, including both dedicated surveys and uses of archival data. Rather than focusing on characterising variability, as the previous imaging surveys had done, this wave of surveys had the stated aim of finding explosive ‘transient’ objects. Here (and in Section 4.3.4), astronomers made use of existing single-epoch large-scale surveys. The properties of some of the key large-scale continuum surveys are summarised in Table 3. By comparing sources between individual surveys, multi-epoch transient searches could be done.

The first of these was Levinson et al. (2002), who used two of the primary radio continuum reference surveys, Faint Images of the Radio Sky at Twenty centimeters (FIRST; Becker et al. 1995; White et al. 1997) and the NRAO VLA Sky Survey (NVSS; Condon et al. 1998), to search for isolated compact sources (with

a flux density limit of 6 mJy beam $^{-1}$  at 1.4 GHz) that were present in one catalogue but not detected in the other. They found nine candidate afterglows, and identified that the most likely confusing source types were radio-loud AGN and radio supernovae. Subsequent radio and optical follow-up of these candidates by Gal-Yam et al. (2006) found that five were not true variables, one was an AGN and one a known pulsar. One of the objects was likely to be a radio supernova, and the other remained unidentified, but the authors concluded it was unlikely to be a GRB afterglow. The analysis presented in this pair of papers provided a foundation for radio transient searches for the next decade.

Several 2–3 epoch VLA surveys followed, each exploring different timescales and sensitivities. Carilli et al. (2003) explored timescales of 19 days and 17 months, at submillijansky sensitivities in the Lockman Hole region. de Vries et al. (2004) used a repeat observation of the FIRST Southern Galactic Cap zero-declination strip region to explore timescales of 7 years at millijansky sensitivities. Neither survey found any transients (objects that had appeared or disappeared between the epochs) and the authors set limits on the expected transient rate, as well as calculating the percentage of highly variable objects.

In the following decade, Croft et al. (2010) used the Allen Telescope Array Twenty-Centimetre Survey (ATATS) to do a two-epoch comparison with NVSS. They took the combined catalogue of 12 epochs of ATATS and compared to the NVSS, observed 15 years earlier. At the same time, Bower et al. (2010) conducted a similar analysis with the ATA Pi GHz Sky Survey (PiGSS) with a smaller sky area but better sensitivity. Neither survey found any radio transients, and both put limits on the number of transients and variables expected in an all-sky survey.

Most surveys in future years were much better sampled than these. However, there were a few more widefield few-epoch surveys, such as Heywood et al. (2016) and Murphy et al. (2017). Both of these found one candidate transient or highly variable object, but did not have enough information to identify the likely source class.

These few-epoch transient surveys provided a good starting point for initial characterisation of the dynamic radio sky. However, it was evident that to do useful science, it would be necessary to have more observation epochs, better sensitivity, and timely analysis to enable follow-up.

#### 4.3.4. Exploring archival data and surveys

To get more information about the dynamic radio sky before future surveys became available, researchers delved deeper into archival datasets in order to exploit repeated observations that had been done for other purposes, for example calibration. The first example of this was by Bower et al. (2007) who searched 5 and 8.4 GHz observations from the VLA data archives. The dataset consisted of 944 epochs of the same calibrator field, taken over 22 years. They found 10 transients, which had no optical counterparts (Ofek et al. 2010), and were not able to be identified. Later re-analysis by Frail et al. (2012) showed that most of these were likely to be imaging and calibration artefacts, but at the time the results motivated the exploration of a number of other archival searches.

Bower & Saul (2011) built on this work to conduct a search using 1.4 GHz observations of the same calibrator field (3C 286). Using more stringent criteria, they found no transient candidates, and calculated limits on the expected all-sky rate. Bell et al. (2011) further expanded on the work, using an automatic pipeline developed for the LOFAR transients project (Fender et al. 2008). They

analysed 5037 observations of seven calibrator fields, primarily at 5 and 8.4 GHz. They also found no transient sources on timescales of 4–45 days, and reported new limits on the all-sky rate.

Bannister et al. (2011) conducted an analysis of the Molonglo Observatory Synthesis Telescope (MOST; Bock et al. 1999) archive, consisting of 22 years of observations at 843 MHz. Although most of the fields were only observed once as part of the Sydney University Molonglo Sky Survey (SUMSS; Mauch et al. 2003) and Molonglo Galactic Plane Surveys (Green et al. 1999; Murphy et al. 2007), about 30% of the fields were observed multiple times for calibration, data quality, or monitoring of specific objects. This search found 15 transients, some of which were identified with known objects (e.g. Nova Muscae 1991) and some of which remained unknown.

Thyagarajan et al. (2011) conducted a similar analysis of repeated observations from the FIRST survey. Each field was observed 2–7 times, and a large number of variable sources (but no transients) were identified. These projects demonstrated the challenges of working with an extremely inhomogeneous dataset in terms of time sampling, and the challenge of doing meaningful follow-up and analysis of transients that occurred many years before discovery. To make substantial progress, continuum surveys designed specifically for time domain science were required.

#### 4.3.5. Multi-epoch radio transient surveys (2010s)

The 2010s saw the emergence of designed-for-purpose multi-epoch radio transient surveys. Some of the first of these were conducted with the Allen Telescope Array (ATA; DeBoer 2006), an instrument designed for SETI searches. Croft et al. (2011) published results from the 12-epoch, 690 deg<sup>2</sup> survey (ATATS) at 1.4 GHz. Bower & Saul (2011) and Croft et al. (2013) presented results from the PiGSS survey at 3 GHz. Neither of these surveys detected any transients (which they defined as varying by a factor of  $> 10$ ). However, they set more stringent limits on transient rates. Unfortunately, due to funding changes, radio imaging surveys did not continue after these initial results, and the full potential of the array as a transient machine was not realised.

There were also a set of relatively small area (0.02 to 60 deg<sup>2</sup>) multi-epoch surveys conducted with the VLA (e.g. Ofek et al. 2011; Hodge et al. 2013; Mooley et al. 2013; Alexander et al. 2015) and the ATCA (e.g. Bell et al. 2015; Hancock et al. 2016). Only one of these, Ofek et al. (2011), detected a transient object, which, although not unambiguously identified, they state is consistent with being from a neutron star merger. These more sensitive surveys, with multiple epochs, were able to be used to start characterising the variability of the radio source population beyond a single numerical metric, for example looking at how variability changed with flux density, timescale and Galactic latitude. Radcliffe et al. (2019) was notable for exploring the variability of radio sources at  $\mu$ Jy sensitivities (and finding the rates comparable to those at mJy sensitivities).

The re-evaluation of the Bower et al. (2007) transient results and the subsequent reduction of the derived rates by Frail et al. (2012), motivated Aoki et al. (2014) to revisit the rates that had been reported from the 1.4 GHz Nasu Sky Survey. Although not strictly an imaging survey (transients were detected directly in drift scan fringe data), 11 extreme transients had been reported over a number of years (see Kuniyoshi et al. 2007; Niinuma et al. 2007; Matsumura et al. 2009, and others). The derived transient rate was inconsistent with other rates reported at the time. However,

in the re-analysis, only a single transient passed the more rigorous thresholds applied by Aoki et al. (2014), giving a rate more consistent with other projects.

The first results from the Australia SKA Pathfinder Boolardy Engineering Test Array (ASKAP-BETA; Hotan et al. 2014) came in 2016, with Heywood et al. (2016) and Hobbs et al. (2016) publishing transient surveys covering timescales of days and minutes to hours, respectively. These surveys used the 6-dish ASKAP test array, operating at  $\sim 1$  GHz. This work was followed by Bhandari et al. (2018) who conducted a pilot survey at 1.4 GHz using a 12-dish array, in the Early Science phase of ASKAP operations. None of these surveys detected any transient sources, but provided the first demonstration of ASKAP’s capabilities for transient science. In particular, the prospect of imaging of long integration observations on short timescales (Hobbs et al. 2016).

A big step forward came with the Caltech-NRAO Stripe 82 Survey (CNSS; Mooley et al. 2016), a multi-year, sensitive (rms  $\sim 40 \mu$ Jy beam<sup>-1</sup>) survey of the 270 deg<sup>2</sup> Stripe 82 region. The survey was conducted with the VLA at 3 GHz, and the Stripe 82 region was chosen for its existing multi-wavelength coverage, to improve the chances of identifying transients. By many measures this could be considered the most successful radio transient imaging survey to date, at that time. In addition to characterising the variability of the 3 GHz source population, the initial pilot survey over 50 deg<sup>2</sup> detected two transients serendipitously, which were both identified — as an RS CVn binary and a dKe star. Further studies discovered a tidal disruption event (Anderson et al. 2020) and identified state changes in AGN (Kunert-Bajraszewska et al. 2020; Wolowska et al. 2021).

Another novel aspect of CNSS was a contemporaneous optical survey carried out with the Palomar Transient Factory (Law et al. 2009). This allowed a comparison of the dynamic sky in optical and radio wavebands; the main finding being that they are quite distinct, something that needs to be considered in planning for complementarity with, for example, the SKAO and Rubin Observatory (Ivezic et al. 2019) transient surveys.

#### 4.3.6. Multi-epoch radio transient surveys (2020s)

By the start of the 2020s, roughly 50 untargeted radio transient imaging surveys had been conducted using both dedicated observations and commensal data obtained for other purposes, and yet only a handful of radio transients had been discovered via those surveys, most of which had not been conclusively classified. The main reasons for this were (i) the lack of surveys that were able to optimise the metrics presented in Equations 4 and 5 — all were limited in either sensitivity, sky coverage, or time sampling; and (ii) processing limitations meant that in many cases candidates were identified long after the event, limiting the potential for multi-wavelength follow-up.

The promise of large scale, well-sampled radio transient imaging surveys was finally (partially) realised, with the arrival of three SKAO pathfinder telescopes: ASKAP, MeerKAT and LOFAR, along with the VLA and MWA. The specifications for the major transient surveys on these telescopes are given in Section 4.4. In this section we will summarise some of the key results that have been published to date.

On ASKAP, the dedicated Variables and Slow Transients survey (VAST; Murphy et al. 2013, see Section 4.4.3) has both a Galactic and extragalactic component. The pilot survey, conducted at 888 MHz (Murphy et al. 2021), consisted of 12 minute observations (with typical sensitivity of  $0.24 \text{ mJy beam}^{-1}$ ), repeated with

cadences of 1 day to 8 months. This survey detected 28 highly variable and transient sources including: known pulsars, new radio stars, sources associated with AGN and galaxies, and some sources yet to be identified. A pilot survey search of the Galactic Centre by Wang et al. (2022a) resulted in the detection of a new GCRT (see Section 3.9).

Dobie et al. (2019, 2022) conducted 10 observations of a single ASKAP field ( $30\text{ deg}^2$ ) which covered 87% of the localisation area of the gravitational event GW190814 localisation area. They reported a single synchrotron transient, which was not associated with the neutron star-black hole merger. Further multi-wavelength observations were conducted, but are so far inconclusive (D. Dobie, *private communication*). Reprocessing of a subset of this data on 15-minute timescales resulted in the discovery of 6 rapid scintillators in a linear arrangement on the sky (Wang et al. 2021a). These were used to constrain the physical properties of a degrees-long plasma filament in our own Galaxy.

Wang et al. (2023) extended this short-timescale (15 min) imaging approach to 505 hours of data from several ASKAP pilot surveys, with typical frequency  $\sim 1\text{ GHz}$ . Their search found 38 variable and transient sources, which is enough to start characterising the fraction of different source types on these timescales. They found 22 AGN or galaxies, 8 stars, 7 (known) pulsars and one unknown source, somewhat similar to the population found by Murphy et al. (2021).

On MeerKAT there have also been several surveys that sample a range of timescales, often resulting from data focused on monitoring other sources (e.g. Driessen et al. 2020, 2022a; Andersson et al. 2022). Rowlinson et al. (2022) searched data from a monitoring campaign of MAXI J1820+070. There were 64 weekly observations with a typical integration time of 15 minutes and typical sensitivity of  $1\text{ mJy beam}^{-1}$ . This resulted in 4 AGN, a pulsar and one unidentified object. Driessen et al. (2022b) searched data from weekly observations of GX 339–4 and identified 21 variable sources, most of which have low-level variability consistent with refractive scintillation from AGN. On shorter timescales, Fijma et al. (2024) re-imaged 5.45 hours of MeerKAT data, centred on NGC 5068, on timescales of 8 s, 128 s, and 1 hr, but did not find any transients.

On the VLA, the CHILES Variable and Explosive Radio Dynamic Evolution Survey (Sarbadhicary et al. 2021) was designed to study radio variability in the extragalactic COSMOS deep field. It had 960 h of 1–2 GHz data, observed over 209 epochs, with typical sensitivity of  $\sim 10\text{ }\mu\text{Jy beam}^{-1}$ . They found 18 moderately variable sources, all of which were identified as AGN or galaxies.

The VLA Sky Survey (VLASS; Lacy et al. 2020) is underway and producing results (see Section 4.4.5) but no general transient survey paper has been published yet. At low frequencies, the MWA Galactic Plane Monitor and LOFAR transient surveys are discussed in Sections 4.4.2 & 4.4.1.

We have now reached a regime where radio transient imaging surveys are detecting significant numbers of transient and highly variable objects. Equally importantly, they have sufficient time sampling and resolution, along with multi-wavelength information, to allow the class of most of the objects to be identified. We discuss these populations further in Section 6.2.

#### 4.3.7. Low frequency surveys

In the decades leading up to the mid-2010s, a majority of radio transient imaging surveys were conducted at gigahertz frequencies, predominantly with the VLA. There were a small number of exceptions, for example Lazio et al. (2010) conducted a survey at 73.8 MHz with the Long Wavelength Demonstrator Array (LWDA), finding no transients above 500 Jy, and Jaeger et al. (2012), who found one (unidentified) transient source in a search of 6 archival VLA fields observed at 325 MHz.

However, the advent of three new wide-field, low-frequency telescopes — the Long Wavelength Array (LWA1; Ellingson et al. 2013), the Murchison Widefield Array (MWA; Tingay et al. 2013) and the Low Frequency Array (LOFAR; van Haarlem et al. 2013) — opened up the possibility of more fully characterising the time domain radio sky at  $< 300\text{ MHz}$ .

The LWA1 enabled very widefield surveys at low frequencies (10 – 88 MHz), but with relatively poor sensitivity (10s – 100s of Jy). Surveys by Obenberger et al. (2014, 2015) detected fireballs from meteors, but no transients originating outside the Solar System.

The next set of results were from early surveys with the MWA and LOFAR. Bell et al. (2014) conducted a survey on timescales of 26 minutes and 1 yr with MWA at 154 MHz. They found no transients above 5.5 Jy. Carbone et al. (2016) reported on a LOFAR survey of 4 fields, observed on cadences between 15 min and several months. The frequency of the observations were between 115 and 190 MHz. They found no transients above 0.3 Jy. Stewart et al. (2016) reported results from a 4 month monitoring campaign of the Northern Galactic Cap as part of the Multifrequency Snapshot Sky Survey. The survey consisted of 2149 11-min snapshots, each covering  $175\text{ deg}^2$ . They reported the discovery of one transient source, with no optical or high-energy counterpart. Despite an extensive investigation, the source class was not identified, and future attempts to discover more sources from this hypothetical population were unsuccessful (e.g. Huang et al. 2022).

The Stewart et al. (2016) transient increased the motivation for low frequency transient surveys. However, the next set of surveys yielded no new candidates. These included: Rowlinson et al. (2016); Feng et al. (2017); Tingay & Hancock (2019); Kemp et al. (2024) all with the MWA at 150–190 MHz; Polisensky et al. (2016) with the Jansky Very Large Array Low-band Ionosphere and Transient Experiment (VLITE) survey at 340 MHz; Anderson et al. (2019) taking advantage of the wide field of view of the Owens Valley Radio Observatory Long Wavelength Array (OVRO-LWA) at  $< 100\text{ MHz}$  and Hajela et al. (2019a) with the GMRT at 150 MHz. Even with improved sensitivity, a significant population of low frequency transients remained elusive.

The lack of radio transients at low frequencies is partly expected from predictions of synchrotron transient rates (e.g. Metzger et al. 2015b). As emission from, for example, GRBs evolves, the brightness decreases as the spectral peak moves to lower frequencies and the evolution slows, meaning they are less likely to be detectable given the sensitivity of low frequency telescopes (Ghirlanda et al. 2014). Recently there has been a shift in focus towards searching for shorter timescale Galactic transients: these often have coherent emission mechanisms, leading to much faster variability. For example, de Ruiter et al. (2024) present an analysis of the LOFAR Two-metre Sky Survey (LoTSS; Shimwell et al. 2017) on 8-second timescales, which resulted in

the detection of a new magnetic white dwarf M-dwarf binary system (de Ruiter et al. 2025). See Sections 4.4.2 and 4.4.1 for work currently underway at low frequencies.

#### 4.3.8. High frequency surveys

All of the surveys discussed so far have been conducted at or below frequencies of a few gigahertz. At higher radio frequencies (and in the millimetre regime), telescope fields of view are much smaller. For example, the field of view of the Australia Telescope Compact Array is  $\sim 2$  arcminutes at 20 GHz, and the field of view of the Atacama Large Millimeter Array (ALMA; Wootten & Thompson 2009) is  $\sim 19''$  at 300 GHz. As a result, there are very few large scale continuum surveys at frequencies  $> 10$  GHz. Two examples are the 9C survey (Waldrum et al. 2003) covering  $520 \text{ deg}^2$  at 15 GHz and the AT20G survey (Murphy et al. 2010) covering  $20\,626 \text{ deg}^2$  at 20 GHz. Two conclusions from these projects were that (i) the overall properties of the source population at high frequencies can not be extrapolated from the  $\sim 1$  GHz population; (ii) the high frequency radio sky has a comparable level of variability to gigahertz frequencies: ( $\sim 5\%$  of bright sources were variable on 1 – 2 year timescales; Sadler et al. 2006).

The challenges of conducting large-scale high frequency radio surveys means that there have been a limited number of studies of high frequency radio variability. Bolton et al. (2006) selected 51 sources from the 9C survey for further monitoring. The motivation for 9C was to identify foreground contaminants for cosmic microwave background (CMB) maps; and variability could impact the completeness of such a sample. Monitoring over 3 years confirmed that about half of the steep spectrum objects (likely to be compact young radio galaxies), and none of the flat spectrum objects, were highly variable. There are various other high frequency monitoring programs in which sources have been selected from surveys (e.g. Franzen et al. 2009), however there have not been any untargeted multi-epoch imaging surveys, as such.

At even higher (millimetre) frequencies there have been a relatively small number of transient surveys using bolometric arrays on single-dish telescopes. Several of these are with the South Pole Telescope (SPT; Carlstrom et al. 2011). Whitehorn et al. (2016) searched for transients in the SPT 100 Square Degree Survey at 95 and 150 GHz, finding a single transient consistent with an extragalactic synchrotron source. Guns et al. (2021) searched at 95, 150, and 220 GHz, resulting in the detection of 15 transient events including stellar flares and possible AGN activity. Other examples are Chen et al. (2013) who searched for transients using the combined Wilkinson Microwave Anisotropy Probe and Planck epochs at 4 bands between 33 and 94 GHz; Naess et al. (2021), Li et al. (2023) and Biermann et al. (2025) using the Atacama Cosmology Telescope at 77 to 277 GHz.

We note that the majority of these surveys have been designed for cosmological purposes and hence have focused on high Galactic latitudes, where the transient targets are largely extragalactic synchrotron transients (although the actual discoveries often include Galactic stars). Therefore they have excluded low-latitude sources like X-ray binaries, which can show high levels of variability at millimetre frequencies associated with state transitions (e.g. Fender et al. 2000; Russell et al. 2020). Future low-latitude surveys will doubtless identify more Galactic sources.

We will not discuss millimetre transient surveys further in this review. An analysis of the expected populations of extragalactic transients detectable in future CMB surveys (including long and

short GRBs, tidal disruption events and fast blue optical transients) is given by Eftekhari et al. (2022).

#### 4.3.9. Galactic Centre and Galactic plane surveys

Parallel to the efforts to characterise variability in the extragalactic radio sky, there were a number of surveys of the Galactic Centre, Galactic bulge and the Galactic plane more generally. These surveys were motivated by the dense stellar and compact object environment in the plane (and centre) of our Galaxy, making it a likely rich source of transient events (e.g. Munoz et al. 2003; Morris & Serabyn 1996; Calore et al. 2016). However, radio imaging of Galactic regions comes with additional challenges, including (a) producing high quality images in regions of significant diffuse emission; and (b) identifying multi-wavelength counterparts when the optical and infrared source density is high, and there is substantial extinction.

One of the first Galactic surveys was a 5-year monitoring program of the northern Galactic plane, conducted between 1977 and 1981 with the NRAO 91m transit telescope, operating at 6 GHz (Gregory & Taylor 1981, 1986). This survey explored timescales from days to  $\sim 1$  year. A key motivation was to find more sources like the high mass X-ray binary Cyg X-3, which had recently been discovered to have large radio outbursts (Gregory et al. 1972). About 5% of the 1274 sources monitored showed significant variability on either short or long timescales. The authors were not able to identify any of these objects, but determined that most were likely to be extragalactic.

The next major long-term Galactic centre monitoring program was conducted by Hyman et al. (2002). This project used archival and new widefield images of the Galactic centre taken with the VLA at 0.33 GHz, with targeted follow-up of objects of interest at 1.4 and 4.8 GHz. They introduced the nomenclature Galactic Centre Radio Transient (GCRT) to describe these sources, as their nature was unknown. Subsequent work by Hyman et al. (2005, 2006, 2007, 2009) resulted in the discovery of three GCRTs. These sources shared some common properties (highly variable, steep spectrum, circularly polarised) but their identity has remained elusive (see Section 3.9).

The challenges presented by imaging near the Galactic region, and difficulty of identifying potential transients has limited the number of surveys with a Galactic focus. Becker et al. (2010) searched for transients in three epochs of the Multi-Array Galactic Plane Imaging Survey, a collection of VLA observations conducted at 4.8 GHz. The observations spanned 15 years, with a sky area of  $23.2 \text{ deg}^2$ . They found no transients, and a number of highly variable sources (at a higher source density than found by extragalactic surveys at that time). However, they were not able to conclusively identify their object class.

Williams et al. (2013) conducted a two-year survey with the Allen Telescope Array at 3 GHz, with weekly visits to  $23 \text{ deg}^2$  in two fields in the Galactic plane. This was a substantial improvement on previous surveys, but did not detect any transient sources, pointing to lower frequencies potentially being more productive for Galactic transient discovery. The capabilities of SKAO pathfinder and precursor telescopes has seen a renewed interest in transient surveys of the Galactic centre and Galactic bulge (e.g. Hyman et al. 2021; Wang et al. 2022a; Frail et al. 2024) as well as the re-exploration of archival data (e.g. Chiti et al. 2016). Some of the large-scale Galactic plane surveys currently underway are outlined in Section 4.4.

#### 4.3.10. Circular polarisation surveys

A vast majority of radio sources are driven by synchrotron emission and so do not show significant levels of circular polarisation (Saikia & Salter 1988). For example, AGN, by far the most populous objects in the radio sky, are typically  $< 0.1\%$  circularly polarised (e.g. Rayner et al. 2000). However, some highly variable radio source classes do have significant fractions of circularly polarised emission, including pulsars (Section 3.8), radio stars (Section 3.5), and unusual transients like GCRTs and LPTs (Section 3.9).

Circular polarisation surveys provide an alternative way of discovering and identifying these objects. Historically, most large radio surveys have only produced total intensity (Stokes I) data products (see Table 3). For example the Westerbork Northern Sky Survey (Rengelink et al. 1997), SUMSS (Mauch et al. 2003) and the GMRT 150 MHz All-sky Radio Survey First Alternative Data Release (Intema et al. 2017). The NRAO VLA Sky Survey (Condon et al. 1998) produced linear polarisation products (Stokes Q and U) but did not produce circular polarisation products.

When circular polarisation is available, it provides a method for easily identifying many interesting objects (e.g. Kaplan et al. 2019; Wang et al. 2021b, 2022b) while filtering out the non-variable sources. In the cases where sensitivity in Stokes I is limited by confusion, Stokes V can also often have better sensitivity. Finally, unlike linear polarisation no correction for Faraday rotation (Burn 1966) is needed, which eliminates the need for multiple frequency channels and hence provides better sensitivity (cf. Brentjens & de Bruyn 2005) and easier processing.

The first all-sky circular polarisation survey was conducted using the MWA at 200 MHz (Lenc et al. 2018). An untargeted search of this data resulted in detections of Jupiter, some known pulsars, several artificial satellites, and the tentative detection of two known flare stars. Several large survey telescopes now produce circular polarisation products by default, enabling searches for new objects via their circularly polarised emission. For example, Pritchard et al. (2021) detected 33 radio stars in the ASKAP RACS survey at 888 MHz; and Callingham et al. (2023) produced a catalogue of 68 circularly polarised sources from V-LoTSS (the circularly polarised LOFAR Two-metre Sky Survey). These sources consisted of radio stars, pulsars, and several that remain unidentified. This is an area that the SKAO pathfinder and precursor surveys are opening up for discovery.

### 4.4. Current large-scale radio transient surveys

There are a number of large image domain radio transient surveys underway (or recently completed). In this section we briefly describe their properties in the context of the history we have presented in Section 4.3, and the future plans for the SKAO, ngVLA, DSA-2000 and other instruments, that we will discuss in Section 7. The specifications of these current surveys are summarised in Table 4, in order of increasing frequency. The specifications of major single-epoch radio continuum surveys are summarised in Table 3, for comparison.

Note that we are not including the many smaller-scale transient searches (e.g. of various archival datasets) that are underway but not-yet-published. Also, our focus remains on imaging surveys, so we do not include other ongoing radio transients surveys such as CHIME (e.g. CHIME/FRB Collaboration et al. 2021, which primarily looks for dispersed signals in beamformed data) and MeerTRAP (e.g. Turner et al. 2025).

#### 4.4.1. The LOFAR Two-metre Sky Survey

The LOFAR Two-metre Sky Survey (LoTSS; Shimwell et al. 2017) is a 150 MHz survey of the sky north of  $\delta = 0^\circ$ . Each LoTSS image is an 8-hour observation, resulting in a typical sensitivity of  $83 \mu\text{Jy beam}^{-1}$  and a resolution of  $6''$ , with full Stokes parameters. The most recent data release covers 27% of the sky (Shimwell et al. 2022), with an upcoming data release expected to cover 70% of the sky.<sup>1</sup>

Although LoTSS is essentially a single-epoch continuum survey, we have included it here because there is a substantial short-time scale imaging project underway that will search for transients on timescales of 8 s, 2 min and 1 h (de Ruiter et al. 2024). The discovery of a white dwarf binary system from this survey was reported by de Ruiter et al. (2025).

In addition, there are other LOFAR surveys underway that will be useful for transient searches, for example the LoTSS Deep Fields which consist of hundreds of hours of repeated observations of three fields (ELIAS-N1, Boötes and the Lockman Hole), with observing blocks scheduled months to years apart (Best et al. 2023; Shimwell et al. 2025), with eventual sensitivities of  $\approx 10 \mu\text{Jy beam}^{-1}$ .

#### 4.4.2. The MWA Galactic Plane Monitor

The MWA Galactic Plane Monitoring program (MWA GPM; project code G0080)<sup>m</sup> is a transient survey being conducted at 185–215 MHz. It covers the Galactic plane south of  $\delta < +15^\circ$  with  $|b| < 15^\circ$ , with longitude coverage changing through the year and 30 min integrations on a bi-weekly cadence. It has a resolution of  $45''$  and a typical sensitivity of  $10 \text{ mJy beam}^{-1}$  on 5 minute timescales (N. Hurley-Walker, *private communication*).

The main scientific goal of the survey is to discover long-period transients. The survey parameters are briefly described in the Methods section of Hurley-Walker et al. (2023), which reports the discovery of GPM J1839–10, a new long period transient, and will be fully described in a paper in preparation.

#### 4.4.3. The ASKAP VAST Survey

The ASKAP Variables and Slow Transients survey (VAST; Murphy et al. 2013, 2021) is one of nine key survey projects on the ASKAP telescope. The survey is being conducted at 887.5 MHz, and produces total intensity (Stokes I) and circular polarisation (Stokes V) data products. There are two components to the survey: an extragalactic component covering 10 954 square degrees, with typical sensitivity of  $220 \mu\text{Jy beam}^{-1}$ , and a Galactic component covering 2 402 square degrees with a typical sensitivity of  $250 \mu\text{Jy beam}^{-1}$ . Note that the Galactic survey also includes two fields that cover the Large and Small Magellanic Clouds. The extragalactic fields are sampled with a median cadence of 2 months, and the Galactic fields are sampled with a median cadence of 2 weeks.

The survey was designed to cover a wide range of science goals, and these goals have evolved over time since the original proposal (Murphy et al. 2013). Results from the VAST pilot survey, a 200 hour test of the observing strategy, data quality and data processing approach have confirmed the survey is effective for a

<sup>1</sup><https://lofar-surveys.org/>

<sup>m</sup><https://mwatelescope.atlassian.net/wiki/spaces/MP/pages/24969577/2022-A+and+2022-B+Extended>

**Table 3.** Specifications of past large scale single-epoch radio continuum surveys, in order of observing frequency.

Survey	GLEAM	GLEAM-X	VLSS	TGSS	WENSS	SUMSS	MGPS-2	NVSS	FIRST
Telescope	MWA	MWA-II	VLA	GMRT	WSRT	MOST	MOST	VLA	VLA
Frequency (MHz)	72–231	72–231	74	150	325	843	843	1400	1400
Bandwidth (MHz)	31	31	1.56	16.7	5	3	3	100	100
Resolution (arcsec)	150 <sup>a,c</sup>	66 <sup>c</sup>	80	25 <sup>a</sup>	54 <sup>a</sup>	43 <sup>a</sup>	43 <sup>a</sup>	45	5.4
Sky coverage (deg <sup>2</sup> )	29 300	30 900	30 939	36 900	10 300	8 000	2 400	33 800	10 600
Sky region	$\delta \leq +25^\circ$	$\delta \leq +30^\circ$	$\delta \geq -30^\circ$	$\delta \geq -53^\circ$	$\delta \geq +30^\circ$	$\delta \leq -30^\circ$	$ b  < 10^\circ, l > 245^\circ$	$\delta \geq -40^\circ$	Galactic caps
Sensitivity (mJy beam <sup>-1</sup> )	25 <sup>d</sup>	1.3 <sup>e</sup>	100	5.0	3.5	1.0	1.0–2.0	0.45	0.2
Stokes products			I	I	IQUV	I	I	IQU	
Reference	Wayth et al. (2015)	Hurley-Walker et al. (2022a)	Cohen et al. (2007)	Intema et al. (2017)	Rengelink et al. (1997)	Bock et al. (1999)	Murphy et al. (2007) <sup>b</sup>	Condon et al. (1998)	Becker et al. (1995)

<sup>a</sup> The resolution depends on the declination as  $\csc |\delta|$ .

<sup>b</sup> There was an earlier epoch of MGPS (Green et al. 1999). However, only images were released, not a source catalogue.

<sup>c</sup> At 154 MHz.

<sup>d</sup> At 154 MHz, roughly.

<sup>e</sup> For the combined 170–231 MHz image.

**Table 4.** Specifications of current large scale radio transient surveys in the image domain. See the main text for the key reference papers.

Survey	LoTSS		MWA GPM <sup>a</sup>	VAST		RACS <sup>b</sup>			VLASS
	Deep	Extragal		Gal	RACS-low	RACS-mid	RACS-high		
Telescope	LOFAR	MWA	ASKAP		ASKAP				VLA
Frequency (MHz)	144	144	200	887.5	887.5	887.5 <sup>c</sup>	1295.5	1655.5	3000
Bandwidth (MHz)	48	48	30	288	288	288	144	288	2000
Resolution	6"	6"	45"	12–24"	12–24"	15–25"	$\gtrsim 8''$	$\gtrsim 8''$	2.5"
Sky coverage (deg <sup>2</sup> )	20 627	30	2 700–4 200	12 279	2 402	34 240	36 200	35 955	33 885
Sensitivity ( $\mu$ Jy beam <sup>-1</sup> )	2 000 (1 h)	10	10 000 (5 min) <sup>d</sup>	220	250	250	200	195	70
Polarisation	IQUV	IQUV	IV	IV	IV		IQUV		IQU
N repeats	1 <sup>e</sup>	ongoing	ongoing	21 <sup>f</sup>	120 <sup>f</sup>	3	1	1	3.5
Typical cadence	8 s, 2 min, 1 h	months	~2 weeks	~2 months	~2 weeks	12–24 months			32 months
Total time span	N/A	N/A	ongoing	4 years	4 years	4.5 years			10 years

<sup>a</sup> At the time of writing the MWA GPM survey paper has not been published, but has been briefly described in the Methods section of Hurley-Walker et al. (2023).

The other MWA GPM specifications listed here have been provided by N. Hurley-Walker (private communication). The sky coverage changes throughout the year.

<sup>b</sup> RACS can be considered as a 5-epoch survey at 3 comparable frequencies, see Section 4.4.4.

<sup>c</sup> RACS-low3 was observed at a slightly different frequency, 943.5 MHz.

<sup>d</sup> The estimated sensitivity is 7–10 mJy beam<sup>-1</sup> on 5 minute timescales and 70–100 mJy beam<sup>-1</sup> on 4 second timescales.

<sup>e</sup> Note that although LoTSS was conceived as single-epoch survey, it can be reprocessed on short timescales to allow for transient searches see Section 4.4.1.

<sup>f</sup> At the time of writing VAST is 50% complete.

number of these goals. Two examples are the multi-epoch sampling of the radio star population (Pritchard et al. 2024), and the discovery of unusual Galactic transients (e.g. Wang et al. 2021b).

#### 4.4.4. The Rapid ASKAP Continuum Survey

The Rapid ASKAP Continuum Survey (RACS; McConnell et al. 2020) was designed to produce a reference image of the entire sky visible to ASKAP ( $\delta < +50^\circ$ ), that would help in calibration of all ASKAP surveys. The first epoch (RACS-low1) was conducted at 887.5 MHz, starting in April 2019, with a resolution of 15" and typical rms sensitivity of 250  $\mu$ Jy beam<sup>-1</sup>. There have been five subsequent epochs, two in the higher ASKAP bands: RACS-mid1 at 1367.5 MHz starting December 2020 (Duchesne et al. 2023, 2024); and RACS-high1 at 1665.5 MHz, starting in December 2021 (Duchesne et al. 2025); and two repeats of RACS-low starting in March 2022 and December 2023. See Table 4 for the detailed specifications of these surveys.

The RACS data products include total intensity, linear and circular polarisation (Stokes I, Q, U, V). The repeated epochs were designed to allow exploration of the time variable sky. Early results have demonstrated the effectiveness for RACS for this. For example, in the detection of late-time radio counterparts for optically detected tidal disruption events (Anumarlapudi et al. 2024).

#### 4.4.5. The Very Large Array Sky Survey

The VLA Sky Survey (VLASS; Lacy et al. 2020) is an all-sky survey conducted at 2–4 GHz, with 2.5" resolution. It covers the entire sky above  $\delta > -40^\circ$ , with typical rms sensitivity of 120  $\mu$ Jy beam<sup>-1</sup>. It was designed to have a time domain component: one of the four science goals is ‘*Hidden Explosions and Transient Events*’. Hence the survey has three repeated epochs separated by  $\sim 32$  months, with a fourth epoch partially completed. The VLASS data products include total intensity and linear polarisation images (Stokes I, Q, U) but, at the time of writing, no public circular polarisation (Stokes V).

The science goals for VLASS are outlined in Lacy et al. (2020). In the time domain, the survey is best suited to search for objects that vary on timescales of  $\sim$ months, such as gamma-ray burst afterglows, radio supernovae and tidal disruption events, although it will also detect bursts from radio stars and Galactic transients. Indeed, early results have demonstrated the survey’s effectiveness for finding synchrotron transients, for example: a merger-triggered core collapse supernova (Dong et al. 2021), and a sample of radio-detected tidal disruption events (Somalwar et al. 2025b). However, the sparse sampling has meant that extensive followup is needed to fully characterise the discoveries.

#### 4.5. Trends and developments in survey design

As we look at the progression of surveys over time (see Figure 7 and Table 4) and consider the developments in the last  $\sim 5$  years (see Sections 4.3.6 and 4.4), some trends emerge. These include:

- **Wider surveys:** Some surveys go deep (e.g. Sarbadhicary et al. 2021), but more surveys are going as wide as feasible (e.g. Murphy et al. 2021; Lacy et al. 2020) at the expense of depth. The advantages this offers in terms of transient rates can be debated, but having brighter sources certainly makes followup and classification easier. Planned future surveys will be able to go both deeper and wider than currently possible (Adams & van Leeuwen 2019).
- **Galactic transients:** More surveys are concentrating on Galactic sources (Murphy et al. 2021; Frail et al. 2024; Hurley-Walker et al. 2023), especially in the Galactic plane. This represents a shift from the extragalactic synchrotron transients targeted in previous surveys (e.g. Mooley et al. 2016), and is related to instruments that focus on lower frequencies ( $\lesssim 1.4$  GHz) where the synchrotron transients are slow and faint. Instead, searches for faster, often coherent, sources in the Galactic plane (Wang et al. 2022a; Pritchard et al. 2021) are becoming prominent.
- **Polarisation products:** Surveys are increasingly producing full polarisation products (e.g. Shimwell et al. 2017; Murphy et al. 2021), and in particular, circular polarisation. This works together with the targeting of Galactic sources mentioned above.
- **Many epochs:** Surveys are increasing from 2–3 epochs that are only sufficient for identification/discovery, to multiple ( $\gtrsim 10$ ) epochs (e.g. Murphy et al. 2021), which enables source classification and probing of different timescales.
- **Short-timescale imaging:** Even when a survey only has a small number of observing epochs (including single-epoch surveys), it is now possible to reprocess the data on multiple timescales to reveal faster behaviour (e.g. Wang et al. 2023; de Ruiter et al. 2024). This approach is most relevant to Galactic sources (de Ruiter et al. 2025), and a major early driver was detecting fast radio bursts (e.g. Tingay et al. 2015), but it has also revealed some scintillating extragalactic sources (Wang et al. 2021a).

The VLA Sky Survey (Lacy et al. 2020) stands apart from some of these trends, drawing on the success of the Caltech-NRAO Stripe 82 Survey (Mooley et al. 2016, and following papers). It operates at 3 GHz, consists of 3–4 epochs, and has yet to release circular polarisation data. Note that unlike some other surveys, VLASS was designed not solely as a transients survey, but with a broad set of science goals, even though much of the justification for the multiple epochs do come from the time domain. Perhaps

because of these aspects, it has been very successful in discovering extragalactic synchrotron transients that other current surveys do not probe as well (Somalwar et al. 2023; Stroh et al. 2021; Dong & Hallinan 2023; Dong et al. 2021; Somalwar et al. 2025b,a).

Overall, the combination of newer instruments (e.g. ASKAP, MeerKAT), newer techniques (Wang et al. 2023; Fijma et al. 2024; Smirnov et al. 2025a) and new targets along with increasing investment of telescope time has allowed both the scope of the surveys to increase together with their yield. We expect that future developments in instrumentation (SKAO, ngVLA, DSA-2000, LOFAR2.0) will allow this to continue into the next decade. These telescopes, and the prospective surveys that may run on them, are discussed in Section 7.

#### 5. Detection methods and approaches

In optical astronomy, the well-established method of finding transient sources in the image domain is via image subtraction (e.g. Zackay et al. 2016). This approach has been used in major projects, for example, the Palomar Transient Factory (Law et al. 2009) and the Zwicky Transient Facility (Bellm et al. 2019). However, the limited sampling of the  $uv$ -plane makes this less straightforward in radio astronomy, and in general, a catalogue cross-matching approach has proved more successful. Catalogue cross-matching is also used in some major optical projects, for example the Catalina Real-Time Transients Survey (Drake et al. 2009).

Regardless of the approach, calibration and imaging artefacts are a significant issue in radio transient surveys, and, as in optical surveys, can result in false ‘transients’. For example, many of the transient candidates reported by Bower et al. (2007) from their analysis of archival VLA data were later found to be artefacts, or the result of calibration errors (Frail et al. 2012).

In this section we review the main transient detection methods used in radio transient surveys, as well as some of the main approaches to follow-up, monitoring and source identification.

##### 5.1. Image subtraction and difference imaging

In the optical domain, image subtraction is a core part of most transient detection pipelines. The typical approach used is to form a reference image from the first  $n$  observations of a given field (or from dedicated deep observations). Each subsequent observation of that field is then astrometrically aligned with the reference image using a catalogue of extracted sources, and convolved to a common resolution. The new image is subtracted from the reference image following Alard & Lupton (1998); Alard (2000) or similar (e.g. Zackay et al. 2016). Sources that are unchanged are effectively removed, leaving sources that have appeared, disappeared or changed substantially in brightness between the observations. These transient sources are detected in the subtracted images using source finding software such as SExtractor (Bertin & Arnouts 1996). This approach (and variations on it) has been used in many major optical transients surveys (e.g. Wozniak 2000; Riess et al. 2004; Law et al. 2009; Bellm et al. 2019).

In radio images, the sparse sampling of the  $uv$ -plane results in artefacts of a number of kinds, including ghost sources (e.g. Grobler et al. 2014) and sidelobes near imperfectly modelled bright sources (e.g. Polisensky et al. 2016). Hence when image subtraction is used, the resulting images are dominated by these artefacts, rather than genuine transient sources. As a result,

although there was a lot of experimentation with image subtraction in early radio transient surveys, it has had very limited use in published results. One example is Varghese et al. (2019) who detect a transient using two Long Wavelength Array stations, via image subtraction, as described by Obenberger et al. (2015).

A variation on image subtraction that is only possible in radio astronomy is visibility differencing and imaging, also just called ‘difference imaging’. In this case, the subtraction can be done using the model visibilities, hence removing the need for the (generally time-consuming) image deconvolution stage. There are a few examples of this (e.g. Law et al. 2018a) but it has not been widely used.

A further variation is making a deep reference image and subtracting this continuum image from snapshot images with much shorter integration times from the same data-set (this is possible since the correlator integration time of 1–10 s is typically much smaller than the image integration time). This is appropriate only for transients with small duty cycles such that they do not appear in the deep image, or significant variability, and has been used in a number of recent projects, for example Wang et al. (2021b, 2023); Fijma et al. (2024); Smirnov et al. (2025a). See also the discussion in Section 5.4.

In current (and future) surveys with improved *uv*-coverage, image subtraction and difference imaging are becoming feasible approaches for radio transient detection. In addition, if there is full control over the observation strategy, some of the above problems mentioned in this section may be mitigated. For example, if the images to be subtracted are observed at the same local sidereal time, it reduces the image of residual synthesised beam sidelobes (although changes in beam shape due to ionospheric refraction or differences in flagging may still be present). In practice, this is difficult to achieve, but should be considered in the design of current and future automatic schedulers.

## 5.2. Other direct image analysis techniques

A technique related to difference imaging is variance imaging. In this approach, an image is created from either a frequency (or time) cube by computing the variance of each pixel across all frequency (or time) channels. This has been proposed as a way of detecting new pulsars via their interstellar scintillation (e.g. Crawford et al. 1996). This technique has not been widely used, but has discovery potential with the increased sensitivity and frequency resolution of current imaging surveys (e.g. Dai et al. 2016, 2017; Morgan et al. 2018).

Another approach is the use of matched filters — which are in general an optimal statistic for detection (e.g. Helstrom 1995) directly on image pixels. One component of the rms noise in radio images is the classical confusion noise, which comes from the background of faint, unresolved sources (Condon 1974). For telescopes with low angular resolution, this can become a dominant factor in the total noise. In this ‘confusion-limited’ regime, matched filter techniques might be useful. Applying a matched filter involves searching for a signal of a known or approximate functional form (e.g. a top-hat), taking advantage of the fact that nearly all of the background sources contributing to the confusion noise are static with time. This approach is used widely in signal processing in engineering, and in gravitational wave detection (e.g. Allen et al. 2012). It has not been used widely in radio transient detection, but one example implementation is given by Feng et al. (2017) for a transient search with the MWA.

Matched filters are also useful when searching for a particular class of transients in catalogue data (rather than image cubes); for example, searching for gamma-ray burst afterglows (Leung et al. 2023). In cases like this, slowly evolving lightcurves mean the sources of interest may not be highly variable using traditional metrics, and hence a matched filter is more effective for discovery. See Section 6.1.5 for further discussion of this topic.

## 5.3. Catalogue cross-matching

A vast majority of radio transient imaging surveys use a transient detection approach that follows these basic steps:

1. **Image** each epoch of data;
2. Run **source-finding** software on each image to extract sources above a noise threshold;
3. **Associate** sources from different epochs with each other via positional cross-matching;
4. **Measure** upper limits in cases where a previously detected object is not detected;
5. Create **lightcurves** for each detected object;
6. Use various metrics to **identify** transients and highly variable objects.

There are many variations on how each of these steps is implemented (or whether the step is done at all). Two key examples of this approach that have been formalised into software pipelines are the LOFAR Transients Pipeline (Trap; Swinbank et al. 2015) and the VAST Pipeline (Pintaldi et al. 2022). In an ideal survey, transient detection would work in real time, as part of the imaging processing pipeline; to allow immediate identification and follow-up of transients. However, to date, the computational challenges of rapid imaging have meant that most projects have done their image-based transient detection in an offline or batch mode. See, for example, recent results from ASKAP VAST (Murphy et al. 2021), LOFAR (Kuiack et al. 2021) and MeerKAT (Rowlinson et al. 2022).

In the rest of this subsection we briefly describe each of the steps in the catalogue cross-matching approach, pointing the reader to the relevant papers for more detailed explanations. Discussion of radio interferometric imaging is beyond the scope of this paper, so we will assume the imaging has already been done on the relevant timescale. Transient and variability metrics will be discussed in Section 6.1.

### 5.3.1. Source finding

The goal of source finding software is to identify astronomical objects in radio images. The typical approach to this is to identify statistically significant collections of pixels (‘sources’) and ‘extract’ them by fitting elliptical Gaussians to measure their properties: position, angular size and flux density (note that the more general radio source finding approach can consider more complex source shapes, but transients are assumed to be point sources, although they can be in complex regions).

In optical astronomy, one of the most well-used source finding packages is SExtractor (Bertin & Arnouts 1996), and many large projects use their own custom software (e.g. Masci et al. 2019) that works in a similar way. However, the needs for radio source finding can be both more complex and simpler than in the optical. For instance, in the radio the typical noise properties of the images are different (adjacent pixels in a restored image are

correlated in the radio, but not in the optical); images are usually restored with a single beam shape that is not subject to seeing variations (although there can be ionospheric effects and variations due to RFI flagging); there are often multiple simultaneous images to search (e.g. as a function of frequency or polarisation), and imaging artefacts are usually deconvolution sidelobes rather than halos, satellite trails, and cosmic rays. These limitations and differences led to the development of radio-specific source finding packages for continuum surveys.

Source finding is a significant focus for radio continuum surveys as we prepare for the SKAO. See, for example, the results of the ASKAP Evolutionary Map of the Universe (EMU; Norris et al. 2011; Hopkins et al. 2025) Source Finding Data Challenge (Hopkins et al. 2015) and the Square Kilometre Array Science Data Challenge 1 (Bonaldi et al. 2021). However, many of the most challenging aspects (such as characterising sources that are diffuse or have a complex morphology) are not as relevant for radio transient surveys where the objects of interest are expected to be intrinsically compact<sup>n</sup>.

Nevertheless, there are some aspects of source finding of particular importance to radio transient surveys. For example:

- Speed: if source finding is running as part of real-time processing then it needs to be computationally efficient without reducing reliability and completeness;
- Identifying sources with negative flux density: for example in the case of circular polarisation (Stokes V) images in which sources can have either sign of polarisation;
- Source finding in the  $uv$ -plane: an alternative to image-plane source finding that can be useful when rapid processing is needed, but requires modelled sources to subtract.

Some of the main source finding packages used in current radio transients surveys are: Selavy (Whiting & Humphreys 2012) used in the ASKAP workflow; AEGEAN (Hancock et al. 2012a, 2018), used in GLEAM-X (Hurley-Walker et al. 2022a); and PyBDSF (Python Blob Detector and Source Finder, Mohan & Rafferty 2015), used in RACS (Hale et al. 2021) and LoTSS (Shimwell et al. 2019). A summary of the main aspects of radio source finding, for example background noise estimation, island-finding and deblending (shared by many of these packages) is given by Lucas et al. (2019). A comparison of the performance of some of these packages (with a focus on continuum survey science applications) is given by Boyce et al. (2023).

### 5.3.2. Source association

Once sources have been identified and fit in each individual epoch, the next step is associating detections of the same object throughout multiple epochs. This is done via positional cross-matching. Both the TraP and VAST pipelines cross-match using the ‘de Ruiter radius’ (de Ruiter et al. 1977): the angular distance on the sky between a source and its potential counterpart in the next epoch, normalised by the positional error of both sources.

To achieve optimal results in source association there are a number of issues to consider. These include how to deal with variable image quality between epochs and how to ensure unique matches in cases where multiple potential matches are identified. There are also computational challenges when scaling this up

<sup>n</sup>There are cases, particularly at lower frequencies, where a compact variable object is embedded in extended or diffuse emission. For example, a pulsar within a supernova remnant, or the core of a radio galaxy within extended lobes.

to large datasets with many repeated fields. These issues are discussed in more detail by Swinbank et al. (2015).

### 5.3.3. Lightcurve creation

Source association produces a lightcurve of flux density measurements with time for all epochs in which the source was detected. To make a more complete lightcurve most pipelines measure either (i) limits or (ii) forced fit parameters for each source in each epoch in which it is not detected (this is also done for optical transient surveys, e.g. Masci et al. 2023). Limits are typically based on the local rms noise in the region of the source (a more computationally efficient but less accurate alternative is to use the overall rms noise of each image). Forced fitting involves fitting an elliptical Gaussian at the known position of the transient source. In both cases, the implementation approach depends on whether the pipelines are running in real time (and hence cannot access previously observed images, beyond a given buffer) or in an offline or batch mode.

Subsequent analysis, such as applying variability metrics, searching for periodic behaviour, or doing automatic classification, is performed on the resulting lightcurves.

## 5.4. Short-timescale (‘fast imaging’) approaches

As mentioned in Section 1.3, almost all radio transient surveys to date have been designed to detect either ‘fast’ (timescales  $<$  seconds) transient behaviour, via single-dish/beamformed observations (with typical time resolution of 10s to 100s of microseconds), or ‘slow’ (timescales  $>$  seconds) transient behaviour via imaging (with maximum time resolution of  $\sim 10+$  seconds). These two regimes have substantially different observational, technical and computational approaches.

However, in recent years, the discovery of (a) very slow pulsars (e.g. Tan et al. 2018; Caleb et al. 2022); (b) long-period radio transients (e.g. Hurley-Walker et al. 2022b; Caleb et al. 2024), and (c) the need to localise fast radio bursts (e.g. Chatterjee et al. 2017; Bannister et al. 2019) has motivated the exploration of the 100 ms – 10 s timescales that fall between these two regimes.

This missing region of parameter space has been approached from opposite directions. The first has been to take the fast transients approach, but incorporate imaging on (relatively) coarse timescales. These systems build on the success of single dish pulsar projects, by taking advantage of the localisation capabilities of interferometers. For example, the *realfast* system (Law et al. 2018a), running on the VLA (and inspired by V-FASTR on the VLBA; Wayth et al. 2011), uses an alternative approach to traditional imaging, made possible by the low density of sources in any given field on timescales of  $\sim 10$  ms. Unlike the image-subtraction below, this subtracts the mean visibilities on  $\sim$ s timescales to remove constant sources, creates ‘dirty’ images for a range of integration time and dispersion measure, and then uses a matched filter to identify dispersed point sources for subsequent analysis. This approach resulted in the first localisation of a fast radio burst (Chatterjee et al. 2017) as well as identification of unusual bursts from a Galactic  $\gamma$ -ray source (Anna-Thomas et al. 2024).

More recently, Wang et al. (2025b) developed the Commensal Realtime ASKAP Fast Transient COherent (CRACO) system, which is another example of a system that comes from a pulsar-inspired background. CRACO images on 110 ms timescales, with plans to increase this to higher resolutions. It works on-the-fly, and can only store a relatively small buffer of

images for sources of interest. An early result from CRACO is the detection of a long period transient with a 44.3 minute period (Wang et al. 2025c).

The second approach is to perform standard radio imaging, on much shorter timescales than the observation length. This has been impractical for most earlier radio surveys due to the limited *uv*-coverage of the instruments. Prior to the past year, there were only a small number of projects that did imaging transient searches on very short ( $\sim 10$  s) timescales (e.g. Obenberger et al. 2015; Kaplan et al. 2015; Tingay et al. 2018). However, the low angular resolution and relatively poor sensitivity of the instruments used in those studies (LWA and MWA) at the time these searches were conducted meant the ability to detect many transient phenomena was limited.

The current set of interferometers, with a large number of dishes or antennas, and hence much improved instantaneous *uv*-coverage have made imaging (or re-imaging) on short timescales possible. One example of this approach is the fast imaging of MeerKAT data on 8 s timescales by Fijma et al. (2024). Another example is the VASTER fast imaging pipeline (Lee et al. 2026) which images ASKAP data on 10 s and 10 min timescales. Both of these projects ran the fast imaging in offline, batch-mode.

A significant step towards online/realtime fast imaging is TRON (Transient Radio Observations for Newbies), which can image MeerKAT data on 8 second timescales (Smirnov et al. 2025a). So far it has been used to search archival imaging data, resulting in the detection of millisecond pulsars (Smirnov et al. 2025a) and a stellar flare (Smirnov et al. 2025b). At the time of writing, work is underway to get TRON running in realtime on MeerKAT (I. Heywood, *private communication*) and VASTER is running in realtime on ASKAP (Y. Wang, *private communication*), although results from these modes have not yet been published.

These early explorations have already produced some interesting results. The next step is to make these approaches more computationally efficient, and integrate them into the standard processing pipelines for current and future telescopes.

### 5.5. Multi-wavelength identification

Radio data alone is rarely sufficient to allow the class of a given transient candidate to be identified. There are a few exceptions, most notably pulsars and fast radio bursts, although if they are discovered in imaging data, beamformed or single-dish observations are needed to confirm them (see Kaplan et al. 2019 for a pulsar example and Bhandari et al. 2020 for an FRB example).

Typically, multi-wavelength data is required to confirm the source type of a radio transient. For example the gamma-ray counterpart of a GRB afterglow, the optical counterpart of a radio supernova, the optical/IR counterpart of a star, or the quasar responsible for observed scintillation. Even within the radio regime, multiple radio frequencies may be needed to understand the nature of a new transient (such as its spectral behaviour and evolution). This multi-wavelength data may exist in archival observations, or may require dedicated follow-up observations. Related to this is dedicated imaging at higher angular resolution (which might require different instruments, different frequencies, or both). Such data can be vital for establishing precise positions for counterpart identification, such as in crowded regions of the Galactic plane (Caleb et al. 2024) or within a host galaxy (Dong & Hallinan 2023).

It is beyond the scope of this paper to discuss the many ways of identifying different classes of objects, and all their associated challenges and subtleties. However, we have summarised some of

the common checks that are conducted in Table 5. This is intended as a high-level guide to common practice, rather than a detailed implementable method.

The relatively small number of radio transients detected in surveys to date means that this exploration has been done manually. However, as the number of detections increases, automatic methods are becoming more important, and we discuss these in Section 5.7.

### 5.6. VLBI observations

For the most part, observations using Very Long Baseline Interferometry (VLBI) function as a follow up technique for radio transients identified elsewhere. VLBI can provide a critical role in determining the geometry and expansion rate of relativistic explosions (e.g. Taylor et al. 2004; Bloom et al. 2011; Mooley et al. 2018a; Giarratana et al. 2024), separating the components of gravitational lenses (e.g. Springola et al. 2016), identifying jet ejection and kinematics in X-ray binary microquasars (e.g. Dhawan et al. 2000, 2007; Stirling et al. 2001; Miller-Jones et al. 2019; Wood et al. 2021), or eliminating star-formation regions from searches for FRB persistent radio sources (e.g. Bruni et al. 2024b). Similarly, for Galactic sources it can be used to determine parallax distances and help constrain energetics (e.g. Miller-Jones et al. 2021).

However, we do note that VLBA-like systems can be used for transient discovery, such as the VLBA Fast Radio Transients Experiment (V-FASTR; Wayth et al. 2011). In this case it is searching for events like FRBs, evaluating incoherent sums between antennas on ms timescales. A detailed discussion of this approach is outside the scope of this review.

### 5.7. Machine learning and classification

The aims of transient searches are to: (a) identify, and study the nature of, individual objects; (b) understand populations of variable sources; or (c) use the transient objects as probes of our Galaxy or extragalactic space. To achieve any of these aims, classifying the source is critical. Typically this involves measuring radio properties of the source either from radio images or its lightcurve, and searching for multi-wavelength associations. Doing this work manually is laborious, and consists of making decisions based on an extensive list of parameters and rules — some of which are strictly deterministic and others of which require judgement. These factors make transient source classification an ideal task for supervised machine learning.

Supervised machine learning is the use of algorithms that improve automatically through experience, to classify data (Mitchell 1997). The basic methodology involves extracting features (measuring properties) from the dataset; then training a model that maps these features to a set of known classes. The model is evaluated using metrics such as precision, recall and overall accuracy. When suitable performance is achieved, the model can then be applied to new datasets.

Machine learning has been widely used in astronomy: see Ball & Brunner (2010), Fluke & Jacobs (2020) and Huertas-Company & Lanusse (2023) for overviews, and see Buchner & Fotopoulou (2024) for a useful how-to guide for beginners. A variety of algorithms have been applied to time-domain astronomy, tackling a wide range of classification tasks. For example, the classification of variable stars using random forests (Richards et al. 2011b), photometric supernova classification (Lochner et al. 2016)

**Table 5.** A high-level summary of the types of multi-wavelength data and checks used to identify radio transient candidates.

Waveband	Check	What it tells us	Relevant classes	Notes
Radio	Detection in archival reference surveys	Long-term variability, spectral index	All	Check for detections in NVSS, SUMSS, FIRST, RACS, GLEAM, TGSS, VLASS...
Radio	Detection in archival targeted observations	Long-term variability, spectral index, astrometry, shape	All	Check for detections in VLA, ATCA, GMRT archival observations
Radio	Linear and circular polarisation	Polarisation properties	Stars, pulsars, LPTs	Linear polarisation may need Faraday rotation check
Radio	Dynamic spectrum	Short-timescale variability, spectral structure	Stars, pulsars, LPTs	Need good signal-to-noise ratio
Radio	Lightcurve periodicity	Whether source has periodic behaviour	Stars, pulsars, LPTs	
Radio	Cross-match with pulsar and FRB catalogues	Whether source is a known pulsar or FRB	Pulsars, FRBs	Sources can be poorly localised, need a careful choice of match radius <sup>a</sup>
Optical/IR	Detection in archival reference surveys	Possible counterpart or host galaxy	All	
Optical/IR	Detection in telescope observing archives	Possible counterpart or host galaxy	All	Check deepest observations available (e.g. ESO archives)
Optical/IR	Cross-match with stellar catalogue	Possible stellar counterpart	Stars	Cross-match with Gaia. Care is needed due to high false-positive rate <sup>b</sup> and large proper motions
Optical/IR	Cross-match with quasar catalogue	Possible AGN counterpart or host galaxy	AGN	Check SDSS, milliquas
Optical/IR	WISE colour-colour plot	Broad classification of source type	Galaxies, AGN, stars	Need to check WISE counterparts are real associations
Optical/IR	Get optical lightcurves	Whether sources is optically variable	All	Check <i>TESS</i> , ZTF, etc.
X-ray	Check X-ray source catalogues and archives <sup>c</sup>	Possible counterpart	All	May need to include variability search within observations
Gamma-ray	<i>Fermi</i> source catalogue	Possible counterpart	GRBs, pulsars, AGN	
General	Cross-match with known objects	Whether source is already catalogued	All	Check for match in SIMBAD, NED, Vizier and other catalogues
General	Cross-match with known transient events	Possible association with known event	GRBs, SNe, TDEs, XRBs, Novae	Check GCNs, ATels, Transient Name Server <sup>d</sup>
General	All solar system planet ephemerides	Whether source is a planet (or the Moon)	Solar system planets	Need accurate position and time of observation

<sup>a</sup> The Pulsar Scraper includes both published, and announced-but-unpublished pulsars, and can be accessed at <https://pulsar.cgca-hub.org/>.<sup>b</sup> See Driessen et al. (2024) for a full analysis of cross-matching with stellar catalogues, including how to select a suitable match radius.<sup>c</sup> NASA's High Energy Astrophysics Science Archive Research Center can be accessed at <https://heasarc.gsfc.nasa.gov/docs/archive.html>.<sup>d</sup> The Transient Name Server can be accessed at <https://www.wis-tns.org/>.

and separating real from bogus events in the Zwicky Transient Facility (Duev et al. 2019).

Most of the work in machine learning classification of radio transients has focused on the fast transients domain, where there are many candidates, significant computational challenges, and a need for real-time (or rapid) detection (e.g. Wagstaff et al. 2016; Agarwal et al. 2020) because the large data volumes prohibit full storage. In the image domain, efforts have been somewhat limited by a lack of training data, and the lack of surveys producing large numbers of transient and highly variable sources. We discuss the key work in the following subsections. Most of the efforts to date have been supervised approaches (see Section 5.7.1), which can only recover class types that have already been identified. However, there has been some exploration of unsupervised approaches, which we touch on briefly in Section 5.7.2.

### 5.7.1. Radio lightcurve classification

One of the primary data products of a multi-epoch survey is radio lightcurves. Radio data alone does not typically provide enough information for a firm classification for many sources types: this usually requires multi-wavelength information (e.g. Mooley et al. 2016; Rowlinson et al. 2022). However, the lightcurves of different source classes do have different time-dependent features, as shown in Figure 8. For example: radio supernovae have a rapid rise followed by a power-law decay; flaring stars show short, discrete bursty behaviour that is sometimes periodic; and scintillation appears as stochastic fluctuations with characteristic amplitudes and timescales. Some sources classes (e.g. synchrotron transients) also show frequency dependent time evolution, and others such as pulsars and long period transients show variability in their polarisation fraction (these dimensions are not captured in Figure 8).

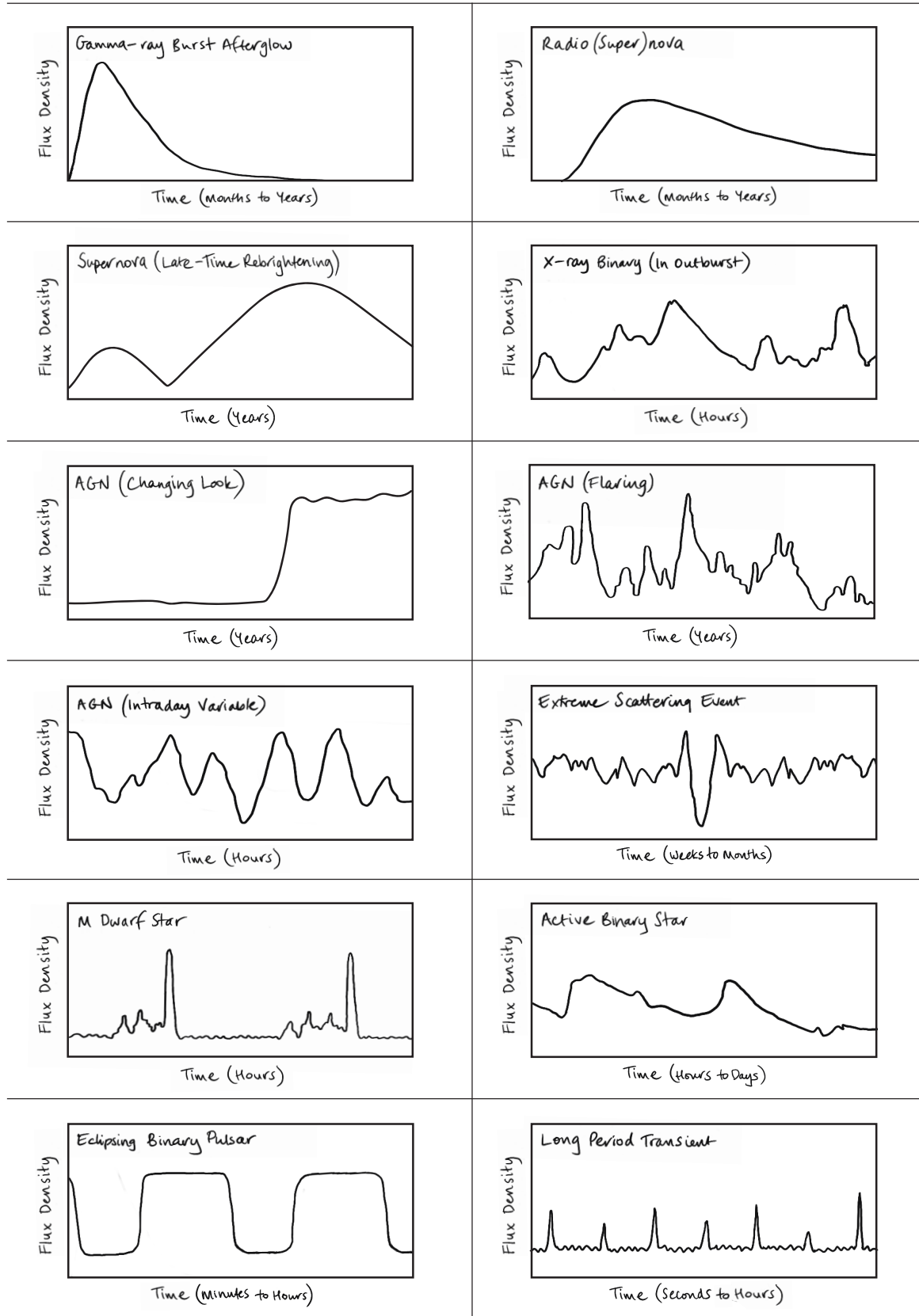


**Figure 8.** Sketches of lightcurves for a range of radio transient source types. The lightcurves capture qualitatively different variability with rough timescales indicated. We have not attempted to capture spectral energy evolution, polarisation fraction, or the typical flux density scale. Not all source types are included; for example other synchrotron transients such as TDEs will show qualitatively the same evolution as GRB afterglows. Note that many source classes exhibit variability on multiple timescales. Most of the sketches are inspired by real data, as listed: AGN intraday variability (Bignall et al. 2003); AGN flaring (Hovatta et al. 2008); Changing look AGN (Meyer et al. 2025); supernova re-brightening (Anderson et al. 2017); active binary star (Osten et al. 2004); X-ray binary (Fender et al. 2023); eclipsing binary pulsar (Zic et al. 2024); M dwarf star (Zic et al. 2019); extreme scattering event (Bannister et al. 2016); long period transient (and long period pulsars) (Wang et al. 2025d).

As a result of the lack of suitable training data (i.e. observed, well-sampled radio lightcurves from a range of source types), the first efforts in automatic classification of radio transients used simulated datasets (e.g. Rebbapragada et al. 2012; Murphy et al. 2013). These were useful as a proof-of-concept, but the simulated lightcurves did not account for the full complexity (or the poor sampling) of real survey data.

Following this, there were various efforts that focused on specific aspects of classification. Pietka et al. (2017) focused on the timescale of variability as a key feature in determining an initial classification for radio transient lightcurves. They automatically measured the rise rate of  $\sim 800$  synchrotron flares from a range of source types to define a probability distribution of timescales for each source type. While the predictive power of a single property is naturally limited, the intention was that this would be a useful component of a more comprehensive classification process.

Along similar lines, Stewart et al. (2018) investigated radio versus optical flux density as a means of making a preliminary classification of radio transients. They showed that different source types do fall (broadly) into different regions of this two-parameter space. For example, quasars tend to have quite a high radio to optical flux density ratio, whereas stars typically have a much lower one. Wang et al. (2022b) took this further and used radio to near-infrared (to be more robust against extinction) flux ratio versus circular polarisation fraction, showing that the locations of pulsars and stellar sources (the two main classes of sources with significant polarisation) were very different. And Wang et al. (2025c) compared X-ray and radio fluxes (drawing on the radio/X-ray correlation plots for accreting sources; e.g. Gallo et al. 2003; Russell et al. 2016; Ridder et al. 2023), showing that LPTs occupied an extreme region of that space distinct from other potentially related populations like low-mass X-ray binaries, stars, and cataclysmic variables, but did resemble magnetars. As with the timescale of variability, these metrics alone are not enough to definitively classify objects, but would be useful parts of a classification pipeline.

The most comprehensive attempt to classify radio transient lightcurves to date is that by Sooknanan et al. (2021), based on an approach presented by Lochner et al. (2016) for optical lightcurves. They addressed the limitations of the currently available data in several ways: (1) they interpolated a set of real lightcurves (from Pietka et al. 2015 and Dobie et al. 2018) so they have equivalent sampling; (2) they augmented this set of lightcurves to produce a larger, more balanced training set; and (3) they incorporated some external contextual information, such as whether the object is in the Galactic plane, and the object's optical flux density. The classifier achieved  $\sim 75\%$  accuracy for a 5-class problem (AGN, GRBs, XRBs, Novae and SNe), a promising result, but with significant room for improvement.

Automatic classification of radio transients is on the cusp of becoming a reality for large surveys. The machine learning techniques are well-established in optical time domain surveys, and some of the additional challenges presented by radio surveys have been investigated in isolation. With the much larger datasets resulting from current surveys, it should be possible to train pipelines that work effectively, at least to provide an initial classification that can be further investigated manually.

### 5.7.2. Anomaly and outlier detection

One of the aims of radio transient surveys is to detect rare classes of objects, or unusual examples of existing classes. Anomaly

detection is a type of unsupervised machine learning that involves searching for data points that do not conform to the normal properties of a given dataset (often called outliers), making it well suited to this task. The methods for identifying anomalies range from well-established statistical techniques, through to more sophisticated algorithms. For a comprehensive review of anomaly detection techniques and applications in science, engineering and business, see Chandola et al. (2009). For a review of anomaly detection methods applied to time series data, see Blázquez-García et al. (2021).

In time-domain astronomy, anomaly detection approaches have been demonstrated on a range of tasks. For example, searching for unusual objects in Kepler light curves (Giles & Walkowicz 2019; Martínez-Galarza et al. 2021). Both of these projects were motivated by the serendipitous discovery of Boyajian's star KIC 8462852 (Boyajian et al. 2016), and the need to prepare for, and capitalise on, the increased discovery potential for unusual objects that will come with the Vera Rubin Observatory 10-year Legacy Survey of Space and Time (LSST; Ivezić et al. 2019).

Lochner & Bassett (2021) present a general framework for anomaly detection aimed at astronomy applications. It incorporates active learning, with the ability for the expert user to rank and categorise the results. Their approach is demonstrated on a set of 50 000 simulated lightcurves that represent typical (99%) and outlier (1%) sources. Andersson et al. (2025) is the first group to apply this approach to observed radio transient lightcurves. Using data from ThunderKAT, they were able to recover interesting outlier sources (as defined by citizen science volunteers — see Section 5.7.3) with some success, giving results that are complementary to other approaches. This area of research shows promise for future, larger, radio transient surveys.

### 5.7.3. Citizen science projects

Citizen science projects (one of the first, and most influential of which, was SETI@HOME; Werthimer et al. 2001) are designed to leverage the enthusiasm of members of the public to help complete large scale scientific data collection and classification, either using only their personal computer facilities (as in the case of SETI@HOME) or using the citizens themselves to help analyse data. In astronomy, a pioneering project in this space was Galaxy Zoo (Lintott et al. 2008) which invited the general public to visually inspect and classify the morphology of nearly a million galaxies from the Sloan Digital Sky survey (Lintott et al. 2011). The success of the initial Galaxy Zoo project led it to broaden its remit to the Zooniverse. This platform, and other similar approaches, have been applied to a wide range of classification tasks including gravitational wave glitch identification (Zevin et al. 2017), exoplanet discovery (Christiansen et al. 2018), and radio galaxy classification (Lukic et al. 2018).

The first (and, to date, only) citizen science project for classifying image domain radio transients is the ‘Bursts From Space’ project on MeerKAT (Andersson et al. 2023). They had  $\sim 1000$  volunteers who provided  $\sim 89$  000 classifications of sources using images and lightcurves. Sources were classified into five classes: Stable, Extended Blobs, Transients/Variables, Artefacts and Unsure. From this, 142 variable sources were identified, most of which the authors conclude are likely to be AGN. The amount of data available from current and future radio surveys should allow similar projects with more detailed classification schema.

## 6. Characterising the time variable sky

There are two major aspects to characterising the dynamic radio sky. The first is how to measure and compare the variability of individual objects. In Section 6.1 we describe some of the main metrics used to do this, and discuss the advantages and disadvantages of each. The second is how to characterise the population of highly variable radio sources, against the background radio source population. In Section 6.2 we discuss this in the context of what we know from current radio transient surveys.

### 6.1. The variability of individual objects

To understand the time variable sky we need a way of identifying and characterising the variability of individual radio sources. There are a range of metrics for identifying variable sources that have been used in the literature. In some cases, the aim is to identify the most highly variable objects for further monitoring, in other cases the aim is to characterise the time behaviour of the entire radio source population.

In this section we focus on metrics for identifying variability. Classification of sources into different discrete types (e.g. supernovae vs. stars) is covered in Section 5.7.

#### 6.1.1. Basic metrics

For surveys with a small number of epochs, the simplest way of measuring the variability of a source is to take the maximum difference between the observed flux density values at different times. For example, Carilli et al. (2003) used:

$$\Delta S = |S_1 - S_2| \quad (6)$$

the absolute change in flux density,  $S$ , between two pairs of two epochs (in their case, 19 days and 17 months apart). To determine if this difference was significant, they compared the value of  $\Delta S$  to the  $5\sigma$  image rms noise. Sources that exhibited the most extreme variability of 100%, would be detected in one epoch and not the other. These have typically been referred to as transients in the literature (but see Section 1.3 for a discussion of terminology).

This approach was also used by Levinson et al. (2002) in their search for orphan afterglows between the FIRST and NVSS surveys. When the two epochs have significantly different sensitivity limits, additional care is required. Levinson et al. (2002) chose a flux density cutoff designed to exclude (most) persistent sources fluctuating around the sensitivity limit.

A related approach is the fractional variability  $V$  used by Gregory & Taylor (1986):

$$V = \frac{S_{\max} - S_{\min}}{S_{\max} + S_{\min}}, \quad (7)$$

where  $S_{\min}$  and  $S_{\max}$  are the minimum and maximum flux density, respectively. This metric is only appropriate for data with a small number of measurements. However, the modulation index below can be considered a more sophisticated version of this metric.

Rather than consider a difference between values, de Vries et al. (2004) looked at the ratio between two flux densities  $S_1$  and  $S_2$ , which they called the variability ratio,  $VR$ :

$$VR = S_1/S_2 \quad (8)$$

This was modified to account for the varying noise levels in the different epochs, which could be functions of the flux densities themselves (most appropriate for bright sources).

All of these metrics are inherently limited, and for surveys with many observations of each source, a more sophisticated approach is preferred.

#### 6.1.2. $\chi^2$ probability

Another way of measuring overall variability is to calculate the  $\chi^2$  value for a model where the source remained constant over the observing period:

$$\chi^2_{lc} = \sum_{i=1}^n \frac{(S_i - \bar{S})^2}{\sigma_i^2} \quad (9)$$

where  $S_i$  is the  $i$ th flux density measurement with variance  $\sigma_i^2$  within a source light curve, and  $n$  is the total number of flux density measurements in the light curve.  $\bar{S}$  is the weighted mean flux density defined as:

$$\bar{S} = \sum_{i=1}^n \frac{S_i}{\sigma_i^2} / \sum_{i=1}^n \frac{1}{\sigma_i^2} \quad (10)$$

This has been used for a number of variability monitoring programs, for example Kesteven et al. (1976); Gaensler & Hunstead (2000); Bell et al. (2014). Kesteven et al. (1976) considered a source ‘variable’ if the probability  $p(\chi^2_{lc})$  of exceeding the observed  $\chi^2_{lc}$  by chance is  $\leq 0.1\%$  and ‘possibly variable’ if  $0.1\% \leq p \leq 1\%$ . Care must be taken to consider the number of sources measured (effectively a ‘trials factor’), since with 1000 sources a single-source probability of 0.1% becomes insignificant (e.g. Bannister et al. 2011).

The probability  $p$  is independent of the number of data points, so this method can be used to compare lightcurves with different numbers of observations. However, as identified by the authors, a limitation of this metric is that it is independent of the order of the flux density measurements, and hence is not sensitive to slowly increasing or decreasing variability with time, much less more complex behaviour (cf. Leung et al. 2023).

#### 6.1.3. Modulation index

Together with  $\chi^2$ , a popular statistic is the modulation index, which is the standard deviation of the flux density divided by the (weighted) mean (e.g. Narayan 1992; Rickett 1990). This can also be written as

$$V = \frac{1}{\bar{S}} \sqrt{\frac{N}{N-1} (\bar{S}^2 - \bar{S}^2)}, \quad (11)$$

with

$$\bar{S}^2 = \sum_{i=1}^n \frac{S_i^2}{\sigma_i^2} / \sum_{i=1}^n \frac{1}{\sigma_i^2}, \quad (12)$$

and where the use of  $N-1$  in the denominator means we are using the unbiased estimator of the sample variance. This has been used extensively in radio transients analysis (for example, see Gaensler & Hunstead 2000; Bannister et al. 2011; Swinbank et al. 2015; Rowlinson et al. 2019). The modulation index, which is also called the ‘coefficient of variation,’ is often written as  $V$ , but also as  $m$  (especially in the literature around scintillation). It is an extension of the fractional variability that makes use of more than two measurements. Different authors also use weighted or unweighted means.

Yet another variant on this is also seen: a ‘debiased’ variability index (Akritas & Bershady 1996; Barvainis et al. 2005; Sadler

et al. 2006):

$$V_d = \frac{1}{\bar{S}} \sqrt{\frac{\sum (S_i - \bar{S})^2 - \sum \sigma_i^2}{N}}, \quad (13)$$

which also has extensive use in the X-ray literature (e.g., Green et al. 1999; Vaughan et al. 2003; Markowitz & Edelson 2004). This is similar to Eqn. 11 in presenting fractional variability. It typically has not used weighted sums, but attempts to account for the range in individual measurement error through the subtraction of the per-observation variance inside the radical. A downside to this is that the factor inside the radical can easily be negative for non-variable sources (rather than deal with this issue directly, other authors use a ‘normalised excess variance’ which is  $V_d^2$ ; e.g. Nandra et al. 1997; Vaughan et al. 2003). Barvainis et al. (2005) and Sadler et al. (2006) handle this in slightly different ways. They generally allow  $V_d$  to be negative when the factor inside the radical is negative, and then present the results either as a negative value or use the range of small negative and positive values to define a minimum threshold for variability, and assign this value to all numbers below it. However, we note that  $\sum (S_i - \bar{S})^2$  is distributed as a scaled  $\chi^2$  distribution for  $N - 1$  degrees-of-freedom. For well-detected sources but with minimal excess variability, the fraction of values that have the factor inside the radical negative is  $> 50\%$ . Also, as discussed extensively in the literature the exact value of this metric will depend on how the cadence of the observations compares to a typical variability timescale (when known), so in some cases more explicit parameterisations or functional forms could be used (Section 6.1.5).

#### 6.1.4. $\eta$ - $V$ parameters

It has become standard to consider both the reduced  $\chi^2$ :

$$\eta = \frac{1}{N-1} \chi_{\text{lc}}^2 \quad (14)$$

(where there are  $N - 1$  degrees of freedom) and the modulation index  $V$  together in finding variables which would have high values of  $\eta$ ,  $V$ , or both (e.g. Swinbank et al. 2015; Rowlinson et al. 2019).

Both of these statistics are based on the second moments of the flux density (i.e. variance or standard deviation), and both are independent of data order. So they should convey some similar information. However, while correlated, the outliers in  $\eta$  or  $V$  are not always the same. As discussed by Rowlinson et al. (2019), sources with high  $\eta$  usually are brighter, have some large flares or similar excursions from the mean, and have low uncertainties relative to the mean. Such lightcurves are statistically distinguishable from a constant value, although this relies on accurate calibration and error analysis at high signal-to-noise, which is not always reliable. In contrast, sources with high  $V$  typically have lower average flux densities.

This is illustrated in Figure 9, which consists entirely of simulated data with Gaussian noise and a range of signal-to-noise ratios (SNRs)<sup>9</sup> but no transients or variables beyond those expected from the noise realisations. As expected, at high  $V$  the data are dominated by low SNR sources that just happened to have slightly higher noise realisations. The trend with  $\eta$  is harder to see, but at a constant  $V$  there is a trend toward higher  $\eta$  at higher SNR. We also show the theoretical predictions for the marginal

<sup>9</sup>Note that SNR is used as acronym both for supernova remnant and signal-to-noise ratio in this review, and in the wider literature. The context usually makes it clear which meaning is intended.

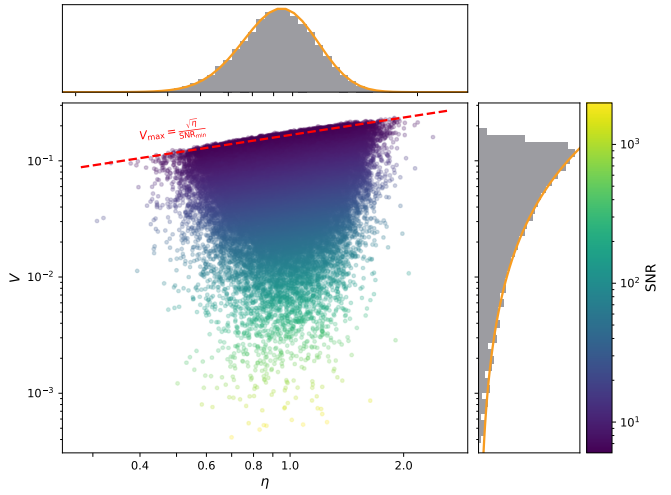


**Figure 9.** Standard  $\eta$ - $V$  plot for identifying variable sources, following Swinbank et al. (2015). The data here were simulated and consist entirely of Gaussian noise with constant amplitude. The distribution of source brightnesses are a power-law with cumulative distribution  $N(>S) \propto S^{-1.5}$ , appropriate for standard candles in a Euclidean universe (e.g., Hoyle & Narlikar 1961; Longair & Scott 1965), with SNR ranging from 6 to 2000. The points are coloured by SNR (with a colour-scale to the right). We also show marginal distributions for  $\eta$  (top) and  $V$  (right), along with theoretical predictions (solid orange lines). Finally, we show the line  $V_{\text{max}} = \sqrt{\eta}/\text{SNR}_{\text{min}}$  which bounds the top of the distribution (red dashed line).

distributions. In the case of  $\eta$  it is a scaled  $\chi^2$  distribution (as expected), which indeed resembles a log-normal distribution as discussed by Rowlinson et al. (2019). For  $V$  the distribution is largely just the distribution of  $1/\text{SNR}$ , which will depend on the underlying flux density distribution: since in this simulation  $S$  has a power-law distribution and  $\text{SNR} \propto S$  (constant noise),  $V$  also has a power-law distribution up to the maximum value but with an inverted index,  $N(>V) \propto V^{1.5}$ . This can change in other samples, though. Finally, we also see a cutoff at high  $V$  that depends on  $\eta$  as  $V_{\text{max}} = \sqrt{\eta}/\text{SNR}_{\text{min}}$ : such cutoffs are observed in real data (e.g. Rowlinson et al. 2019; Murphy et al. 2021).

This demonstration serves several purposes. Firstly, the use of both  $\eta$  and  $V$ , while common, is not necessarily optimal since they are related to each other as a function of SNR. A better second metric in addition to  $\eta$  or  $V$  might be something optimised for detecting short-timescale variability such as the result of an outlier search or a matched filter, or some other metric that incorporates information about the order of the data. Secondly, the background distribution of  $\eta$  should follow a  $\chi^2$  distribution, while that of  $V$  depends on the range of SNRs considered, and both can be used to determine thresholds for investigation.

#### 6.1.5. Other variability metrics

The metrics discussed in the previous section are related: they are both second-order statistics that depend on the degree of variability but ignore any shape/ordering of the lightcurve. Hence a number of other metrics or analyses have been used in different cases.

Perhaps the simplest is the temporal gradient  $\nabla_F \equiv dS/dt$  used by Bell et al. (2019), who also divided the gradient by its uncertainty,  $\nabla_S \equiv \nabla_F/\sigma_F$  to identify statistically significant changes. They also found that higher-order polynomial changes were not needed to describe the data.

More general parameterisations use the autocorrelation function:

$$ACF(\tau) = \langle S(t + \tau)S(t) \rangle, \quad (15)$$

which is sometimes replaced by the autocovariance function (also ACF):

$$ACF(\tau) = \langle [S(t + \tau) - \bar{S}][S(t) - \bar{S}] \rangle, \quad (16)$$

where the means are subtracted before calculation. Both of these determine the ACF as a function of lag  $\tau$ . The autocorrelation function can be used to study the timescale of variations (Rickett 1977), especially for diffractive scintillation in pulsars. A similar concept is the structure function:

$$D(\tau) = \langle [F(t + \tau) - F(t)]^2 \rangle \quad (17)$$

for all measurements in some bin with lag  $\tau$ , where  $F$  can be the raw flux density measurements (Hughes et al. 1992; Kumamoto et al. 2021), but also measurements with the mean subtracted and then normalised by the standard deviation (Gaensler & Hunstead 2000), or just normalised by the mean (Rickett & Lyne 1990; Kaspi & Stinebring 1992; Lovell et al. 2008). This is commonly used to study variability in AGN (Hughes et al. 1992; Lovell et al. 2008; Gaensler & Hunstead 2000) and pulsars (Rickett & Lyne 1990; Kaspi & Stinebring 1992; Kumamoto et al. 2021) which can be compared against the predictions for refractive scintillation (e.g. Hancock et al. 2019). Using expectations for the behaviour of the structure function with lag, it can be used to give a better definition of the modulation index and its associated timescale (e.g. Kaspi & Stinebring 1992). In both cases effort must be taken to do this correctly for irregularly-sampled data (Edelson & Krolik 1988; Kreutzer et al. 2023).

These functions are also intrinsically related to the Fourier power spectrum and its extension for irregularly-sampled data, the Lomb-Scargle power spectrum (Scargle 1982, 1989). Such power spectra can be estimated directly when searching for explicitly periodic emission, such as from eclipsing pulsar systems (e.g. Zic et al. 2024; Petrou et al. 2025). There are also many refinements to these broad techniques such as Gaussian processes (Aigrain & Foreman-Mackey 2023), but in the cases of radio lightcurves with only a few tens of data-points for most examples, the differences between the techniques are small.

Furthermore, Fourier techniques can be seen as matched filters with sine/cosine kernel functions with unknown period. This can be explored further with more specific kernels that are appropriate to specific transient types. For example, Leung et al. (2023) designed a matched filter around the expected shape of a GRB afterglow, especially orphan afterglows, parameterised as a power-law lightcurve with an optional break. Compared to selection via a standard techniques selecting sources compared to a constant model (effectively the  $\chi^2_{\text{IC}}$  in Equation 9), none of the five selected sources from that paper would have passed a more basic  $3\sigma$  threshold due to their slow evolution. Such a strategy can of course be adopted for an arbitrary light-curve shape, such as a generic burst. All of these techniques, though, require richer data sets with at least tens (if not more) samples, which are only becoming common with the latest generation of surveys.

#### 6.1.6. Burst detection

In time-domain surveys with small numbers of temporal samples (observing epochs or otherwise), there is in general no need for explicit burst detection beyond the variability analysis presented above. But as the number of samples grows, especially with short

integrations from longer images (Section 5.1), the need for explicit burst detection grows.

Historically, there has not been a large focus on burst detection from radio images, largely due to the small number of samples available. This is in contrast to the significant literature in finding and classifying bursts in other domains such as FRBs (e.g., Rajwade & van Leeuwen 2024) or XRBs and GRBs (e.g., Barthelmy et al. 2005; Meegan et al. 2009). Those cases are made further difficult by the need to examine large data-sets in real time — leading to efficient hardware implementations, machine learning classifiers, and distributed architectures — something which radio imaging surveys are only now starting to confront.

Beyond initial approaches using the metrics above or variants, there can be techniques that segment the data into ‘background’ and ‘burst’. At the simplest level, iterative sigma clipping (e.g., Leroy & Rousseeuw 1987) is often used for outlier excision (Vallisneri & van Haasteren 2017), but can be used for outlier identification as well. More complex approaches can be taken to the same problem (e.g., Hogg et al. 2010) with robust statistical models that attempt to assign probabilities to each data point regarding whether it is part of the background or not. However, these approaches may be limited in that they consider each observation independently. If the burst duration is less than the sampling time that is fine, but if bursts can last longer then techniques which take into account the temporal relation between data points may be preferred.

The basic techniques used in those cases are typically variants of matched filtering (also see Section 5.2), which is also commonly used for FRB detection (after dedispersion). Typically a Gaussian or boxcar filter (if there is *a priori* knowledge that the burst shape should be different that could of course be used instead, or a more complex basis like wavelets if there are enough samples) of a given width is convolved with the data to identify bursts, and then this is repeated for a range of widths. And as with the outlier detection metrics above, a more formal Bayesian approach can be taken here too. For instance, Scargle et al. (2013) offer an efficient algorithm that can identify segments of arbitrary length which differ from the background, and which can be applied to data arriving in real time and to data which have already been collected. This algorithm achieves similar sensitivity to the theoretical limit.

## 6.2. Populations and rates

In many previous papers, where transients were identified from 2-epoch searches in small numbers, often years after the fact (limiting followup possibilities), the results were presented as a limit or constraint on the rate (areal density) of transient sources (e.g., Bower & Saul 2011; Croft et al. 2010, 2011; Stewart et al. 2016; Rowlinson et al. 2016; Bell et al. 2011, 2015, 2014; Bhandari et al. 2018; Mooley et al. 2013); see Mooley et al. (2016) for a nice compilation that has been recently updated<sup>P</sup>. This served to help develop expectations for improved surveys, as well as understand the discovery rate relative to the expected rates of various source populations (e.g., Metzger et al. 2015b). This analysis particularly applied to synchrotron transients, which have very similar lightcurves.

However, the changes outlined in Section 4.5 have changed this practice. Firstly, using multi-epoch surveys makes the distinction between transients and variables less clear. Although

<sup>P</sup>See <http://www.tauceti.caltech.edu/kunal/radio-transient-surveys/index.html>.

some sources are clearly explosive in origin and hence intrinsically ‘transient’, many of the sources identified by earlier surveys are more clearly examples of variable sources when richer data sets are used (e.g., Murphy et al. 2021). This also means that lightcurve shape can influence the inferred transient rate explicitly, as described in detail by Carbone et al. (2016); Carbone et al. (2017). Those works include more powerful but also more specific techniques to constrain the rates of individual source populations. These approaches rely on assumptions about the underlying source properties and distributions, as well as detailed knowledge of the observing strategy (similar to Feindt et al. 2019). For a general review such as this, it is difficult to do a comprehensive analysis for a large set of previous surveys and sources. Secondly, faster identification has allowed much more reliable followup and classification (e.g., Law et al. 2018b; Anderson et al. 2020; Dong et al. 2021; Dong & Hallinan 2023). Thirdly, searches for shorter-duration events and polarised sources have allowed discovery of new classes of sources besides synchrotron transients (e.g., Hurley-Walker et al. 2022b, 2023; Caleb et al. 2024; Lee et al. 2025; Wang et al. 2021b, 2025c; Dong et al. 2025b). Finally, the latest generation of surveys (VLASS, VAST, LoTSS, MWA GPM) are still ongoing, with individual sources being published and final tallies of discoveries still to come. All of these make the continuation of overall rate projections less valuable. Rates are extremely valuable still for studying individual classes of objects (e.g., Beniamini et al. 2023) but we do not focus on the ‘transient rate’.

These recent surveys have allowed us to start to characterise the overall populations of radio transients and variables for the first time. Figure 10 shows the number of each source type found in a selection of recent surveys. Most surveys found AGN/galaxies as the dominant class (except for Dobie et al. (2023) who deliberately excluded them), followed by radio stars and pulsars.

We have looked at the potential discovery volume from different past/ongoing surveys (Figure 7) but more to show the overall progression with time, rather than to allow direct comparison. The proliferation of survey strategies probing different timescales with different techniques has made such comparisons increasingly hard (e.g., Rowlinson et al. 2016). In the following section, we look toward future facilities (for which the details of potential surveys are still unclear) to see broadly where they might excel, but we still do not give detailed projections for yields. This is best left to in-depth analyses that examine specific source classes.

## 7. Previewing future transient surveys

The substantial amount of effort that has been put into conducting image domain radio transient surveys over the past 15 years has resulted in significant steps forward in our understanding of individual radio transient source types, of the overall populations, and of the advantages and limitations of various approaches to transient identification and classification.

It is critical that we draw on this experience to optimise the scientific benefit of the surveys that will be possible on upcoming radio telescopes. In this section we outline the specifications of three major future instruments, summarise some of the other planned facilities, and reflect on lessons learned from current transient surveys.

We summarise the basic properties of the telescopes in Table 6. Note that this does not contain details of prospective surveys. Some of the facilities will be primarily survey-driven,

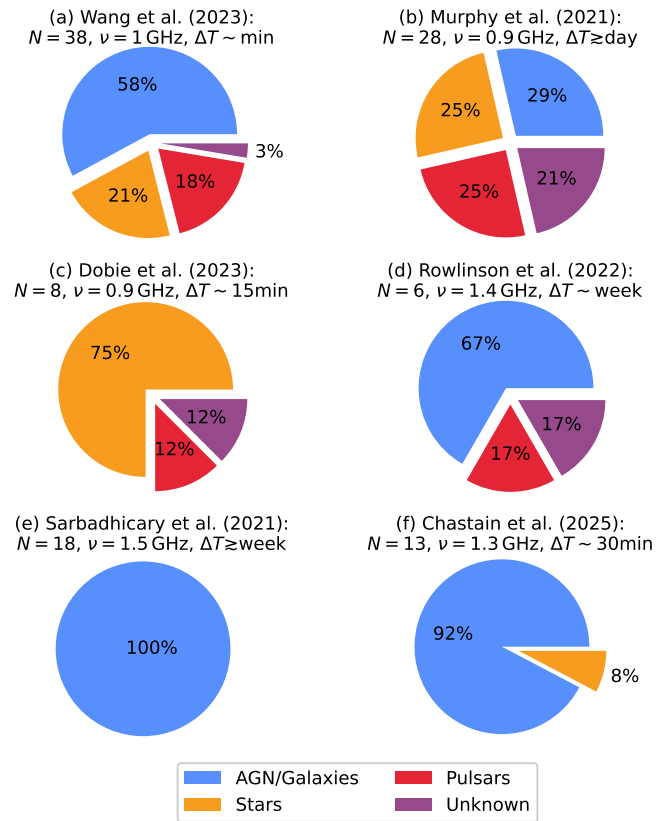


**Figure 10.** Source class distribution for the transient and variable sources found in a selection of recent image-domain surveys: Wang et al. (2023), who searched for minute-scale variability at frequencies near 1 GHz with ASKAP; Murphy et al. (2021), who searched for longer-scale variability at 888 MHz with ASKAP; Dobie et al. (2023), who searched for fast variability at 943 MHz with ASKAP; Rowlinson et al. (2022), who searched for variability on timescales of weeks at 1.4 GHz with MeerKAT; Sarbadhicary et al. (2021), who searched for longer-scale variability in deep images with the VLA at 1–2 GHz; and Chastain et al. (2025), who searched for short-term variability with MeerKAT at 1.3 GHz. Most surveys show AGN & galaxies as the dominant class, except for Dobie et al. (2023) who deliberately excluded them. Since each survey had very different fields-of-view and total numbers of epochs we do not present absolute numbers, but just relative populations, and even those will change for different surveys (e.g. stars and pulsars will be over-represented on shorter timescales).

while others will be used more for PI-led science including transient followup. So focusing on the ‘survey speed’ may not be the most relevant metric. Nonetheless, we do present a survey speed calculated for each facility as:

$$SS \equiv \Omega_{\text{inst}} \frac{A_{\text{eff}}^2}{T_{\text{sys}}^2}. \quad (18)$$

Unlike in Section 4.2.1,  $\Omega_{\text{inst}}$  here is the instantaneous telescope field-of-view, since we are discussing telescopes and not surveys. In principle this should actually be an integral of the sensitivity over solid angle (e.g., Hotan et al. 2021), but such information is not always available. In some uses survey speed can also include a bandwidth factor (so that it more directly reflects the time needed to achieve a given flux density limit over a given area), but we do not do that here.

This survey speed is intended to be proportional to the expected speed it would take to survey the sky down to a constant limiting flux density (and higher is better), although it does ignore

some elements like changing bandwidth between telescopes or other sources of noise like confusion (compared to Eqn. 5 which uses the delivered noise). Note that we can relate the survey speed to the system equivalent flux density:

$$\text{SEFD} \equiv \frac{2k_B T_{\text{sys}}}{A_{\text{eff}}} \quad (19)$$

via

$$\text{SS} = \Omega_{\text{inst}} \frac{4k_B^2}{\text{SEFD}^2} \quad (20)$$

and the continuum sensitivity

$$\sigma = \frac{\text{SEFD}}{\sqrt{N_p \Delta t \Delta v}} \quad (21)$$

with  $N_p = 2$  the number of polarisations,  $\Delta t$  the integration time, and  $\Delta v$  the bandwidth (and this ignores any loss of sensitivity from  $uv$  tapering or weighting). So we also have

$$\text{SS} = \Omega_{\text{inst}} \frac{4k_B^2}{N_p \Delta t \Delta v \sigma^2} \quad (22)$$

In addition, comparisons between telescopes operating at very different frequencies are complicated by the changing sensitivities and bandwidths, together with expected source characteristics. Instead of an explicit spectral correction like in Eqn. 5 we separate the high ( $\sim 1.4$  GHz) and low ( $\lesssim 200$  MHz) facilities (especially as the contribution from Galactic synchrotron emission in the latter can be highly significant and highly variable with position).

In Figure 11 we plot the capabilities of the future facilities from Table 6 (which we discuss more below) along with current-generation facilities. We include both the survey speed, relevant for wide-field discovery, as well as the sensitivity (inverse of the SEFD), which is relevant for pointed followup. It is clear that the future facilities will have big improvements in both metrics, although the survey speed improvements will be most significant, and overall the boost at lower frequencies with the SKA-Low will be more significant than at higher frequencies.

### 7.1. The SKA Observatory

The SKA Observatory (SKAO) consists of two telescopes (SKA-Low and SKA-Mid), currently under construction<sup>9</sup>. SKA-Low will consist of 512 low frequency aperture array stations, spread over an area 80 km in diameter, located in Western Australia. Each station will have 256 wire antennas in a 38-m diameter area. It will observe in the frequency range 50–350 MHz. SKA-Mid will consist of 197 mid frequency dishes (64 from the existing MeerKAT array) spread over an area 160 km in diameter. It will be located in the Karoo region of South Africa. The telescope will operate in 6 frequency bands (3 initially) ranging from 350 MHz to 15.4 GHz. Full details and technical specifications of the telescopes are given in the Design Baseline Description and the SKAO Staged Delivery, Array Assemblies And Layouts documents and summarised in Table 6.

The SKAO telescopes are being constructed in stages, as outlined in the SKAO construction timeline<sup>10</sup>. A key milestone will

<sup>9</sup>The specifications given in this Section are based on the official SKAO documents available in this Zenodo collection: <https://zenodo.org/communities/skaokeydocuments/>, in particular the ‘SKAO Staged Delivery, Array Assemblies And Layouts’ document: Seethapuram Sridhar et al. (2025) and the ‘Design Baseline Description’: Dewdney et al. (2022).

<sup>10</sup><https://www.skao.int/en/science-users/timeline-science>

be the completion of the AA\* arrays, which will consist of 307 SKA-Low stations and 144 SKA-Mid dishes. These arrays are expected to be completed in 2029 and 2031, respectively, with the specifications summarised in Table 6.

The science case for the SKAO telescopes has been outlined in two paper collections. Firstly, in ‘*Science with the Square Kilometre Array*’ (Carilli & Rawlings 2004), and then, a decade later, in ‘*Advancing Astrophysics with the Square Kilometre Array*’ (Braun et al. 2015). A new science book, stemming from the 2025 SKAO General Science Meeting, ‘*A new era in astrophysics: Preparing for early science with the SKAO*’ is currently in preparation.

The exact operating model of the SKAO telescopes (including how time is allocated, and potential survey design) is yet to be determined. However, the current plan is that PI-led science would start in 2030 on AA\* and larger observing programs led by the Key Science Projects would start several years later.

### 7.2. DSA-2000

The DSA-2000 telescope is a planned instrument that, as originally scoped, will consist of 2000  $\times$  5-m dishes spanning an area of 19 km  $\times$  15 km in Nevada, USA (Hallinan et al. 2019). However, the array specification has changed to 1650  $\times$  6.15-m (along with a new name, still to be determined), which will have a similar survey speed but a better point-source sensitivity (G. Hallinan, pers. comm.). The telescope will operate at radio frequencies of 700 MHz to 2 GHz. The baseline reference design specifications are summarised in Table 6. The aim is to survey the sky repeatedly with a logarithmic cadence, with more of a focus on the Galactic plane.

The science case for DSA-2000 has been outlined in the Community Science Book<sup>8</sup>. There are four main science areas, two of which are directly relevant to this review: ‘*the dynamic radio sky*’ and ‘*multi-messenger astronomy*’. Unlike the SKAO and ngVLA, there are no receivers to switch, so the DSA-2000 is planning on surveying the sky for its main science goals (with some time devoted to followup of multi-messenger transients). This, combined with the small element diameter and consequent large field-of-view, gives DSA-2000 a considerable advantage in survey speed compared to the other facilities at the same frequency.

### 7.3. The next-generation VLA

The next-generation Very Large Array (ngVLA; Murphy 2018) is a planned instrument that will consist of a Main array of 214  $\times$  18 m off-axis parabolic antennas distributed across the USA and Mexico, out to baselines of 1000 km, plus another 30  $\times$  18 m dishes on continental baselines (out to 9000 km) in the Long Baseline Array (LBA) and 19  $\times$  6 m dishes in the Short Baseline Array for diffuse sources (which is of less interest for transient science). The array will operate in a frequency range from 1 to 116 GHz, with maximum bandwidth 20 GHz.

In contrast to the SKAO and DSA-2000, the ngVLA is designed to be primarily a PI-driven instrument. It has 5 key science drivers, the most relevant to this review being: ‘*Understanding the Formation and Evolution of Stellar and Supermassive Black Holes in the Era of Multi-Messenger Astronomy*’. For the most part it is not planned that there will

<sup>8</sup>[https://www.dropbox.com/scl/fi/579zwhw5r8pt5o45tsn0/DSA-2000\\_Community-Science\\_Book.pdf](https://www.dropbox.com/scl/fi/579zwhw5r8pt5o45tsn0/DSA-2000_Community-Science_Book.pdf)

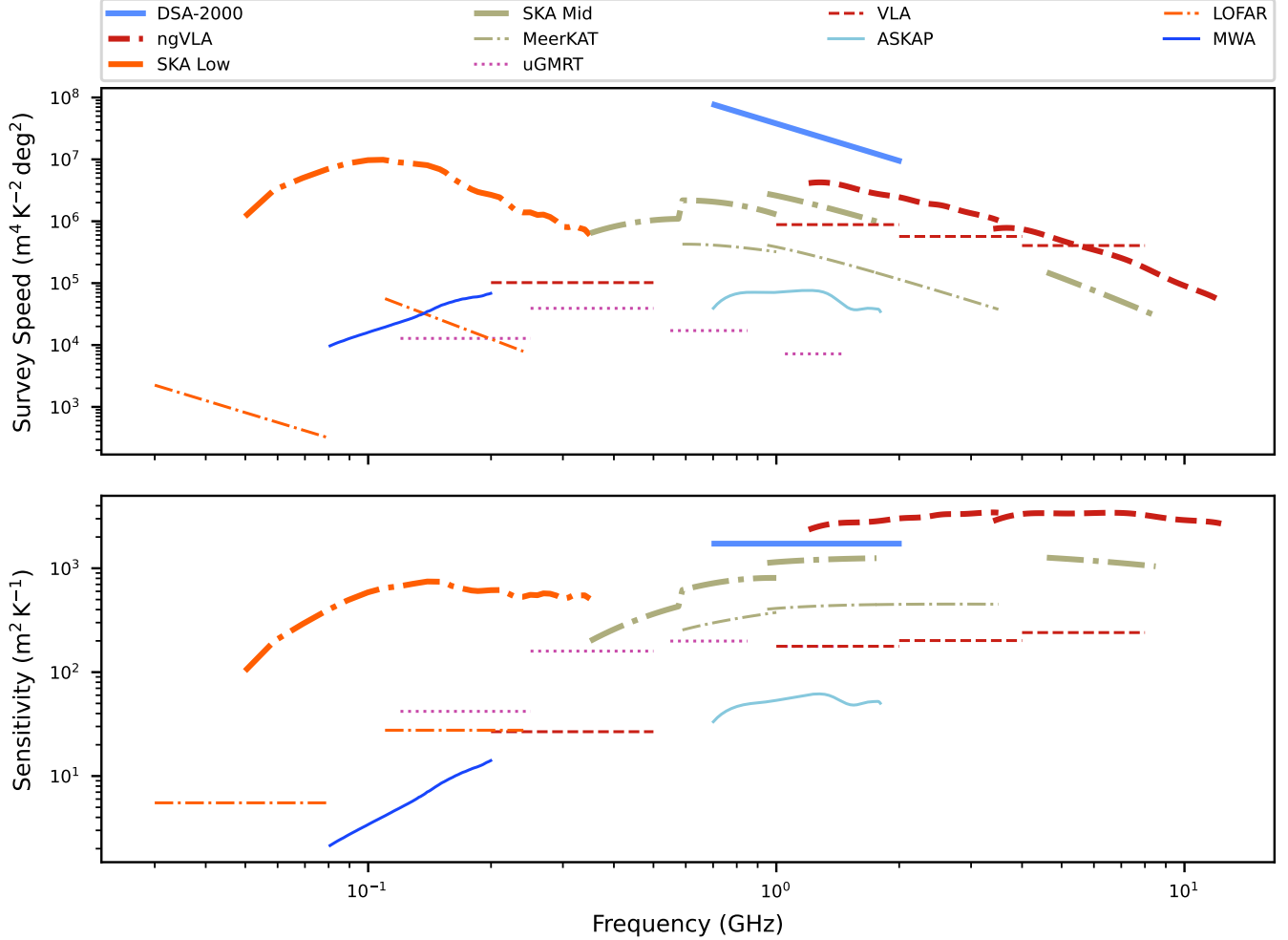


**Figure 11.** Sensitivity of planned future radio facilities. We show the survey speed (Eqn. 18) in the top panel and the sensitivity ( $A_{\text{eff}}/T_{\text{sys}}$ , from Eqn. 19) in the bottom panel as a function of frequency. Current facilities are shown with thinner lines, while future facilities are with thicker lines. The data are a mix of detailed calculations and simplistic projection (e.g., ignoring effective area changes within a frequency band). Data sources for future facilities are: DSA-2000 from G. Hallinan (pers. comm.), ngVLA from <https://github.com/dlakaplan/>, SKA1-low from <http://skalowsensitivitybackup-env.eba-daehsrjt.ap-southeast-2.elasticbeanstalk.com>, and SKA1-mid from <https://gitlab.com/ska-telescope/ost/ska-ost-senscale>. Data sources for current facilities are: MeerKAT from <https://gitlab.com/ska-telescope/ost/ska-ost-senscale>, upgraded GMRT (uGMRT) from Gupta et al. (2017), VLA from <https://science.nrao.edu/facilities/vla/docs/manuals/oss/performance>, ASKAP from Hotan et al. (2021) and E. Lenc (pers. comm.), LOFAR from van Haarlem et al. (2013) for the Dutch array but with double the number of LBA antennas per station, and MWA from Ung (2019) via <https://github.com/ysimonov/MWA-Sensitivity>. Facilities at  $< 300$  MHz include contributions from the sky temperature, although we use a pointing location away from the Galactic plane.

**Table 6.** Specifications for future radio telescopes

Telescope	LOFAR 2.0 LBA <sup>a</sup>	SKA Low	LOFAR2.0 HBA <sup>a</sup>	SKA Mid <sup>b</sup>	DSA-2000	ngVLA <sup>c</sup>
Collecting area (m <sup>2</sup> )	70 192	419 000	41 226	33 000	49 000	54 000
Frequency range (GHz)	0.01–0.08	0.05–0.35	0.12–0.24	0.35–15.4	0.7–2.0	1.2–116
Bandwidth (MHz)	48	300	48	720	1300	2300
Angular resolution (arcsec)	0.5	3.3–23	0.2	0.7	3	0.08
Field-of-view (deg <sup>2</sup> )	12	2.3–113	12	0.7	7.0	0.55
1 h continuum sensitivity (μJy beam <sup>-1</sup> )	3000	14–26	85	0.9	1 <sup>d</sup>	0.27 <sup>d</sup>
Survey speed <sup>e</sup> (10 <sup>6</sup> deg <sup>2</sup> m <sup>4</sup> K <sup>-2</sup> )	$\sim 10^{-3}$	0.6–10	0.01–0.1	2.6	13	2.1

<sup>a</sup> Multiple configurations trading bandwidth between HBA and LBA arrays and multiple beams are possible. Most specifications are for the full EU array.

<sup>b</sup> Based on <https://www.astron.nl/telescopes/square-kilometre-array>, Dewdney et al. (2022), and <https://sensitivity-calculator.skao.int/mid>. Most specifications are for Band 2, containing 1.4 GHz. Sensitivity and resolution can be changed with different weighting schemes.

<sup>c</sup> Based on <https://ngett.nrao.edu>. Most specifications are for the ‘main’ (core plus spiral out to 1000 km) array and for Band 1 (centred at 2.4 GHz).

<sup>d</sup> At 1.4 GHz.

<sup>e</sup> Defined as  $\Omega A_{\text{eff}}^2 / T_{\text{sys}}^2$ .

be large-scale surveys with the ngVLA, but it will certainly participate in dedicated time-domain followup studies, and the capabilities of the LBA for astrometry and precision measurements enable new science compared to what SKA and DSA-2000 offer on their own (e.g. Section 5.6).

#### 7.4. LOFAR 2.0

The LOw-Frequency ARray (LOFAR; van Haarlem et al. 2013) is a network of 24 Core stations located near Dwingeloo in the Netherlands, 14 Remote stations distributed across the Netherlands and 14 larger International stations distributed over Europe. Each station consists of low band antennas (LBAs) that operate at 10–90 MHz and high band antennas (HBAs) that operate at 110–240 MHz.

LOFAR 2.0<sup>1</sup> is a major upgrade to the LOFAR telescope. Two new stations will be added. New low-noise amplifiers will be added to all antennas (Wang et al. 2025a), and processing improvements will allow simultaneous use of both LBAs and HBAs, or using two beams for each HBA station. There are also improvements in the clock distribution and central processing facility used for calibration and imaging, as well as a 24/7 transient buffer for imaging and localisation. The net result will be a considerably more powerful and flexible system capable of optimising its operation for many different transient cases (timescales, sensitivities, etc), as well as general improvements in image fidelity and processing (enabling faster followup with better localisation).

The science case is outlined in the LOFAR 2.0 White Paper<sup>2</sup>. Transient science (including supernova, gamma-ray bursts, stellar activity and exploring the unknown), forms a major part of the science case.

#### 7.5. All-sky radio transient monitors

To maximise the chance of detecting very rare, very bright events (e.g. fast radio bursts, long period transients, extreme stellar bursts, or coherent signals from neutron star mergers) it is desirable to maximise the time on sky. These can be achieved with existing and proposed facilities that can continuously monitor large fractions of the sky (e.g. Prasad et al. 2016; Bochenek et al. 2020a; Sokolowski et al. 2021; Connor et al. 2021; Lin et al. 2022; Luo et al. 2024; Kosogorov et al. 2025), which are being developed with increasing sensitivity and other capabilities. This strategy achieved notable success in detecting a FRB-like burst from a Galactic magnetar (Bochenek et al. 2020b), which served to motivate future experiments.

All-sky monitors have typically been designed to detect ‘fast’ transients, using multiple receivers or digital beamforming techniques rather than imaging. This leads to good performance for short-duration signals, especially those that have detectable dispersion across the band (helping with interference rejection), but means they have reduced sensitivity to longer-duration signals due to fluctuations in the receiver electronics. Nonetheless, there is overlap in the type of sources these systems can detect and those discussed in this review, such as the discovery of a LPT with period of 14 min by the CHIME FRB system (Dong et al. 2025a, although note that the same source was independently detected through LOFAR imaging by Bloot et al. 2025). This discovery

was helped by the relatively short pulse period and narrow duty cycle, such that individual pulses were short enough to be detected by the FRB system. Future explorations of the overlap between all-sky beamformed searches and more targeted imaging searches will help map out the underlying distribution of periods and fluences from sources like these.

#### 8. Summary and outlook

Time domain studies have been important since the dawn of radio astronomy, and give us insight into physical phenomena that span orders of magnitude in luminosity (from stars in our local neighbourhood through to distant gamma-ray bursts); in timescale (from nanosecond pulses through to afterglows that evolve over years); and in physical properties (from highly dense, magnetised compact objects to scintillation caused by interstellar plasma). These regimes are often inaccessible via other observations and have led to numerous breakthroughs.

The field of image-domain transients has evolved from targeted studies of individual objects, to serendipitous coverage by generic surveys, through to custom designed large scale surveys. In the current decade (the 2020s), the plans mapped out many years ago have started to come to fruition, with a suite of telescopes reaching the sensitivity, resolution, and survey speed required to detect a wide range of radio transients at megahertz and gigahertz radio frequencies.

Some of the scientific highlights of the past decade (from both targeted and untargeted observations) include (with tentative results in italics):

- Detection of an extreme scattering event in real time (Bannister et al. 2016);
- Identification of persistent radio sources associated with Fast Radio Bursts (Chatterjee et al. 2017);
- Radio detection and monitoring of the afterglow from GW170817 (Hallinan et al. 2017);
- *Detection of a possible gamma-ray burst orphan afterglow* (Law et al. 2018b; Mooley et al. 2022);
- Discovery of fast blue optical transients (FBOTs; Ho et al. 2019);
- *Tentative signs of radio emission from star-planet interactions* (Vedantham et al. 2020).
- Detection of delayed radio flares from a tidal disruption event (Horesh et al. 2021a);
- Precision measurement of the distance to and mass of the black hole X-ray binary Cygnus X-1 (Miller-Jones et al. 2021);
- Detection of merger-triggered core collapse supernova (Dong et al. 2021);
- Discovery of long period transients (Hurley-Walker et al. 2022b; Caleb et al. 2022);
- First detection of radio emission from Type Ia supernova (Kool et al. 2023);
- Substantial expansion of the known radio star population (Driessen et al. 2024);
- Identification of Type II radio burst from an M dwarf, suggestive of a coronal mass ejection (Callingham et al. 2025).

Many of these discoveries are only the first in their class (e.g. long period transients and fast blue optical transients), and have already been supplemented by further discoveries. Future surveys

<sup>1</sup>See <https://www.lofar.eu/lofar2-0-documentation/>.

<sup>2</sup>[https://www.lofar.eu/wp-content/uploads/2023/04/LOFAR2\\_0\\_White\\_Paper\\_v2023.1.pdf](https://www.lofar.eu/wp-content/uploads/2023/04/LOFAR2_0_White_Paper_v2023.1.pdf)

will continue to detect more examples, allowing us to understand the full underlying populations.

The diversity of these results show that we are long past the point of exploring the radio transient sky in a way that is uninformed by the properties of the underlying populations. While early surveys emphasised searching in ways that were independent of the time domain properties of the potential populations, we can now characterise the populations on very different timescales (contrast long period transients, with periods of seconds to hours; with gamma-ray bursts that evolve over months). Rather than counting the number of ‘transients’, we can instead study multiple classes.

Much of the planning over the past few decades has been framed in the context of preparation for SKAO-era radio transient surveys. With this in mind, we end with some reflections on lessons learned from the pathfinder and precursor surveys that we hope feed into the plans for upcoming surveys with the telescopes discussed in Section 7. Some of the things we think will be important are:

- **Real-time imaging and transient detection:** No major radio transient imaging survey so far has had the capability to detect transients in real time (unlike FRB surveys). This will be critical in opening up shorter timescales (by enabling rapid follow-up or more complex analysis), which are currently proving very productive in finding new classes of radio transients, and in enabling rapid follow-up of new detections.
- **Commensal transient surveys:** Serendipity is an important part of transient astronomy. To discover rare objects, it is important to maximise the time on sky. Hence continuing to have full commensal access to other large surveys, with dedicated rapid processing, for the purpose of transient detection is critical, and helps maximise the scientific output of our telescopes. Of course data processing in the era of massive datasets is not ‘free’, but the benefits of commensal transient surveys are likely to make this relatively minimal extra cost worthwhile.
- **Custom-designed transient surveys:** It is important to state that commensal observing is not enough to reveal and study populations of radio transients. We have now begun to characterise the time domain, spectral, and polarisation properties of a range of source classes. To maximise the chance of detection of the most interesting sources, custom-designed surveys that consider the time domain properties of specific populations are required.
- **Radio follow-up capability:** Large-scale widefield surveys are key to discovering rare events. However, understanding them often requires detailed radio monitoring across a range of frequencies. For example, to establish the spectral evolution of synchrotron sources, or establish periodic behaviour in stellar objects. Hence it is critical in the SKAO era that we maintain access to facilities that can be used for this follow-up, including VLBI.
- **Multiwavelength coverage:** Multiwavelength (optical, near-infrared, X-ray, gamma-ray) survey data is vital for assessing the nature of new discoveries. In general this does not have to be contemporaneous, although this is beneficial for some scientific goals. For example, stellar flares show significant structure within an event, so modelling requires multi-wavelength data, but triggering is impractical. For synchrotron transients, optical/IR data is required to identify a host galaxy, and archival high-energy data can be vital to determining whether it is a novel event like an orphan afterglow.
- **Automatic classification of radio transients:** Now we are detecting significant numbers of radio transients in untargeted

surveys, it is important to have automatic methods for removing poor quality data, and for classifying transients and identifying the most interesting outliers. There are well-established approaches in optical transient surveys that are in relative infancy in radio. These should be developed and refined.

In addition, the capabilities identified in Section 4.5 are important considerations for future surveys.

Enormous progress has been made in the field of radio transient surveys in the past decades. The surveys (and targeted monitoring) conducted to date have been fruitful, and in some cases revealed new populations of objects. However, there are still many unanswered questions that we will be able to address when the telescopes currently under development come online. With such a substantial investment of time and resources, it is important we incorporate the lessons learned from our existing experience as we head into this new era of radio transients.

## Acknowledgements

Thank you to the anonymous reviewer whose comments were very helpful in improving this manuscript, and to the editor, Minh Huynh, for advice and assistance throughout the publication process.

Huge thanks to Ron Ekers, Elaine Sadler, Dougal Dobie and Iris de Ruiter for feedback on parts of our draft manuscript. In preparing this review we drew on the very useful compilation of radio transient surveys and rates by Kunal Mooley. Thanks to Kunal (and Deepika Yadav) for updating their online table in time for this review. Thank you to Laura Driessen for permission to adapt the colour-magnitude diagram in Figure 5. Romy Pearse created the lightcurve sketches in Figure 8. Thank you also to Ashna Gulati for help preparing Figures 4 and 8. Finally, thanks to Lirov Lourenço for his help with references and the formatting of this manuscript. Of course any remaining errors in the text are our own.

We had useful interactions and discussions with many people in the preparation of this review. Particular thanks to Gemma Anderson, Shari Breen, Manisha Caleb, Fernando Camilo, Lauren Carter, Shami Chatterjee, Barnali Das, Paul Demorest, Iris de Ruiter, Dougal Dobie, Laura Driessen, Ashna Gulati, Gregg Hallinan, Natasha Hurley-Walker, Scott Hyman, Francois Kapp, Emil Lenc, Walter Max-Moerbeck, Eric Murphy, Joshua Pritchard, Kovi Rose, Antonia Rowlinson, Sarvesh Sridhar, Randall Wayth, Michael Wheatland and Andrew Zic.

This research has made use of the Astrophysics Data System, funded by NASA under Cooperative Agreement 80NSSC21M00561. In conducting this review, generative AI tools (ChatGPT-4) were used to help search for relevant papers in the literature. No information or text directly from generative AI was used in the preparation of this manuscript.

This research was supported by the Australian Research Council Centre of Excellence for Gravitational Wave Discovery (OzGrav), project number CE230100016, and by National Science Foundation grant AST-2511757.

## References

Abbott D. C., Bieging J. H., Churchwell E., 1984, *The Astrophysical Journal*, **280**, 671  
 Abbott D. C., Beiging J. H., Churchwell E., Torres A. V., 1986, *The Astrophysical Journal*, **303**, 239

Abbott B. P., et al., 2016, *Phys. Rev. Lett.*, **116**, 061102

Abbott B. P., et al., 2017a, *Physical Review Letters*, **119**, 161101

Abbott B. P., et al., 2017b, *The Astrophysical Journal*, **848**, L12

Ackermann M., et al., 2011, *The Astrophysical Journal*, **741**, 30

Ackermann M., et al., 2014, *Science*, **345**, 554

Adams E. A. K., van Leeuwen J., 2019, *Nature Astronomy*, **3**, 188

Agarwal D., Aggarwal K., Burke-Spolaor S., Lorimer D. R., Garver-Daniels N., 2020, *Monthly Notices of the Royal Astronomical Society*, **497**, 1661

Agazie G., et al., 2023a, *The Astrophysical Journal*, **951**, L8

Agazie G., et al., 2023b, *The Astrophysical Journal*, **952**, L37

Aigrain S., Foreman-Mackey D., 2023, *Annual Review of Astronomy and Astrophysics*, **61**, 329

Akritas M. G., Bershady M. A., 1996, *The Astrophysical Journal*, **470**, 706

Alard C., 2000, *Astronomy and Astrophysics Supplement Series*, **144**, 363

Alard C., Lupton R. H., 1998, *The Astrophysical Journal*, **503**, 325

Alexander K. D., Soderberg A. M., Chomiuk L. B., 2015, *The Astrophysical Journal*, **806**, 106

Alexander K. D., Berger E., Guillochon J., Zauderer B. A., Williams P. K. G., 2016, *The Astrophysical Journal*, **819**, L25

Alexander K. D., Wieringa M. H., Berger E., Saxton R. D., Komossa S., 2017a, *The Astrophysical Journal*, **837**, 153

Alexander K. D., et al., 2017b, *The Astrophysical Journal*, **848**, L21

Alexander K. D., van Velzen S., Horesh A., Zauderer B. A., 2020, *Space Science Reviews*, **216**, 81

Allen B., Anderson W. G., Brady P. R., Brown D. A., Creighton J. D. E., 2012, *Physical Review D*, **85**, 122006

Alsabti A. W., Murdin P., eds, 2017, *Handbook of Supernovae*. Springer International Publishing, Cham, Switzerland, doi:10.1007/978-3-319-21846-5, <https://ui.adsabs.harvard.edu/abs/2017hsn.book.....A>

An T., Baan W. A., Wang J.-Y., Wang Y., Hong X.-Y., 2013, *Monthly Notices of the Royal Astronomical Society*, **434**, 3487

Anderson G. E., et al., 2017, *Monthly Notices of the Royal Astronomical Society*, **466**, 3648

Anderson G. E., et al., 2018, *Monthly Notices of the Royal Astronomical Society*, **473**, 1512

Anderson M. M., et al., 2019, *The Astrophysical Journal*, **886**, 123

Anderson M. M., et al., 2020, *The Astrophysical Journal*, **903**, 116

Anderson G. E., et al., 2024, *The Astrophysical Journal*, **975**, L13

Andersson A., et al., 2022, *Monthly Notices of the Royal Astronomical Society*, **513**, 3482

Andersson A., et al., 2023, *Monthly Notices of the Royal Astronomical Society*, **523**, 2219

Andersson A., et al., 2025, *Monthly Notices of the Royal Astronomical Society*, **538**, 1397

Andreoni I., et al., 2022, *Nature*, **612**, 430

Andrew B. H., Purton C. R., 1968, *Nature*, **218**, 855

Anna-Thomas R., Burke-Spolaor S., Law C. J., Schinzel F. K., Aggarwal K., Bower G. C., Connor L., Demorest P. B., 2024, *The Astrophysical Journal*, **974**, 72

Anumarlapudi A., et al., 2023, *The Astrophysical Journal*, **956**, 28

Anumarlapudi A., et al., 2024, *The Astrophysical Journal*, **974**, 241

Anumarlapudi A., et al., 2025, *Monthly Notices of the Royal Astronomical Society*, **542**, 1208

Aoki T., et al., 2014, *The Astrophysical Journal*, **781**, 10

Archibald A. M., et al., 2009, *Science*, **324**, 1411

Archibald A. M., et al., 2018, *Nature*, **559**, 73

Backer D. C., 1970, *Nature*, **228**, 42

Backer D. C., Kulkarni S. R., Heiles C., Davis M. M., Goss W. M., 1982, *Nature*, **300**, 615

Balasubramanian A., et al., 2022, *The Astrophysical Journal*, **938**, 12

Ball N. M., Brunner R. J., 2010, *International Journal of Modern Physics D*, **19**, 1049

Bannister K. W., Murphy T., Gaensler B. M., Hunstead R. W., Chatterjee S., 2011, *Monthly Notices of the Royal Astronomical Society*, **412**, 634

Bannister K. W., Stevens J., Tuntsov A. V., Walker M. A., Johnston S., Reynolds C., Bignall H., 2016, *Science*, **351**, 354

Bannister K. W., et al., 2019, *Science*, **365**, 565

Barnacka A., Glicenstein J. F., Moudden Y., 2011, *Astronomy and Astrophysics*, **528**, L3

Barnes J., Duffell P. C., Liu Y., Modjaz M., Bianco F. B., Kasen D., MacFadyen A. I., 2018, *The Astrophysical Journal*, **860**, 38

Barthelmy S. D., et al., 2005, *Space Science Reviews*, **120**, 143

Bartos I., Lee K. H., Corsi A., Márka Z., Márka S., 2019, *Monthly Notices of the Royal Astronomical Society*, **485**, 4150

Barvainis R., Lehár J., Birkinshaw M., Falcke H., Blundell K. M., 2005, *The Astrophysical Journal*, **618**, 108

Bastian T. S., 1990, *Solar Physics*, **130**, 265

Bastian T. S., Benz A. O., Gary D. E., 1998, *Annual Review of Astronomy & Astrophysics*, **36**, 131

Bastian T. S., Dulk G. A., Leblanc Y., 2000, *The Astrophysical Journal*, **545**, 1058

Basu R., Athreya R., Mitra D., 2011, *The Astrophysical Journal*, **728**, 157

Bates S. D., Lorimer D. R., Verbiest J. P. W., 2013, *Monthly Notices of the Royal Astronomical Society*, **431**, 1352

Becker R. H., White R. L., Helfand D. J., 1995, *The Astrophysical Journal*, **450**, 559

Becker R. H., Helfand D. J., White R. L., Proctor D. D., 2010, *The Astronomical Journal*, **140**, 157

Bell M. E., et al., 2011, *Monthly Notices of the Royal Astronomical Society*, **415**, 2

Bell M. E., et al., 2014, *Monthly Notices of the Royal Astronomical Society*, **438**, 352

Bell M. E., Huynh M. T., Hancock P., Murphy T., Gaensler B. M., Burlon D., Trott C., Bannister K., 2015, *Monthly Notices of the Royal Astronomical Society*, **450**, 4221

Bell M. E., et al., 2019, *Monthly Notices of the Royal Astronomical Society*, **482**, 2484

Bellm E. C., et al., 2019, *Publications of the Astronomical Society of the Pacific*, **131**, 018002

Belloni T. M., 2010, in Belloni T. M., ed., *Lecture Notes in Physics*, Vol. 794, *The Jet Paradigm*. Springer International Publishing, Berlin, Germany, p. 53, doi:10.1007/978-3-540-76937-8\_3, <https://ui.adsabs.harvard.edu/abs/2010LNP...794...53B>

Beniamini P., Wadiasingh Z., Hare J., Rajwade K. M., Younes G., van der Horst A. J., 2023, *Monthly Notices of the Royal Astronomical Society*, **520**, 1872

Benz A. O., Güdel M., 2010, *Annual Review of Astronomy and Astrophysics*, **48**, 241

Berger E., 2014, *Annual Review of Astronomy and Astrophysics*, **52**, 43

Berger E., et al., 2000, *The Astrophysical Journal*, **545**, 56

Berger E., et al., 2001a, *Nature*, **410**, 338

Berger E., et al., 2001b, *The Astrophysical Journal*, **556**, 556

Berger E., Kulkarni S. R., Frail D. A., 2001c, *The Astrophysical Journal*, **560**, 652

Berger E., Soderberg A. M., Frail D. A., Kulkarni S. R., 2003, *The Astrophysical Journal*, **587**, L5

Berger E., et al., 2005, *Nature*, **438**, 988

Bertin E., Arnouts S., 1996, *Astronomy and Astrophysics Supplement Series*, **117**, 393

Best P. N., et al., 2023, *Monthly Notices of the Royal Astronomical Society*, **523**, 1729

Bhandari S., et al., 2018, *Monthly Notices of the Royal Astronomical Society*, **478**, 1784

Bhandari S., et al., 2020, *The Astrophysical Journal*, **901**, L20

Bhandari S., et al., 2023, *The Astrophysical Journal*, **958**, L19

Bieging J. H., Abbott D. C., Churchwell E. B., 1989, *The Astrophysical Journal*, **340**, 518

Biermann E., et al., 2025, *The Astrophysical Journal*, **986**, 7

Bieterholz M. F., Bartel N., Argo M., Dua R., Ryder S., Soderberg A., 2021, *The Astrophysical Journal*, **908**, 75

Biggs A. D., 2021, *Monthly Notices of the Royal Astronomical Society*, **505**, 2610

Biggs A. D., 2023, *Monthly Notices of the Royal Astronomical Society*, **522**, 426

Bignall H. E., et al., 2003, *The Astrophysical Journal*, **585**, 653

Bignall H. E., Croft S., Hovatta T., Koay J. Y., Lazio J., Macquart J. P., Reynolds C., 2015, in Advancing Astrophysics with the Square Kilometre Array. SKA Organization, eprint: arXiv:1501.04627, doi:10.22323/1.215.0058, <https://ui.adsabs.harvard.edu/abs/2015aska.confE..58B>

Blandford R., Narayan R., Romani R. W., 1986, *The Astrophysical Journal*, **301**, L53

Blandford R., Meier D., Readhead A., 2019, *Annual Review of Astronomy and Astrophysics*, **57**, 467

Bloemen S., et al., 2016, in Hall H. J., Gilmozzi R., Marshall H. K., eds., Vol. 9906, Ground-based and Airborne Telescopes VI. SPIE, p. 990664, doi:10.1117/12.2232522, <https://ui.adsabs.harvard.edu/abs/2016SPIE.9906E..64B>

Blomme R., van Loo S., De Becker M., Rauw G., Runacles M. C., Setia Gunawan D. Y. A., Chapman J. M., 2005, *Astronomy and Astrophysics*, **436**, 1033

Blomme R., De Becker M., Volpi D., Rauw G., 2010, *Astronomy and Astrophysics*, **519**, A111

Blondin S., 2024, in Mandel I., ed., *Encyclopedia of Astrophysics*. Elsevier, <https://ui.adsabs.harvard.edu/abs/2024arXiv241109740B>

Bloom J. S., et al., 2011, *Science*, **333**, 203

Bloot S., et al., 2025, *Astronomy and Astrophysics*, **699**, A341

Blázquez-García A., Conde A., Mori U., Lozano J. A., 2021, *ACM Comput. Surv.*, **54**, 56:1

Bochenek C. D., McKenna D. L., Belov K. V., Kocz J., Kulkarni S. R., Lamb J., Ravi V., Woody D., 2020a, *Publications of the Astronomical Society of the Pacific*, **132**, 034202

Bochenek C. D., Ravi V., Belov K. V., Hallinan G., Kocz J., Kulkarni S. R., McKenna D. L., 2020b, *Nature*, **587**, 59

Bock D. C. J., Large M. I., Sadler E. M., 1999, *The Astronomical Journal*, **117**, 1578

Bode M. F., Seaquist E. R., Evans A., 1987, *Monthly Notices of the Royal Astronomical Society*, **228**, 217

Bolton R. C., Chandler C. J., Cotter G., Pearson T. J., Pooley G. G., Readhead A. C. S., Riley J. M., Waldram E. M., 2006, *Monthly Notices of the Royal Astronomical Society*, **370**, 1556

Bonaldi A., et al., 2021, *Monthly Notices of the Royal Astronomical Society*, **500**, 3821

Bond H. E., White R. L., Becker R. H., O'Brien M. S., 2002, *Publications of the Astronomical Society of the Pacific*, **114**, 1359

Bonnell J. T., Klebesadel R. W., 1996, in Koutoulou C., Briggs M. F., Fishman G. J., eds., Vol. 384, Gamma-ray bursts: 3rd Huntsville symposium. AIP, pp 977–980, doi:10.1063/1.51630, <https://ui.adsabs.harvard.edu/abs/1996AIPC..384..977B>

Bower G. C., 2011, *The Astrophysical Journal*, **732**, L12

Bower G. C., Saul D., 2011, *The Astrophysical Journal*, **728**, L14

Bower G. C., Saul D., Bloom J. S., Bolatto A., Filippenko A. V., Foley R. J., Perley D., 2007, *The Astrophysical Journal*, **666**, 346

Bower G. C., et al., 2010, *The Astrophysical Journal*, **725**, 1792

Bower G. C., Metzger B. D., Cenko S. B., Silverman J. M., Bloom J. S., 2013, *The Astrophysical Journal*, **763**, 84

Boyajian T. S., et al., 2016, *Monthly Notices of the Royal Astronomical Society*, **457**, 3988

Boyce M. M., et al., 2023, *Publications of the Astronomical Society of Australia*, **40**, e027

Braes L. L. E., Miley G. K., 1972, *Nature*, **237**, 506

Braun R., Bourke T., Green J. A., Keane E., Wagg J., 2015, in Advancing Astrophysics with the Square Kilometre Array. SKA Organization, p. 174, doi:10.22323/1.215.0174, <https://ui.adsabs.harvard.edu/abs/2015aska.confE.174B>

Brentjens M. A., de Bruyn A. G., 2005, *Astronomy and Astrophysics*, **441**, 1217

Briggs M. S., et al., 1996, *The Astrophysical Journal*, **459**, 40

Bright J. S., et al., 2022, *The Astrophysical Journal*, **926**, 112

Broderick J. W., et al., 2016, *Monthly Notices of the Royal Astronomical Society*, **459**, 2681

Bromberg O., Nakar E., Piran T., 2011a, *The Astrophysical Journal*, **739**, L55

Bromberg O., Nakar E., Piran T., Sari R., 2011b, *The Astrophysical Journal*, **740**, 100

Brown A., Veale A., Judge P., Bookbinder J. A., Hubeny I., 1990, *The Astrophysical Journal*, **361**, 220

Brown G. C., et al., 2017, *Monthly Notices of the Royal Astronomical Society*, **472**, 4469

Browning M. K., 2008, *The Astrophysical Journal*, **676**, 1262

Bruni G., et al., 2024a, *Nature*, **632**, 1014

Bruni G., et al., 2024b, *Astronomy and Astrophysics*, **695**, L12

Buchner J., Fotopoulou S., 2024, *Nat Rev Phys*, **6**, 535

Budding E., Carter B. D., Mengel M. W., Slee O. B., Donati J.-F., 2002, *Publications of the Astronomical Society of Australia*, **19**, 527

Burke B. F., Franklin K. L., 1955, *Journal of Geophysical Research (1896-1977)*, **60**, 213

Burn B. J., 1966, *Monthly Notices of the Royal Astronomical Society*, **133**, 67

CHIME/FRB Collaboration et al., 2021, *The Astrophysical Journal Supplement Series*, **257**, 59

Caleb M., et al., 2022, *Nature Astronomy*, **6**, 828

Caleb M., et al., 2024, *Nature Astronomy*, **8**, 1159

Callingham J. R., et al., 2021, *Nature Astronomy*, **5**, 1233

Callingham J. R., et al., 2023, *Astronomy and Astrophysics*, **670**, A124

Callingham J. R., et al., 2024, *Nature Astronomy*, **8**, 1359

Callingham J. R., et al., 2025, *Nature*, **647**, 603

Calore F., Di Mauro M., Donato F., Hessels J. W. T., Weniger C., 2016, *The Astrophysical Journal*, **827**, 143

Camilo F., Ransom S. M., Halpern J. P., Reynolds J., Helfand D. J., Zimmerman N., Sarkissian J., 2006, *Nature*, **442**, 892

Camilo F., et al., 2007, *The Astrophysical Journal*, **663**, 497

Campana S., et al., 2006, *Nature*, **442**, 1008

Cano Z., Wang S.-Q., Dai Z.-G., Wu X.-F., 2017, *Advances in Astronomy*, **2017**, 8929054

Carbone D., et al., 2016, *Monthly Notices of the Royal Astronomical Society*, **459**, 3161

Carbone D., van der Horst A. J., Wijers R. A. M. J., Rowlinson A., 2017, *Monthly Notices of the Royal Astronomical Society*, **465**, 4106

Carilli C. L., Rawlings S., eds., 2004, *Science with the Square Kilometre Array* New Astronomy Reviews Vol. 48. ([arXiv:astro-ph/0409274](https://arxiv.org/abs/astro-ph/0409274)), doi:10.1016/j.newar.2004.09.001

Carilli C. L., Ivison R. J., Frail D. A., 2003, *The Astrophysical Journal*, **590**, 192

Carlstrom J. E., et al., 2011, *Publications of the Astronomical Society of the Pacific*, **123**, 568

Castro Segura N., et al., 2025, *Monthly Notices of the Royal Astronomical Society*, **543**, 2116

Cendes Y., Alexander K. D., Berger E., Eftekhari T., Williams P. K. G., Chornock R., 2021, *The Astrophysical Journal*, **919**, 127

Cendes Y., et al., 2022, *The Astrophysical Journal*, **938**, 28

Cendes Y., et al., 2024, *The Astrophysical Journal*, **971**, 185

Cenko S. B., et al., 2006, *The Astrophysical Journal*, **652**, 490

Cenko S. B., et al., 2011, *The Astrophysical Journal*, **732**, 29

Cenko S. B., et al., 2012, *The Astrophysical Journal*, **753**, 77

Chandola V., Banerjee A., Kumar V., 2009, *ACM Comput. Surv.*, **41**, 15:1

Chandra P., 2016, *Advances in Astronomy*, **2016**, 296781

Chandra P., 2018, *Space Science Reviews*, **214**, 27

Chandra P., Frail D. A., 2012, *The Astrophysical Journal*, **746**, 156

Chandra P., et al., 2008, *The Astrophysical Journal*, **683**, 924

Chandra P., et al., 2010, *The Astrophysical Journal*, **712**, L31

Chastain S. I., et al., 2025, *The Astrophysical Journal*, **988**, 227

Chatterjee S., et al., 2017, *Nature*, **541**, 58

Chattopadhyay D., Stevenson S., Hurley J. R., Rossi L. J., Flynn C., 2020, *Monthly Notices of the Royal Astronomical Society*, **494**, 1587

Chauhan J., et al., 2021, *Publications of the Astronomical Society of Australia*, **38**, e045

Chen C., Shen R.-F., 2022, *Research in Astronomy and Astrophysics*, **22**, 035017

Chen X., Rachen J. P., López-Caniego M., Dickinson C., Pearson T. J., Fuhrmann L., Krichbaum T. P., Partridge B., 2013, *Astronomy and Astrophysics*, **553**, A107

Chevalier R. A., 1981, *The Astrophysical Journal*, **251**, 259

Chevalier R. A., 1982, *The Astrophysical Journal*, **259**, 302

Chevalier R. A., 1998, *The Astrophysical Journal*, **499**, 810

Chevalier R. A., Li Z.-Y., 2000, *The Astrophysical Journal*, **536**, 195

Chhetri R., Ekers R. D., Morgan J., Macquart J. P., Franzen T. M. O., 2018, *Monthly Notices of the Royal Astronomical Society*, **479**, 2318

Chiti A., Chatterjee S., Wharton R., Cordes J., Lazio T. J. W., Kaplan D. L., Bower G. C., Croft S., 2016, *ApJ*, **833**, 11

Chomiuk L., et al., 2012, *The Astrophysical Journal*, **750**, 164

Chomiuk L., et al., 2014, *The Astrophysical Journal*, **788**, 130

Chomiuk L., Metzger B. D., Shen K. J., 2021a, *Annual Review of Astronomy and Astrophysics*, **59**, 391

Chomiuk L., et al., 2021b, *The Astrophysical Journal Supplement Series*, **257**, 49

Chrimes A. A., et al., 2024a, *Monthly Notices of the Royal Astronomical Society*, **527**, L47

Chrimes A. A., Coppejans D. L., Jonker P. G., Levan A. J., Groot P. J., Mummery A., Stanway E. R., 2024b, *Astronomy and Astrophysics*, **691**, A329

Christiansen J. L., et al., 2018, *The Astronomical Journal*, **155**, 57

Churchwell E., Bieging J. H., van der Hucht K. A., Williams P. M., Spoelstra T. A. T., Abbott D. C., 1992, *The Astrophysical Journal*, **393**, 329

Clarke M., 1964, Phd thesis, University of Cambridge

Clegg A. W., Fey A. L., Lazio T. J. W., 1998, *The Astrophysical Journal*, **496**, 253

Cognard I., Bourgois G., Lestrade J.-F., Biraud F., Aubry D., Darchy B., Drouhin J.-P., 1993, *Nature*, **366**, 320

Cohen M. H., Gundermann E. J., Hardebeck H. E., Harris D. E., Salpeter E. E., Sharp L. E., 1966, *Science*, **153**, 745

Cohen M. H., Gundermann E. J., Hardebeck H. E., Sharp L. E., 1967, *The Astrophysical Journal*, **147**, 449

Cohen A. S., Lane W. M., Cotton W. D., Kassim N. E., Lazio T. J. W., Perley R. A., Condon J. J., Erickson W. C., 2007, *The Astronomical Journal*, **134**, 1245

Condon J. J., 1974, *The Astrophysical Journal*, **188**, 279

Condon J. J., Ransom S. M., 2016, *Essential Radio Astronomy*. Princeton Series in Modern Observational Astronomy, Princeton University Press, Princeton, USA, <https://ui.adsabs.harvard.edu/abs/2016era.book.....C>

Condon J. J., Cotton W. D., Greisen E. W., Yin Q. F., Perley R. A., Taylor G. B., Broderick J. J., 1998, *The Astronomical Journal*, **115**, 1693

Condon J. J., Cotton W. D., Broderick J. J., 2002, *The Astronomical Journal*, **124**, 675

Connor L., et al., 2021, *Publications of the Astronomical Society of the Pacific*, **133**, 075001

Cooke W. J., Moser D. E., 2012, in Rudawska R., Rendtel J., Powell C., Lunsford R., Verbeeck C., Knofel A., eds, *Proceedings of the IMC International Meteor Organization*, pp 9–12, <https://ui.adsabs.harvard.edu/abs/2012pimo.conf....9C>

Cooper A. J., Wadiasingh Z., 2024, *Monthly Notices of the Royal Astronomical Society*, **533**, 2133

Cooper A. J., Gupta O., Wadiasingh Z., Wijers R. A. M. J., Boersma O. M., Andreoni I., Rowlinson A., Gourdjii K., 2023, *Monthly Notices of the Royal Astronomical Society*, **519**, 3923

Coppejans D. L., et al., 2020, *The Astrophysical Journal*, **895**, L23

Corbel S., et al., 2015, in *Advancing Astrophysics with the Square Kilometre Array (AASKA14)*. SKA Organization, eprint: arXiv:1501.04716, p. 53, doi:10.22323/1.215.0053, <https://ui.adsabs.harvard.edu/abs/2015aska.confE..53C>

Cordes J. M., Chatterjee S., 2019, *Annual Review of Astronomy and Astrophysics*, **57**, 417

Cordes J. M., Lazio T. J., 1991, *The Astrophysical Journal*, **376**, 123

Cordes J. M., Lazio T. J. W., 2002, *arXiv e-prints*, pp astro-ph/0207156

Cordes J. M., Rickett B. J., 1998, *The Astrophysical Journal*, **507**, 846

Cordes J. M., Romani R. W., Lundgren S. C., 1993, *Nature*, **362**, 133

Cordes J. M., Lazio T. J. W., McLaughlin M. A., 2004, *New Astronomy Reviews*, **48**, 1459

Coriat M., Fender R. P., Dubus G., 2012, *Monthly Notices of the Royal Astronomical Society*, **424**, 1991

Corsi A., et al., 2018, *The Astrophysical Journal*, **861**, L10

Corsi A., et al., 2023, *The Astrophysical Journal*, **953**, 179

Corsi A., Eddins A., Lazio T. J. W., Murphy E. J., Osten R. A., 2024, *Frontiers in Astronomy and Space Sciences*, **11**, 1401792

Costa E., et al., 1997, *Nature*, **387**, 783

Coulter D. A., et al., 2017, *Science*, **358**, 1556

Crane P. C., Napier P. J., 1989, in Perley R. A., Schwab F. R., Bridle A. H., eds, Vol. 6, *Synthesis imaging in radio astronomy, A collection of Lectures from the Third NRAO Synthesis Imaging Summer School*. Astronomical Society of the Pacific, p. 139, <https://ui.adsabs.harvard.edu/abs/1989ASPC...6..139C>

Crawford D. F., Robertson J. G., Davidson G., 1996, *Monthly Notices of the Royal Astronomical Society*, **283**, 336

Croft S., et al., 2010, *The Astrophysical Journal*, **719**, 45

Croft S., Bower G. C., Keating G., Law C., Whysong D., Williams P. K. G., Wright M., 2011, *The Astrophysical Journal*, **731**, 34

Croft S., Bower G. C., Whysong D., 2013, *The Astrophysical Journal*, **762**, 93

Crosley M. K., Osten R. A., 2018, *The Astrophysical Journal*, **862**, 113

Crowther P. A., 2007, *Annual Review of Astronomy and Astrophysics*, **45**, 177

Czerny B., Siemiginowska A., Janiuk A., Nikiel-Wroczyński B., Stawarz Ł., 2009, *The Astrophysical Journal*, **698**, 840

Dai S., Johnston S., Bell M. E., Coles W. A., Hobbs G., Ekers R. D., Lenc E., 2016, *Monthly Notices of the Royal Astronomical Society*, **462**, 3115

Dai S., Johnston S., Hobbs G., 2017, *Monthly Notices of the Royal Astronomical Society*, **472**, 1458

Dai S., et al., 2019, *The Astrophysical Journal*, **874**, L14

Das B., et al., 2022, *The Astrophysical Journal*, **925**, 125

Das B., et al., 2025, *Publications of the Astronomical Society of Australia*, **42**, e147

Davies R. D., Walsh D., Browne I. W. A., Edwards M. R., Noble R. G., 1976, *Nature*, **261**, 476

Davis R. J., Lovell B., Palmer H. P., Spencer R. E., 1978, *Nature*, **273**, 644

De Becker M., 2007, *Astronomy and Astrophysics Review*, **14**, 171

DeBoer D. R., 2006, *Acta Astronautica*, **59**, 1153

DeMarchi L., et al., 2022, *The Astrophysical Journal*, **938**, 84

Demorest P. B., Pennucci T., Ransom S. M., Roberts M. S. E., Hessels J. W. T., 2010, *Nature*, **467**, 1081

Dent W. A., 1965, *Science*, **148**, 1458

Dessart L., 2024, *Astronomy and Astrophysics*, **692**, A204

Dewdney P., et al., 2022, *SKA1 Design Baseline Description*, doi:10.5281/zenodo.16895574

Dhawan V., Mirabel I. F., Rodríguez L. F., 2000, *The Astrophysical Journal*, **543**, 373

Dhawan V., Mirabel I. F., Ribó M., Rodrigues I., 2007, *The Astrophysical Journal*, **668**, 430

Dichiara S., Troja E., O'Connor B., Marshall F. E., Beniamini P., Cannizzo J. K., Lien A. Y., Sakamoto T., 2020, *Monthly Notices of the Royal Astronomical Society*, **492**, 5011

Djorgovski S. G., Frail D. A., Kulkarni S. R., Bloom J. S., Odewahn S. C., Diercks A., 2001, *The Astrophysical Journal*, **562**, 654

Dobie D., et al., 2018, *The Astrophysical Journal*, **858**, L15

Dobie D., et al., 2019, *The Astrophysical Journal*, **887**, L13

Dobie D., Kaplan D. L., Hotokezaka K., Murphy T., Deller A., Hallinan G., Nissanka S., 2020, *Monthly Notices of the Royal Astronomical Society*, **494**, 2449

Dobie D., Murphy T., Kaplan D. L., Hotokezaka K., Bonilla Ataides J. P., Mahony E. K., Sadler E. M., 2021, *Monthly Notices of the Royal Astronomical Society*, **505**, 2647

Dobie D., et al., 2022, *Monthly Notices of the Royal Astronomical Society*, **510**, 3794

Dobie D., et al., 2023, *Monthly Notices of the Royal Astronomical Society*, **519**, 4684

Dobie D., et al., 2024, *Monthly Notices of the Royal Astronomical Society*, **535**, 909

Dong D. Z., Hallinan G., 2023, *The Astrophysical Journal*, **948**, 119

Dong L., Petropoulou M., Giannios D., 2018, *Monthly Notices of the Royal Astronomical Society*, **481**, 2685

Dong D. Z., et al., 2021, *Science*, **373**, 1125

Dong Y., et al., 2024, *The Astrophysical Journal*, **961**, 44

Dong F. A., et al., 2025a, *The Astrophysical Journal*, **988**, L29

Dong F. A., et al., 2025b, *The Astrophysical Journal Letters*, **990**, L49

Dougherty S. M., Beasley A. J., Claussen M. J., Zauderer B. A., Bolingbroke N. J., 2005, *The Astrophysical Journal*, **623**, 447

Drake S. A., Abbott D. C., Bastian T. S., Biegling J. H., Churchwell E., Dulk G., Linsky J. L., 1987, *The Astrophysical Journal*, **322**, 902

Drake S. A., Simon T., Linsky J. L., 1989, *The Astrophysical Journal Supplement Series*, **71**, 905

Drake S. A., Simon T., Brown A., 1993, *The Astrophysical Journal*, **406**, 247

Drake A. J., et al., 2009, *The Astrophysical Journal*, **696**, 870

Driessen L. N., et al., 2020, *Monthly Notices of the Royal Astronomical Society*, **491**, 560

Driessen L. N., Williams D. R. A., McDonald I., Stappers B. W., Buckley D. A. H., Fender R. P., Woudt P. A., 2022a, *Monthly Notices of the Royal Astronomical Society*, **510**, 1083

Driessen L. N., et al., 2022b, *Monthly Notices of the Royal Astronomical Society*, **512**, 5037

Driessen L. N., Lenc E., Kaplan D., Murphy T., Gaensler B. M., Sivakoff G. R., 2023, *The Astronomer's Telegram*, **15920**, 1

Driessen L. N., et al., 2024, *Publications of the Astronomical Society of Australia*, **41**, e084

Drout M. R., et al., 2014, *The Astrophysical Journal*, **794**, 23

Duchesne S. W., et al., 2023, *Publications of the Astronomical Society of Australia*, **40**, e034

Duchesne S. W., et al., 2024, *Publications of the Astronomical Society of Australia*, **41**, e003

Duchesne S., et al., 2025, *Publications of the Astronomical Society of Australia*, **42**, 38

Duev D. A., et al., 2019, *Monthly Notices of the Royal Astronomical Society*, **489**, 3582

Dulk G. A., 1985, *Annual Review of Astronomy and Astrophysics*, **23**, 169

Dwek E., 2016, *The Astrophysical Journal*, **825**, 136

Dykaa H., et al., 2024, *The Astrophysical Journal*, **973**, 104

EPTA Collaboration et al., 2023, *Astronomy and Astrophysics*, **678**, A50

Edelson R. A., Krolik J. H., 1988, *The Astrophysical Journal*, **333**, 646

Eftekhari T., Berger E., Williams P. K. G., Blanchard P. K., 2018, *The Astrophysical Journal*, **860**, 73

Eftekhari T., et al., 2019, *The Astrophysical Journal*, **876**, L10

Eftekhari T., et al., 2022, *The Astrophysical Journal*, **935**, 16

Eichler D., Livio M., Piran T., Schramm D. N., 1989, *Nature*, **340**, 126

Eisenberg M., Gottlieb O., Nakar E., 2022, *Monthly Notices of the Royal Astronomical Society*, **517**, 582

Ekers R. D., Culler K., Billingham J., Scheffer L., 2002, SETI 2020 : a roadmap for the search for extraterrestrial intelligence / produced for the SETI Institute by the SETI Science & Technology Working Group. SETI Press, Mountain View, CA

Ellingson S. W., et al., 2013, *IEEE Transactions on Antennas and Propagation*, **61**, 2540

Esposito P., Turolla R., de Luca A., Israel G. L., Possenti A., Burrows D. N., 2011, *Monthly Notices of the Royal Astronomical Society*, **418**, 170

Exter K. M., Watson S. K., Barlow M. J., Davis R. J., 2002, *Monthly Notices of the Royal Astronomical Society*, **333**, 715

Fabian A. C., 2009, Serendipity in Astronomy, doi:10.48550/arXiv.0908.2784, <https://ui.adsabs.harvard.edu/abs/2009arXiv0908.2784F>

Falcke H., Lehár J., Barvainis R., Nagar N. M., Wilson A. S., 2001, in Peterson B. M., Pogge R. W., Polidan R. S., eds., Vol. 224, Probing the Physics of Active Galactic Nuclei. Astronomical Society of the Pacific, San Francisco, USA, p. 265, doi:10.48550/arXiv.astro-ph/0009457, <https://ui.adsabs.harvard.edu/abs/2001ASP..224..265F>

Fan Y.-N., Xu K., Chen W.-C., 2024, *The Astrophysical Journal*, **967**, 24

Fanaroff B. L., Riley J. M., 1974, *Monthly Notices of the Royal Astronomical Society*, **167**, 31P

Farrell W. M., Desch M. D., Zarka P., 1999, *Journal of Geophysical Research*, **104**, 14025

Feindt U., Nordin J., Rigault M., Brinnel V., Dhawan S., Goobar A., Kowalski M., 2019, *Journal of Cosmology and Astroparticle Physics*, **2019**, 005

Feldman P. A., Taylor A. R., Gregory P. C., Seaquist E. R., Balonek T. J., Cohen N. L., 1978, *The Astronomical Journal*, **83**, 1471

Fender R., 2006, in Lewin W. H. G., van der Klis M., eds., , Vol. 39, Compact stellar X-ray sources. Cambridge University Press, Cambridge, UK, pp 381–419, doi:10.48550/arXiv.astro-ph/0303339, <https://ui.adsabs.harvard.edu/abs/2006csxs.book..381F>

Fender R., 2016, *Astronomische Nachrichten*, **337**, 381

Fender R. P., Bell M. E., 2011, *Bulletin of the Astronomical Society of India*, **39**, 315

Fender R., Gallo E., 2014, *Space Science Reviews*, **183**, 323

Fender R. P., Pooley G. G., Durouchoux P., Tilanus R. P. J., Brocksopp C., 2000, *Monthly Notices of the Royal Astronomical Society*, **312**, 853

Fender R. P., Belloni T. M., Gallo E., 2004a, *Monthly Notices of the Royal Astronomical Society*, **355**, 1105

Fender R., Wu K., Johnston H., Tzioumis T., Jonker P., Spencer R., van der Klis M., 2004b, *Nature*, **427**, 222

Fender R. P., Maccarone T. J., van Kesteren Z., 2005, *Monthly Notices of the Royal Astronomical Society*, **360**, 1085

Fender R. P., Stirling A. M., Spencer R. E., Brown I., Pooley G. G., Muxlow T. W. B., Miller-Jones J. C. A., 2006, *Monthly Notices of the Royal Astronomical Society*, **369**, 603

Fender R., Wijers R., Stappers B., LOFAR Transients Key Science Project t., 2008, LOFAR Transients and the Radio Sky Monitor, doi:10.48550/arXiv.0805.4349, <https://ui.adsabs.harvard.edu/abs/2008arXiv0805.4349F>

Fender R., Stewart A., Macquart J. P., Donnarumma I., Murphy T., Deller A., Paragi Z., Chatterjee S., 2015a, in Advancing Astrophysics with the Square Kilometre Array (AASKA14). SKA Organization, eprint: arXiv:1507.00729, p. 51, doi:10.22323/1.215.0051, <https://ui.adsabs.harvard.edu/abs/2015aska.confE..51F>

Fender R., Anderson G. E., Osten R., Staley T., Rumsey C., Grainge K., Saunders R. D. E., 2015b, *Monthly Notices of the Royal Astronomical Society*, **446**, L66

Fender R., et al., 2016, in MeerKAT Science: On the Pathway to the SKA. eprint: arXiv:1711.04132, p. 13, doi:10.22323/1.277.0013, <https://ui.adsabs.harvard.edu/abs/2016mks..confE..13F>

Fender R. P., et al., 2023, *Monthly Notices of the Royal Astronomical Society*, **518**, 1243

Feng L., et al., 2017, *The Astronomical Journal*, **153**, 98

Fiedler R. L., Dennison B., Johnston K. J., Hewish A., 1987, *Nature*, **326**, 675

Fiedler R., Dennison B., Johnston K. J., Waltman E. B., Simon R. S., 1994, *The Astrophysical Journal*, **430**, 581

Fijma S., et al., 2024, *Monthly Notices of the Royal Astronomical Society*, **528**, 6985

Finzell T., et al., 2018, *The Astrophysical Journal*, **852**, 108

Fluke C. J., Jacobs C., 2020, *WIREs Data Mining and Knowledge Discovery*, **10**, e1349

Fong W., et al., 2014, *The Astrophysical Journal*, **780**, 118

Fong W., Berger E., Margutti R., Zauderer B. A., 2015, *The Astrophysical Journal*, **815**, 102

Fong W., et al., 2021, *The Astrophysical Journal*, **906**, 127

Frail D. A., Kulkarni S. R., Nicastro L., Feroci M., Taylor G. B., 1997, *Nature*, **389**, 261

Frail D. A., Kulkarni S. R., Bloom J. S., 1999a, *Nature*, **398**, 127

Frail D. A., et al., 1999b, *The Astrophysical Journal*, **525**, L81

Frail D. A., et al., 2000a, *The Astrophysical Journal*, **534**, 559

Frail D. A., Waxman E., Kulkarni S. R., 2000b, *The Astrophysical Journal*, **537**, 191

Frail D. A., et al., 2000c, *The Astrophysical Journal*, **538**, L129

Frail D. A., et al., 2001, *The Astrophysical Journal*, **562**, L55

Frail D. A., Kulkarni S. R., Berger E., Wieringa M. H., 2003, *The Astronomical Journal*, **125**, 2299

Frail D. A., Soderberg A. M., Kulkarni S. R., Berger E., Yost S., Fox D. W., Harrison F. A., 2005, *The Astrophysical Journal*, **619**, 994

Frail D. A., et al., 2006, *The Astrophysical Journal*, **646**, L99

Frail D. A., Kulkarni S. R., Ofek E. O., Bower G. C., Nakar E., 2012, *The Astrophysical Journal*, **747**, 70

Frail D. A., et al., 2024, *The Astrophysical Journal*, **975**, 34

Fransson C., et al., 2024, *Science*, **383**, 898

Franzen T. M. O., et al., 2009, *Monthly Notices of the Royal Astronomical Society*, **400**, 995

Franzen T. M. O., et al., 2021, *Publications of the Astronomical Society of Australia*, **38**, e041

Fridman P. A., Baan W. A., 2001, *Astronomy and Astrophysics*, **378**, 327

Fruchter A. S., Stinebring D. R., Taylor J. H., 1988, *Nature*, **333**, 237

Gaensler B. M., Hunstead R. W., 2000, *Publications of the Astronomical Society of Australia*, **17**, 72

Gaensler B. M., Slane P. O., 2006, *Annual Review of Astronomy and Astrophysics*, **44**, 17

Gaia Collaboration et al., 2023, *Astronomy and Astrophysics*, **674**, A1

Gal-Yam A., et al., 2006, *The Astrophysical Journal*, **639**, 331

Galama T. J., et al., 1998, *Nature*, **395**, 670

Galama T. J., et al., 2000, *The Astrophysical Journal*, **541**, L45

Galama T. J., Frail D. A., Sari R., Berger E., Taylor G. B., Kulkarni S. R., 2003, *The Astrophysical Journal*, **585**, 899

Gallagher J. S., Starrfield S., 1978, *Annual Review of Astronomy and Astrophysics*, **16**, 171

Gallo E., Fender R. P., Pooley G. G., 2003, *Monthly Notices of the Royal Astronomical Society*, **344**, 60

Gallo E., Fender R., Kaiser C., Russell D., Morganti R., Oosterloo T., Heinz S., 2005, *Nature*, **436**, 819

Gallo E., et al., 2014, *Monthly Notices of the Royal Astronomical Society*, **445**, 290

Gallo E., Degenaar N., van den Eijnden J., 2018, *Monthly Notices of the Royal Astronomical Society*, **478**, L132

Gaspari N., Levan A. J., Chrimes A. A., Nelemans G., 2024, *Monthly Notices of the Royal Astronomical Society*, **527**, 1101

Gezari S., 2021, *Annual Review of Astronomy and Astrophysics*, **59**, 21

Ghirlanda G., et al., 2014, *Publications of the Astronomical Society of Australia*, **31**, e022

Ghirlanda G., et al., 2019, *Science*, **363**, 968

Giannios D., Metzger B. D., 2011, *Monthly Notices of the Royal Astronomical Society*, **416**, 2102

Giarratana S., et al., 2024, *Astronomy and Astrophysics*, **690**, A74

Giles D., Walkowicz L., 2019, *Monthly Notices of the Royal Astronomical Society*, **484**, 834

Giuricin G., Mardirossian F., Mezzetti M., 1983, *The Astrophysical Journal Supplement Series*, **52**, 35

Goldstein A., et al., 2017, *The Astrophysical Journal*, **848**, L14

Goodman J., 1997, *New Astronomy*, **2**, 449

Goodman J. J., Romani R. W., Blandford R. D., Narayan R., 1987, *Monthly Notices of the Royal Astronomical Society*, **229**, 73

Goodwin A. J., et al., 2023, *Monthly Notices of the Royal Astronomical Society*, **518**, 847

Goodwin A. J., et al., 2025, *The Astrophysical Journal Supplement Series*, **278**, 36

Gopal-Krishna Subramanian K., 1991, *Nature*, **349**, 766

Gottesman S. T., Broderick J. J., Brown R. L., Balick B., Palmer P., 1972, *The Astrophysical Journal*, **174**, 383

Granot J., van der Horst A. J., 2014, *Publications of the Astronomical Society of Australia*, **31**, e008

Green A. J., Cram L. E., Large M. I., Ye T., 1999, *The Astrophysical Journal Supplement Series*, **122**, 207

Gregory P. C., Taylor A. R., 1981, *The Astrophysical Journal*, **248**, 596

Gregory P. C., Taylor A. R., 1986, *The Astronomical Journal*, **92**, 371

Gregory P. C., Kronberg P. P., Seaquist E. R., Hughes V. A., Woodsworth A., Viner M. R., Retallack D., 1972, *Nature*, **239**, 440

Greiner J., et al., 2013, *Astronomy and Astrophysics*, **560**, A70

Grießmeier J. M., Zarka P., Spreeuw H., 2007, *Astronomy and Astrophysics*, **475**, 359

Grobler T. L., Nunhokee C. D., Smirnov O. M., van Zyl A. J., de Bruyn A. G., 2014, *Monthly Notices of the Royal Astronomical Society*, **439**, 4030

Gudel M., 1992, *Astronomy and Astrophysics*, **264**, L31

Güdel M., 2002, *Annual Review of Astronomy and Astrophysics*, **40**, 217

Guirado J. C., Climent J. B., Bergasa J. D., Pérez-Torres M. A., Marcaide J. M., Peña-Moñino L., 2025, *The Astrophysical Journal*, **987**, 7

Gulati A., et al., 2023, *Publications of the Astronomical Society of Australia*, **40**, e025

Gulati A., et al., 2025, *Monthly Notices of the Royal Astronomical Society*, **538**, 2676

Guns S., et al., 2021, *The Astrophysical Journal*, **916**, 98

Gupta Y., et al., 2017, *Current Science*, **113**, 707

Hajduk M., Leto P., Vedantham H., Trigilio C., Havercorn M., Shimwell T., Callingham J. R., White G. J., 2022, *Astronomy and Astrophysics*, **665**, A152

Hajela A., Mooley K. P., Intema H. T., Frail D. A., 2019a, *Monthly Notices of the Royal Astronomical Society*, **490**, 4898

Hajela A., et al., 2019b, *The Astrophysical Journal*, **886**, L17

Hajela A., et al., 2022, *The Astrophysical Journal*, **927**, L17

Hajela A., et al., 2025, *The Astrophysical Journal*, **983**, 29

Hale C. L., et al., 2021, *Publications of the Astronomical Society of Australia*, **38**, e058

Hall D. S., 1976, in Fitch W. S., ed., *Astrophysics and Space Science Library* Vol. 60, IAU Colloq. 29: Multiple Periodic Variable Stars. p. 287, doi:10.1007/978-94-010-1175-4\_15

Hallinan G., et al., 2007, *The Astrophysical Journal*, **663**, L25

Hallinan G., Antonova A., Doyle J. G., Bourke S., Lane C., Golden A., 2008, *The Astrophysical Journal*, **684**, 644

Hallinan G., et al., 2015, *Nature*, **523**, 568

Hallinan G., et al., 2017, *Science*, **358**, 1579

Hallinan G., et al., 2019, in *Bulletin of the American Astronomical Society*. p. 255 (arXiv:1907.07648), doi:10.48550/arXiv.1907.07648

Hancock P. J., Gaensler B. M., Murphy T., 2011, *The Astrophysical Journal*, **735**, L35

Hancock P. J., Murphy T., Gaensler B. M., Hopkins A., Curran J. R., 2012a, *Monthly Notices of the Royal Astronomical Society*, **422**, 1812

Hancock P. J., Murphy T., Gaensler B., Zauderer A., 2012b, GRB Coordinates Network, **12804**, 1

Hancock P. J., Drury J. A., Bell M. E., Murphy T., Gaensler B. M., 2016, *Monthly Notices of the Royal Astronomical Society*, **461**, 3314

Hancock P. J., Trott C. M., Hurley-Walker N., 2018, *Publications of the Astronomical Society of Australia*, **35**, e011

Hancock P. J., Charlton E. G., Macquart J.-P., N. Hurley-Walker 2019, Refractive Interstellar Scintillation of Extra-galactic Radio Sources I: Expectations, doi:10.48550/arXiv.1907.08395, <https://ui.adsabs.harvard.edu/abs/2019arXiv190708395H>

Hankins T. H., Kern J. S., Weatherall J. C., Eilek J. A., 2003, *Nature*, **422**, 141

Harrison F. A., et al., 1999, *The Astrophysical Journal*, **523**, L121

Harrison F. A., et al., 2001, *The Astrophysical Journal*, **559**, 123

Harwit M., 1981, *Cosmic discovery. The search, scope, and heritage of astronomy*. Harvester Press, Brighton, UK

Heeschen D. S., Krichbaum T., Schalinski C. J., Witzel A., 1987, *The Astronomical Journal*, **94**, 1493

Helmboldt J. F., Ellingson S. W., Hartman J. M., Lazio T. J. W., Taylor G. B., Wilson T. L., Wolfe C. N., 2014, *Radio Science*, **49**, 157

Helou G., Soifer B. T., Rowan-Robinson M., 1985, *The Astrophysical Journal*, **298**, L7

Helstrom C. W., 1995, *Elements of signal detection and estimation*, 1. print edn. PTR Prentice Hall, Englewood Cliffs, NJ

Henriksen R. N., Widrow L. M., 1995, *The Astrophysical Journal*, **441**, 70

Hess S. L. G., Zarka P., 2011, *Astronomy and Astrophysics*, **531**, A29

Hewish A., Scott P. F., Wills D., 1964, *Nature*, **203**, 1214

Hewish A., Bell S. J., Pilkington J. D. H., Scott P. F., Collins R. A., 1968, *Nature*, **217**, 709

Hey J. S., 1946, *Nature*, **157**, 47

Hey J. S., Parsons S. J., Phillips J. W., 1946, *Nature*, **158**, 234

Heywood I., et al., 2016, *Monthly Notices of the Royal Astronomical Society*, **457**, 4160

Hills J. G., 1975, *Nature*, **254**, 295

Hinse T. C., Dorch B. F., Occhionero L. V. T., Holck J. P., 2023, *Front. Astron. Space Sci.*, **10**

Hjellming R. M., Balick B., 1972, *Nature*, **239**, 443

Hjellming R. M., Wade C. M., 1971, *Science*, **173**, 1087

Hjellming R. M., Hermann M., Webster E., 1972, *Nature*, **237**, 507

Hjellming R. M., Wade C. M., Vandenberg N. R., Newell R. T., 1979, *The Astronomical Journal*, **84**, 1619

Ho W. C. G., Andersson N., 2017, *Monthly Notices of the Royal Astronomical Society*, **464**, L65

Ho A. Y. Q., et al., 2019, *The Astrophysical Journal*, **871**, 73

Ho A. Y. Q., et al., 2020, *The Astrophysical Journal*, **895**, 49

Ho A. Y. Q., et al., 2022, *The Astrophysical Journal*, **932**, 116

Ho A. Y. Q., et al., 2023a, *Nature*, **623**, 927

Ho A. Y. Q., et al., 2023b, *The Astrophysical Journal*, **949**, 120

Hobbs G., et al., 2016, *Monthly Notices of the Royal Astronomical Society*, **456**, 3948

Hodge J. A., Becker R. H., White R. L., Richards G. T., 2013, *The Astrophysical Journal*, **769**, 125

Hogg D. W., Bovy J., Lang D., 2010, Data analysis recipes: Fitting a model to data, doi:10.48550/arXiv.1008.4686, <http://arxiv.org/abs/1008.4686>

Hopkins A. M., et al., 2015, *Publications of the Astronomical Society of Australia*, **32**, e037

Hopkins A., et al., 2025, *Publications of the Astronomical Society of Australia*, **42**, e071

Horesh A., et al., 2012, *The Astrophysical Journal*, **746**, 21

Horesh A., Cenko S. B., Perley D. A., Kulkarni S. R., Hallinan G., Bellm E., 2015, *The Astrophysical Journal*, **812**, 86

Horesh A., Cenko S. B., Arcavi I., 2021a, *Nature Astronomy*, **5**, 491

Horesh A., Sfaradi I., Fender R., Green D. A., Williams D. R. A., Bright J. S., 2021b, *The Astrophysical Journal*, **920**, L5

Hotan A. W., et al., 2014, *Publications of the Astronomical Society of Australia*, **31**, e041

Hotan A. W., et al., 2021, *Publications of the Astronomical Society of Australia*, **38**, e009

Hotokezaka K., Piran T., 2015, *Monthly Notices of the Royal Astronomical Society*, **450**, 1430

Hotokezaka K., Nissance S., Hallinan G., Lazio T. J. W., Nakar E., Piran T., 2016, *The Astrophysical Journal*, **831**, 190

Hotokezaka K., Kiuchi K., Shibata M., Nakar E., Piran T., 2018, *The Astrophysical Journal*, **867**, 95

Hotokezaka K., Nakar E., Gottlieb O., Nissance S., Masuda K., Hallinan G., Mooley K. P., Deller A. T., 2019, *Nature Astronomy*, **3**, 940

Hovatta T., Tornikoski M., Lainela M., Lehto H. J., Valtaoja E., Torniainen I., Aller M. F., Aller H. D., 2007, *Astronomy and Astrophysics*, **469**, 899

Hovatta T., Nieppola E., Tornikoski M., Valtaoja E., Aller M. F., Aller H. D., 2008, *Astronomy and Astrophysics*, **485**, 51

Hoyle F., Narlikar J. V., 1961, *Monthly Notices of the Royal Astronomical Society*, **123**, 133

Huang Y., Anderson M. M., Hallinan G., W. Lazio T. J., Price D. C., Sharma Y., 2022, *The Astrophysical Journal*, **925**, 171

Huang F., Bi Y.-C., Cao Z., Huang Q.-G., 2024, *Chinese Physics C*, **48**, 065103

Huertas-Company M., Lanusse F., 2023, *Publications of the Astronomical Society of Australia*, **40**, e001

Hufnagel B. R., Bregman J. N., 1992, *The Astrophysical Journal*, **386**, 473

Hughes P. A., Aller H. D., Aller M. F., 1989, *The Astrophysical Journal*, **341**, 54

Hughes P. A., Aller H. D., Aller M. F., 1992, *The Astrophysical Journal*, **396**, 469

Hulse R. A., Taylor J. H., 1975, *The Astrophysical Journal*, **195**, L51

Hunstead R. W., 1972, *Astrophysical Letters*, **12**, 193

Hurley-Walker N., et al., 2022a, *Publications of the Astronomical Society of Australia*, **39**, e035

Hurley-Walker N., et al., 2022b, *Nature*, **601**, 526

Hurley-Walker N., et al., 2023, *Nature*, **619**, 487

Hurley-Walker N., et al., 2024, *The Astrophysical Journal*, **976**, L21

Hyman S. D., Lazio T. J. W., Kassim N. E., Bartleson A. L., 2002, *The Astronomical Journal*, **123**, 1497

Hyman S. D., Lazio T. J. W., Kassim N. E., Ray P. S., Markwardt C. B., Yusef-Zadeh F., 2005, *Nature*, **434**, 50

Hyman S. D., Lazio T. J. W., Roy S., Ray P. S., Kassim N. E., Neureuther J. L., 2006, *The Astrophysical Journal*, **639**, 348

Hyman S. D., Roy S., Pal S., Lazio T. J. W., Ray P. S., Kassim N. E., Bhatnagar S., 2007, *The Astrophysical Journal*, **660**, L121

Hyman S. D., Wijnands R., Lazio T. J. W., Pal S., Starling R., Kassim N. E., Ray P. S., 2009, *The Astrophysical Journal*, **696**, 280

Hyman S. D., et al., 2021, *Monthly Notices of the Royal Astronomical Society*, **507**, 3888

Högberg J. A., Shakeshaft J. R., 1961, *Nature*, **189**, 561

Ibik A. L., et al., 2024, *The Astrophysical Journal*, **976**, 199

Intema H. T., Jagannathan P., Mooley K. P., Frail D. A., 2017, *Astronomy and Astrophysics*, **598**, A78

Ivezic Ž., et al., 2019, *The Astrophysical Journal*, **873**, 111

Jaeger T. R., Hyman S. D., Kassim N. E., Lazio T. J. W., 2012, *The Astronomical Journal*, **143**, 96

James C. W., et al., 2025, *The Astrophysical Journal Letters*, **987**, L16

Janiuk A., Czerny B., 2011, *Monthly Notices of the Royal Astronomical Society*, **414**, 2186

Jankowski F., van Straten W., Keane E. F., Bailes M., Barr E. D., Johnston S., Kerr M., 2018, *Monthly Notices of the Royal Astronomical Society*, **473**, 4436

Jauncey D. L., Macquart J. P., 2001, *Astronomy and Astrophysics*, **370**, L9

Jin Z.-P., et al., 2018, *The Astrophysical Journal*, **857**, 128

Johnston S., et al., 2007, *Publications of the Astronomical Society of Australia*, **24**, 174

Jokipii J. R., 1973, *Annual Review of Astronomy and Astrophysics*, **11**, 1

Jonas J., et al., 2016, *MeerKAT Science: On the Pathway to the SKA*, p. 1

Jow D. L., Pen U.-L., Baker D., 2024, *Monthly Notices of the Royal Astronomical Society*, **528**, 6292

Kao M. M., Hallinan G., Pineda J. S., Escala I., Burgasser A., Bourke S., Stevenson D., 2016, *The Astrophysical Journal*, **818**, 24

Kao M. M., Hallinan G., Pineda J. S., Stevenson D., Burgasser A., 2018, *The Astrophysical Journal Supplement Series*, **237**, 25

Kao M. M., Mioduszewski A. J., Villadsen J., Shkolnik E. L., 2023, *Nature*, **619**, 272

Kaplan D. L., Hyman S. D., Roy S., Bandyopadhyay R. M., Chakrabarty D., Kassim N. E., Lazio T. J. W., Ray P. S., 2008, *The Astrophysical Journal*, **687**, 262

Kaplan D. L., et al., 2015, *The Astrophysical Journal*, **809**, L12

Kaplan D. L., et al., 2019, *The Astrophysical Journal*, **884**, 96

Karastergiou A., Johnston S., Posselt B., Oswald L. S., Kramer M., Weltevrede P., 2024, *Monthly Notices of the Royal Astronomical Society*, **532**, 3558

Kasen D., Bildsten L., 2010, *The Astrophysical Journal*, **717**, 245

Kasliwal M. M., et al., 2017, *Science*, **358**, 1559

Kaspi V. M., Beloborodov A. M., 2017, *Annual Review of Astronomy and Astrophysics*, **55**, 261

Kaspi V. M., Stinebring D. R., 1992, *The Astrophysical Journal*, **392**, 530

Katira A., Mooley K. P., Hotokezaka K., 2025, *Monthly Notices of the Royal Astronomical Society*, **539**, 2654

Katz J. I., 2022, *Astrophysics and Space Science*, **367**, 108

Keane E. F., McLaughlin M. A., 2011, *Bulletin of the Astronomical Society of India*, **39**, 333

Keane E. F., Kramer M., Lyne A. G., Stappers B. W., McLaughlin M. A., 2011, *Monthly Notices of the Royal Astronomical Society*, **415**, 3065

Keith M. J., et al., 2024, *Monthly Notices of the Royal Astronomical Society*, **530**, 1581

Kellermann K. I., 1966, *Icarus*, **5**, 478

Kellermann K. I., Pauliny-Toth I. I. K., 1969, *The Astrophysical Journal*, **155**, L71

Kellermann K. I., Verschuur G. L., 1988, *Galactic and Extragalactic Radio Astronomy*. Springer International Publishing, Heidelberg, Germany, <https://ui.adsabs.harvard.edu/abs/1988gera.book.....K>

Kellermann K. I., Sramek R., Schmidt M., Shaffer D. B., Green R., 1989, *The Astronomical Journal*, **98**, 1195

Kellermann K. I., Condon J. J., Kimball A. E., Perley R. A., Ivezic Ž., 2016, *The Astrophysical Journal*, **831**, 168

Kemp I., Tingay S., Midgley S., Mitchell D., 2024, *The Astronomical Journal*, **168**, 153

Kesteven M. J. L., Bridle A. H., Brandie G. W., 1976, *The Astronomical Journal*, **81**, 919

Klebesadel R. W., Strong I. B., Olson R. A., 1973, *The Astrophysical Journal*, **182**, L85

Koay J. Y., Vestergaard M., Bignall H. E., Reynolds C., Peterson B. M., 2016, *Monthly Notices of the Royal Astronomical Society*, **460**, 304

Kochanek C. S., Piran T., 1993, *The Astrophysical Journal*, **417**, L17

Koljonen K. I. I., McCollough M. L., Hannikainen D. C., Droulans R., 2013, *Monthly Notices of the Royal Astronomical Society*, **429**, 1173

Komossa S., 2015, *Journal of High Energy Astrophysics*, **7**, 148

Kool E. C., et al., 2023, *Nature*, **617**, 477

Koopmans L. V. E., de Bruyn A. G., 2000, *Astronomy and Astrophysics*, **358**, 793

Koopmans L. V. E., et al., 2003, *The Astrophysical Journal*, **595**, 712

Kosogorov N., et al., 2025, *The Astrophysical Journal*, **985**, 265

Kouveliotou C., Meegan C. A., Fishman G. J., Bhat N. P., Briggs M. S., Koshut T. M., Paciesas W. S., Pendleton G. N., 1993, *The Astrophysical Journal*, **413**, L101

Kowalski A. F., 2024, *Living Reviews in Solar Physics*, **21**, 1

Kramer M., Lyne A. G., O'Brien J. T., Jordan C. A., Lorimer D. R., 2006, *Science*, **312**, 549

Kramer M., et al., 2021, *Physical Review X*, **11**, 041050

Krauss M. I., et al., 2011, *The Astrophysical Journal*, **739**, L6

Kreuter L. T., Gillen E., Briegal J. T., Queloz D., 2023, *Monthly Notices of the Royal Astronomical Society*, **522**, 5049

Krolik J. H., Piran T., 2011, *The Astrophysical Journal*, **743**, 134

Krolik J., Piran T., Svirski G., Cheng R. M., 2016, *The Astrophysical Journal*, **827**, 127

Kuiack M., Wijers R. A. M. J., Shulevski A., Rowlinson A., Huizinga F., Molenaar G., Prasad P., 2021, *Monthly Notices of the Royal Astronomical Society*, **505**, 2966

Kuin N. P. M., et al., 2019, *Monthly Notices of the Royal Astronomical Society*, **487**, 2505

Kulkarni S. R., et al., 1998, *Nature*, **395**, 663

Kulkarni S. R., et al., 1999, *The Astrophysical Journal*, **522**, L97

Kumamoto H., et al., 2021, *Monthly Notices of the Royal Astronomical Society*, **501**, 4490

Kunert-Bajraszewska M., Wołowska A., Mooley K., Kharb P., Hallinan G., 2020, *The Astrophysical Journal*, **897**, 128

Kuniyoshi M., et al., 2007, *Publications of the Astronomical Society of the Pacific*, **119**, 122

Lacy M., et al., 2020, *Publications of the Astronomical Society of the Pacific*, **132**, 035001

Lähteenmäki A., Valtaoja E., 1999, *The Astrophysical Journal*, **521**, 493

Lamb G. P., et al., 2019, *The Astrophysical Journal*, **883**, 48

Landstreet J. D., 1992, *The Astron Astrophys Rev*, **4**, 35

Laskar T., et al., 2016, *The Astrophysical Journal*, **833**, 88

Laskar T., et al., 2018, *The Astrophysical Journal*, **859**, 134

Laskar T., et al., 2022, *The Astrophysical Journal Letters*, **935**, L11

Laskar T., et al., 2023, *The Astrophysical Journal*, **946**, L23

Law N. M., et al., 2009, *Publications of the Astronomical Society of the Pacific*, **121**, 1395

Law C. J., et al., 2018a, *The Astrophysical Journal Supplement Series*, **236**, 8

Law C. J., Gaensler B. M., Metzger B. D., Ofek E. O., Sironi L., 2018b, *The Astrophysical Journal*, **866**, L22

Law C. J., et al., 2019, *The Astrophysical Journal*, **886**, 24

Law C. J., Connor L., Aggarwal K., 2022, *The Astrophysical Journal*, **927**, 55

Lazio T. J. W., Farrell W. M., 2007, *The Astrophysical Journal*, **668**, 1182

Lazio W. T. J., Farrell W. M., Dietrick J., Greenlees E., Hogan E., Jones C., Hennig L. A., 2004, *The Astrophysical Journal*, **612**, 511

Lazio T. J. W., et al., 2010, *The Astronomical Journal*, **140**, 1995

Lazzati D., Perna R., Morsany B. J., Lopez-Camara D., Cantiello M., Ciolfi R., Giacomazzo B., Workman J. C., 2018, *Physical Review Letters*, **120**, 241103

Lee Y. W. J., et al., 2025, *Nature Astronomy*, **9**, 393

Lee Y. W. J., et al., 2026, *Monthly Notices of the Royal Astronomical Society*, **545**, staf2008

Lefevre E., Klein K. L., Lestrade J. F., 1994, *Astronomy and Astrophysics*, **283**, 483

Leitherer C., Chapman J. M., Koribalski B., 1995, *The Astrophysical Journal*, **450**, 289

Lenc E., Murphy T., Lynch C. R., Kaplan D. L., Zhang S. N., 2018, *Monthly Notices of the Royal Astronomical Society*, **478**, 2835

Leone F., Umana G., 1993, *Astronomy and Astrophysics*, **268**, 667

Leroy A. M., Rousseeuw P. J., 1987, Robust regression and outlier detection. Wiley, <https://ui.adsabs.harvard.edu/abs/1987rrod.book.....L>

Leto P., Trigilio C., Buemi C. S., Umana G., Leone F., 2006, *Astronomy and Astrophysics*, **458**, 831

Leung J. K., et al., 2021, *Monthly Notices of the Royal Astronomical Society*, **503**, 1847

Leung J. K., Murphy T., Lenc E., Edwards P. G., Ghirlanda G., Kaplan D. L., O'Brien A., Wang Z., 2023, *Monthly Notices of the Royal Astronomical Society*, **523**, 4029

Levan A. J., et al., 2011, *Science*, **333**, 199

Levan A. J., et al., 2024, *Nature*, **626**, 737

Levin L., et al., 2010, *The Astrophysical Journal*, **721**, L33

Levin L., et al., 2019, *Monthly Notices of the Royal Astronomical Society*, **488**, 5251

Levinson A., Ofek E. O., Waxman E., Gal-Yam A., 2002, *The Astrophysical Journal*, **576**, 923

Li Z.-Y., Chevalier R. A., 2001, *The Astrophysical Journal*, **551**, 940

Li L.-B., Zhang Z.-B., Rice J., 2015, *Astrophysics and Space Science*, **359**, 37

Li Y., et al., 2023, *The Astrophysical Journal*, **956**, 36

Lim J., White S. M., 1995, *The Astrophysical Journal*, **453**, 207

Lim J., Nelson G. J., Castro C., Kilkenny D., van Wyk F., 1992, *The Astrophysical Journal*, **388**, L27

Lim J., Carilli C. L., White S. M., Beasley A. J., Marson R. G., 1998, *Nature*, **392**, 575

Lin H., Totani T., 2020, *Monthly Notices of the Royal Astronomical Society*, **498**, 2384

Lin H.-H., et al., 2022, *Publications of the Astronomical Society of the Pacific*, **134**, 094106

Linsky J. L., Drake S. A., Bastian T. S., 1992, *The Astrophysical Journal*, **393**, 341

Lintott C. J., et al., 2008, *Monthly Notices of the Royal Astronomical Society*, **389**, 1179

Lintott C., et al., 2011, *Monthly Notices of the Royal Astronomical Society*, **410**, 166

Lister M. L., 2001, *The Astrophysical Journal*, **561**, 676

Liu K., et al., 2021, *The Astrophysical Journal*, **914**, 30

Liu Z.-W., Röpke F. K., Han Z., 2023, *Research in Astronomy and Astrophysics*, **23**, 082001

Lloyd-Ronning N., 2018, *Galaxies*, **6**, 103

Lloyd-Ronning N. M., Fryer C. L., 2017, *Monthly Notices of the Royal Astronomical Society*, **467**, 3413

Lloyd-Ronning N. M., Murphy E. J., 2017, in Science with a Next Generation Very Large Array. Astronomical Society of the Pacific, San Fransisco, USA, p. 701, doi:10.48550/arXiv.1709.08512, <https://ui.adsabs.harvard.edu/abs/2017arXiv170908512L>

Lo K. K., et al., 2012, *Monthly Notices of the Royal Astronomical Society*, **421**, 3316

Lochner M., Bassett B. A., 2021, *Astronomy and Computing*, **36**, 100481

Lochner M., McEwen J. D., Peiris H. V., Lahav O., Winter M. K., 2016, *The Astrophysical Journal Supplement Series*, **225**, 31

Loeb A., Maoz D., 2022, *Research Notes of the American Astronomical Society*, **6**, 27

Loi S. T., et al., 2015a, *Geophysical Research Letters*, **42**, 3707

Loi S. T., et al., 2015b, *Monthly Notices of the Royal Astronomical Society*, **453**, 2731

Longair M. S., Scott P. F., 1965, *Monthly Notices of the Royal Astronomical Society*, **130**, 379

Lorimer D. R., Kramer M., 2012, Handbook of Pulsar Astronomy. Cambridge University Press, Cambridge, UK, <https://ui.adsabs.harvard.edu/abs/2012hpa..book.....L>

Lorimer D. R., Bailes M., McLaughlin M. A., Narkevic D. J., Crawford F., 2007, *Science*, **318**, 777

Lourenço L., et al., 2024, *Publications of the Astronomical Society of Australia*, **41**, e012

Lovell A. C. B., 1964, *The Observatory*, **84**, 191

Lovell B., Whipple F. L., Solomon L. H., 1963, *Nature*, **198**, 228

Lovell J. E. J., Jauncey D. L., Bignall H. E., Kedziora-Chudczer L., Macquart J. P., Rickett B. J., Tzioumis A. K., 2003, *The Astronomical Journal*, **126**, 1699

Lovell J. E. J., et al., 2008, *The Astrophysical Journal*, **689**, 108

Lower M. E., et al., 2025, *Monthly Notices of the Royal Astronomical Society*, **538**, 3104

Lucas L., Staley T., Scaife A., 2019, *Astronomy and Computing*, **27**, 96

Lucas P. W., et al., 2020, *Monthly Notices of the Royal Astronomical Society*, **492**, 4847

Lukic V., Brüggen M., Banfield J. K., Wong O. I., Rudnick L., Norris R. P., Simmons B., 2018, *Monthly Notices of the Royal Astronomical Society*, **476**, 246

Luo R., et al., 2024, *Publications of the Astronomical Society of Australia*, **41**, e109

Luyten W. J., 1949, *The Astrophysical Journal*, **109**, 532

Lynch C., Murphy T., Ravi V., Hobbs G., Lo K., Ward C., 2016, *Monthly Notices of the Royal Astronomical Society*, **457**, 1224

Lynch C. R., Lenc E., Kaplan D. L., Murphy T., Anderson G. E., 2017, *The Astrophysical Journal*, **836**, L30

Lynch C. R., Murphy T., Lenc E., Kaplan D. L., 2018, *Monthly Notices of the Royal Astronomical Society*, **478**, 1763

Lyutikov M., 2022, *Monthly Notices of the Royal Astronomical Society*, **515**, 2293

Lyutikov M., Toonen S., 2019, *Monthly Notices of the Royal Astronomical Society*, **487**, 5618

MacFadyen A. I., Woosley S. E., 1999, *The Astrophysical Journal*, **524**, 262

MacGregor M. A., et al., 2021, *The Astrophysical Journal*, **911**, L25

Macquart J.-P., et al., 2010, *Publications of the Astronomical Society of Australia*, **27**, 272

Maehara H., et al., 2012, *Nature*, **485**, 478

Manchester R. N., Hobbs G. B., Teoh A., Hobbs M., 2005, *The Astronomical Journal*, **129**, 1993

Mao Y.-H., Li X.-D., Lai D., Deng Z.-L., Yang H.-R., 2025, *The Astrophysical Journal Letters*, **988**, L11

Maoz D., Mannucci F., Nelemans G., 2014, *Annual Review of Astronomy and Astrophysics*, **52**, 107

Marcote B., et al., 2017, *The Astrophysical Journal*, **834**, L8

Marcote B., Nimmo K., Salafia O. S., Paragi Z., Hessels J. W. T., Petroff E., Karuppusamy R., 2019, *The Astrophysical Journal*, **876**, L14

Margalit B., Metzger B. D., 2018, *The Astrophysical Journal*, **868**, L4

Margutti R., et al., 2012, *The Astrophysical Journal*, **751**, 134

Margutti R., et al., 2013, *The Astrophysical Journal*, **778**, 18

Margutti R., et al., 2017, *The Astrophysical Journal*, **848**, L20

Margutti R., et al., 2019, *The Astrophysical Journal*, **872**, 18

Markowitz A., Edelson R., 2004, *The Astrophysical Journal*, **617**, 939

Marscher A. P., Gear W. K., 1985, *The Astrophysical Journal*, **298**, 114

Marsh T. R., et al., 2016, *Nature*, **537**, 374

Martínez-Galarza J. R., Bianco F. B., Crake D., Tirumala K., Mahabal A. A., Graham M. J., Giles D., 2021, *Monthly Notices of the Royal Astronomical Society*, **508**, 5734

Masci F. J., et al., 2019, *Publications of the Astronomical Society of the Pacific*, **131**, 018003

Masci F. J., et al., 2023, eprint arXiv:2305.16279, p. arXiv:2305.16279

Matsumura N., et al., 2009, *The Astronomical Journal*, **138**, 787

Matsuoka M., et al., 2009, *Publications of the Astronomical Society of Japan*, **61**, 999

Matthews L. D., 2019, *Publications of the Astronomical Society of the Pacific*, **131**, 016001

Matthews L. D., 2025, *Publications of the Astronomical Society of the Pacific*, **137**, 116001

Matthews A. M., Condon J. J., Cotton W. D., Mauch T., 2021, *The Astrophysical Journal*, **914**, 126

Mattila S., et al., 2018, *Science*, **361**, 482

Mauch T., Murphy T., Buttery H. J., Curran J., Hunstead R. W., Piestrzynski B., Robertson J. G., Sadler E. M., 2003, *Monthly Notices of the Royal Astronomical Society*, **342**, 1117

Mauk B. H., Fox N. J., 2010, *Journal of Geophysical Research: Space Physics*, **115**

Max-Moerbeck W., et al., 2012, OVRO 40m blazar monitoring program: Understanding the relationship between 15 GHz radio variability properties and gamma-ray activity in blazars, doi:10.48550/arXiv.1205.0276, <http://arxiv.org/abs/1205.0276>

Max-Moerbeck W., et al., 2014, *Monthly Notices of the Royal Astronomical Society*, **445**, 428

McClintock J. E., Narayan R., Steiner J. F., 2014, *Space Science Reviews*, **183**, 295

McConnell D., et al., 2020, *Publications of the Astronomical Society of Australia*, **37**, e048

McCrory R., Fransson C., 2016, *Annual Review of Astronomy and Astrophysics*, **54**, 19

McGilchrist M. M., Riley J. M., 1990, *Monthly Notices of the Royal Astronomical Society*, **246**, 123

McLaughlin M. A., et al., 2006, *Nature*, **439**, 817

McMahon E., Kumar P., Piran T., 2006, *Monthly Notices of the Royal Astronomical Society*, **366**, 575

McSweeney S. J., et al., 2025a, *Monthly Notices of the Royal Astronomical Society*, **542**, 203

McSweeney S. J., Moseley J., Hurley-Walker N., Grover G., Horváth C., Galvin T. J., Meyers B. W., Tan C. M., 2025b, *The Astrophysical Journal*, **981**, 143

Mckinven R., et al., 2025, *Nature*, **637**, 43

Meegan C. A., Fishman G. J., Wilson R. B., Paciesas W. S., Pendleton G. N., Horack J. M., Brock M. N., Kouveliotou C., 1992, *Nature*, **355**, 143

Meegan C., et al., 2009, *The Astrophysical Journal*, **702**, 791

Melrose D. B., 1991, *Annual Review of Astronomy and Astrophysics*, **29**, 31

Melrose D. B., 2017, *Reviews of Modern Plasma Physics*, **1**, 5

Men Y., McSweeney S., Hurley-Walker N., Barr E., Stappers B., 2025, *Science Advances*, **11**, eadp6351

Merloni A., Heinz S., di Matteo T., 2003, *Monthly Notices of the Royal Astronomical Society*, **345**, 1057

Mészáros P., Rees M. J., 1997, *The Astrophysical Journal*, **476**, 232

Mészáros P., Waxman E., 2001, *Physical Review Letters*, **87**, 171102

Mészáros P., Rees M. J., Wijers R. A. M. J., 1998, *The Astrophysical Journal*, **499**, 301

Metzger B. D., 2022, *The Astrophysical Journal*, **932**, 84

Metzger B. D., Margalit B., Kasen D., Quataert E., 2015a, *Monthly Notices of the Royal Astronomical Society*, **454**, 3311

Metzger B. D., Williams P. K. G., Berger E., 2015b, *The Astrophysical Journal*, **806**, 224

Meyer E. T., et al., 2025, *The Astrophysical Journal*, **979**, L2

Michilli D., et al., 2018, *Nature*, **553**, 182

Migliari S., Fender R. P., 2006, *Monthly Notices of the Royal Astronomical Society*, **366**, 79

Migliori G., et al., 2024, *The Astrophysical Journal*, **963**, L24

Miles M. T., et al., 2025, *Monthly Notices of the Royal Astronomical Society*, **536**, 1489

Milisavljevic D., Fesen R. A., 2017, in Alsabti A. W., Murdin P., eds., *Handbook of Supernovae*. Springer International Publishing, Cham, Switzerland, p. 2211, doi:10.1007/978-3-319-21846-5\_97, <https://ui.adsabs.harvard.edu/abs/2017hsn..book.2211M>

Milisavljevic D., Patnaude D. J., Chevalier R. A., Raymond J. C., Fesen R. A., Margutti R., Conner B., Banovetz J., 2018, *The Astrophysical Journal*, **864**, L36

Miller-Jones J. C. A., Blundell K. M., Rupen M. P., Mioduszewski A. J., Duffy P., Beasley A. J., 2004, *The Astrophysical Journal*, **600**, 368

Miller-Jones J. C. A., Gallo E., Rupen M. P., Mioduszewski A. J., Brisken W., Fender R. P., Jonker P. G., Maccarone T. J., 2008, *Monthly Notices of the Royal Astronomical Society*, **388**, 1751

Miller-Jones J. C. A., et al., 2019, *Nature*, **569**, 374

Miller-Jones J. C. A., et al., 2021, *Science*, **371**, 1046

Miller M. C., et al., 2021, *The Astrophysical Journal*, **918**, L28

Mimica P., Giannios D., Metzger B. D., Aloy M. A., 2015, *Monthly Notices of the Royal Astronomical Society*, **450**, 2824

Minns A. R., Riley J. M., 2000, *Monthly Notices of the Royal Astronomical Society*, **315**, 839

Mirabel I. F., Rodríguez L. F., 1994, *Nature*, **371**, 46

Mitchell T. M., 1997, Machine learning. Vol. 1, McGraw-hill New York

Mohan N., Rafferty D., 2015, *Astrophysics Source Code Library*, p. [ascl:1502.007](#)

Mohan P., An T., Yang J., 2020, *The Astrophysical Journal*, **888**, L24

Moin A., et al., 2013, *The Astrophysical Journal*, **779**, 105

Molnar L. A., Reid M. J., Grindlay J. E., 1984, *Nature*, **310**, 662

Mooley K. P., Frail D. A., Ofek E. O., Miller N. A., Kulkarni S. R., Horesh A., 2013, *The Astrophysical Journal*, **768**, 165

Mooley K. P., et al., 2016, *The Astrophysical Journal*, **818**, 105

Mooley K. P., et al., 2018a, *Nature*, **554**, 207

Mooley K. P., et al., 2018b, *Nature*, **561**, 355

Mooley K. P., et al., 2018c, *The Astrophysical Journal*, **868**, L11

Mooley K. P., et al., 2022, *The Astrophysical Journal*, **924**, 16

Morgan J. S., et al., 2018, *Monthly Notices of the Royal Astronomical Society*, **473**, 2965

Moroianu A., Wen L., James C. W., Ai S., Kovalam M., Panther F. H., Zhang B., 2023, *Nature Astronomy*, **7**, 579

Morris M., Serabyn E., 1996, *Annual Review of Astronomy and Astrophysics*, **34**, 645

Morton D. C., Wright A. E., 1978, *Monthly Notices of the Royal Astronomical Society*, **182**, 47P

Mundell C. G., Ferruit P., Nagar N., Wilson A. S., 2009, *The Astrophysical Journal*, **703**, 802

Muno M. P., et al., 2003, *The Astrophysical Journal*, **589**, 225

Murphy E., ed. 2018, Science with a Next Generation Very Large Array Astronomical Society of the Pacific Conference Series Vol. 517

Murphy T., Mauch T., Green A., Hunstead R. W., Piestrzynska B., Kels A. P., Sztajer P., 2007, *Monthly Notices of the Royal Astronomical Society*, **382**, 382

Murphy T., et al., 2010, *Monthly Notices of the Royal Astronomical Society*, **402**, 2403

Murphy T., et al., 2013, *Publications of the Astronomical Society of Australia*, **30**, e006

Murphy T., et al., 2015, *Monthly Notices of the Royal Astronomical Society*, **446**, 2560

Murphy T., et al., 2017, *Monthly Notices of the Royal Astronomical Society*, **466**, 1944

Murphy T., et al., 2021, *Publications of the Astronomical Society of Australia*, **38**, e054

Mutel R. L., Lestrade J. F., Preston R. A., Phillips R. B., 1985, *The Astrophysical Journal*, **289**, 262

Mutel R. L., Molnar L. A., Waltman E. B., Ghigo F. D., 1998, *The Astrophysical Journal*, **507**, 371

Naess S., et al., 2021, *The Astrophysical Journal*, **915**, 14

Nakar E., Piran T., 2011, *Nature*, **478**, 82

Nandra K., George I. M., Mushotzky R. F., Turner T. J., Yaqoob T., 1997, *The Astrophysical Journal*, **476**, 70

Narayan R., 1992, *Philosophical Transactions of the Royal Society of London Series A*, **341**, 151

Nayana A. J., Chandra P., 2021, *The Astrophysical Journal*, **912**, L9

Nelson T., et al., 2014, *The Astrophysical Journal*, **785**, 78

Niiuma K., et al., 2007, *The Astrophysical Journal*, **657**, L37

Nimmo K., et al., 2022, *Nature Astronomy*, **6**, 393

Nindos A., Kontar E. P., Oberoi D., 2019, *Advances in Space Research*, **63**, 1404

Niu C. H., et al., 2022, *Nature*, **606**, 873

Norris J. P., Bonnell J. T., 2006, *The Astrophysical Journal*, **643**, 266

Norris R. P., et al., 2011, *Publications of the Astronomical Society of Australia*, **28**, 215

Noyola J. P., Satyal S., Musielak Z. E., 2014, *The Astrophysical Journal*, **791**, 25

Nugis T., Lamers H. J. G. L. M., 2000, *Astronomy and Astrophysics*, **360**, 227

Nyland K., et al., 2020, *The Astrophysical Journal*, **905**, 74

O'Connor B., Beniamini P., Kouveliotou C., 2020, *Monthly Notices of the Royal Astronomical Society*, **495**, 4782

O'Connor B., et al., 2023, *Science Advances*, **9**, eadi1405

O'Gorman E., et al., 2020, *Astronomy and Astrophysics*, **638**, A65

Obenberger K. S., et al., 2014, *The Astrophysical Journal*, **788**, L26

Obenberger K. S., et al., 2015, *Journal of Astronomical Instrumentation*, **4**, 1550004

Ofek E. O., 2017, *The Astrophysical Journal*, **846**, 44

Ofek E. O., Breslauer B., Gal-Yam A., Frail D., Kasliwal M. M., Kulkarni S. R., Waxman E., 2010, *The Astrophysical Journal*, **711**, 517

Ofek E. O., Frail D. A., Breslauer B., Kulkarni S. R., Chandra P., Gal-Yam A., Kasliwal M. M., Gehrels N., 2011, *The Astrophysical Journal*, **740**, 65

Ofek E. O., et al., 2021, *The Astrophysical Journal*, **922**, 247

Offringa A. R., de Bruyn A. G., Biehl M., Zaroubi S., Bernardi G., Pandey V. N., 2010, *Monthly Notices of the Royal Astronomical Society*, **405**, 155

Olmi B., Bucciantini N., 2023, *Publications of the Astronomical Society of Australia*, **40**, e007

Ortiz Ceballos K. N., Cendes Y., Berger E., Williams P. K. G., 2024, *The Astronomical Journal*, **168**, 127

Osborne J. A., Bagheri F., Shahmoradi A., 2021, *Monthly Notices of the Royal Astronomical Society*, **502**, 5622

Osten R. A., et al., 2004, *The Astrophysical Journal Supplement Series*, **153**, 317

Osterbrock D. E., Ferland G. J., 2006, *Astrophysics of gaseous nebulae and active galactic nuclei*. University Science Books, Sausalito, USA, <https://ui.adsabs.harvard.edu/abs/2006agna.book....O>

Owen F. N., Jones T. W., Gibson D. M., 1976, *The Astrophysical Journal*, **210**, L27

Paczynski B., 1998, *The Astrophysical Journal*, **494**, L45

Padovani P., 2016, *Astronomy & Astrophysics Review*, **24**, 13

Pais M., Piran T., Nakar E., 2023, *Monthly Notices of the Royal Astronomical Society*, **519**, 1941

Palenzuela C., Lehner L., Liebling S. L., 2010, *Science*, **329**, 927

Palliyaguru N. T., Corsi A., Pérez-Torres M., Varenius E., Van Eerten H., 2021, *The Astrophysical Journal*, **910**, 16

Palmer D. M., 1993, *The Astrophysical Journal*, **417**, L25

Panagia N., Van Dyk S. D., Weiler K. W., Sramek R. A., Stockdale C. J., Murata K. P., 2006, *The Astrophysical Journal*, **646**, 369

Panaiteescu A., Mészáros P., Rees M. J., 1998, *The Astrophysical Journal*, **503**, 314

Panaiteescu A., Kumar P., Narayan R., 2001, *The Astrophysical Journal*, **561**, L171

Pasham D. R., van Velzen S., 2018, *The Astrophysical Journal*, **856**, 1

Pasham D. R., et al., 2015, *The Astrophysical Journal*, **805**, 68

Pasham D. R., et al., 2021, *Nature Astronomy*, **6**, 249

Pauliny-Toth I. I. K., Kellermann K. I., 1966, *The Astrophysical Journal*, **146**, 634

Pedersen M. G., et al., 2019, *The Astrophysical Journal*, **872**, L9

Pearson A. L., et al., 2022, *The Astrophysical Journal*, **927**, 24

Pelisoli I., et al., 2023, *Nature Astronomy*, **7**, 931

Pellegrino C., et al., 2022, *The Astrophysical Journal*, **926**, 125

Pen U.-L., King L., 2012, *Monthly Notices of the Royal Astronomical Society*, **421**, L132

Pérez-Torres M. A., et al., 2014, *The Astrophysical Journal*, **792**, 38

Perley D. A., et al., 2008, *The Astrophysical Journal*, **688**, 470

Perley D. A., et al., 2014, *The Astrophysical Journal*, **781**, 37

Perley D. A., et al., 2019, *Monthly Notices of the Royal Astronomical Society*, **484**, 1031

Perley D. A., et al., 2021, *Monthly Notices of the Royal Astronomical Society*, **508**, 5138

Perlmutter S., et al., 1999, *The Astrophysical Journal*, **517**, 565

Perna R., Loeb A., 1998, *The Astrophysical Journal*, **509**, L85

Persi P., Tapia M., Rodriguez L. F., Ferrari-Toniolo M., Roth M., 1990, *Astronomy and Astrophysics*, **240**, 93

Peters C., et al., 2019, *The Astrophysical Journal*, **872**, 28

Petroff E., et al., 2015, *Monthly Notices of the Royal Astronomical Society*, **451**, 3933

Petroff E., Hessels J. W. T., Lorimer D. R., 2022, *Astronomy and Astrophysics Review*, **30**, 2

Petrou F., et al., 2025, *Publications of the Astronomical Society of Australia*, **42**, e139

Petrov P., et al., 2022, *The Astrophysical Journal*, **924**, 54

Petruk O., et al., 2023, *Monthly Notices of the Royal Astronomical Society*, **518**, 6377

Philippov A., Kramer M., 2022, *Annual Review of Astronomy and Astrophysics*, **60**, 495

Pietka M., Fender R. P., Keane E. F., 2015, *Monthly Notices of the Royal Astronomical Society*, **446**, 3687

Pietka M., Staley T. D., Pretorius M. L., Fender R. P., 2017, *Monthly Notices of the Royal Astronomical Society*, **471**, 3788

Pineda J. S., Villadsen J., 2023, *Nature Astronomy*, **7**, 569

Pintaldi S., Stewart A., O'Brien A., Kaplan D., Murphy T., 2022, in Ruiz J. E., Pierfederici F., Teuben P., eds, *Astronomical Society of the Pacific Conference Series* Vol. 532, *Astronomical Data Analysis Software and Systems XXX*. p. 333 ([arXiv:2101.05898](https://arxiv.org/abs/2101.05898), doi:10.48550/arXiv.2101.05898)

Piran T., 2004, *Reviews of Modern Physics*, **76**, 1143

Piran T., Nakar E., Rosswog S., 2013, *Monthly Notices of the Royal Astronomical Society*, **430**, 2121

Piran T., Nakar E., Mazzali P., Pian E., 2019, *The Astrophysical Journal*, **871**, L25

Pleunis Z., et al., 2021, *The Astrophysical Journal*, **923**, 1

Plotkin R. M., et al., 2017, *The Astrophysical Journal*, **834**, 104

Polisensky E., et al., 2016, *The Astrophysical Journal*, **832**, 60

Polzin E. J., Breton R. P., Bhattacharyya B., Scholte D., Sobey C., Stappers B. W., 2020, *Monthly Notices of the Royal Astronomical Society*, **494**, 2948

Prabu S., Hancock P. J., Zhang X., Tingay S. J., 2020, *Publications of the Astronomical Society of Australia*, **37**, e010

Prasad P., et al., 2016, *Journal of Astronomical Instrumentation*, **5**, 1641008

Prentice S. J., et al., 2018, *The Astrophysical Journal*, **865**, L3

Preston G. W., 1974, *Annual Review of Astronomy and Astrophysics*, **12**, 257

Price P. A., et al., 2002, *The Astrophysical Journal*, **572**, L51

Pritchard J., et al., 2021, *Monthly Notices of the Royal Astronomical Society*, **502**, 5438

Pritchard J., Murphy T., Heald G., Wheatland M. S., Kaplan D. L., Lenc E., O'Brien A., Wang Z., 2024, *Monthly Notices of the Royal Astronomical Society*, **529**, 1258

Qu Y., Zhang B., 2025, *The Astrophysical Journal*, **981**, 34

Radcliffe J. F., Beswick R. J., Thomson A. P., Garrett M. A., Barthel P. D., Muxlow T. W. B., 2019, *Monthly Notices of the Royal Astronomical Society*, **490**, 4024

Rajwade K. M., van Leeuwen J., 2024, *Universe*, **10**, 158

Rastinejad J. C., et al., 2022, *Nature*, **612**, 223

Ravi V., et al., 2010, *Monthly Notices of the Royal Astronomical Society*, **408**, L99

Ravi V., et al., 2022a, *Monthly Notices of the Royal Astronomical Society*, **513**, 982

Ravi V., et al., 2022b, *The Astrophysical Journal*, **925**, 220

Rayner D. P., Norris R. P., Sault R. J., 2000, *Monthly Notices of the Royal Astronomical Society*, **319**, 484

Rea N., et al., 2022, *The Astrophysical Journal*, **940**, 72

Rea N., et al., 2024, *The Astrophysical Journal*, **961**, 214

Readhead A. C. S., 1994, *The Astrophysical Journal*, **426**, 51

Reardon D. J., et al., 2023, *The Astrophysical Journal*, **951**, L6

Rebbapragada U., Lo K., Wagstaff K. L., Reed C., Murphy T., Thompson D. R., 2012, in Griffin E., Hanisch R., Seaman R., eds, *IAU Symposium Vol. 285, New Horizons in Time Domain Astronomy*. pp 397–399, doi:10.1017/S1743921312001196

Rees M. J., 1988, *Nature*, **333**, 523

Rengelink R. B., Tang Y., de Bruyn A. G., Miley G. K., Bremer M. N., Roettgering H. J. A., Bremer M. A. R., 1997, *Astronomy and Astrophysics Supplement Series*, **124**, 259

Resmi L., 2017, *Journal of Astrophysics and Astronomy*, **38**, 56

Rhoads J. E., 1997, *The Astrophysical Journal*, **487**, L1

Rhoads J. E., 1999, *The Astrophysical Journal*, **525**, 737

Rhoads J. E., 2003, *The Astrophysical Journal*, **591**, 1097

Rhodes L., Caleb M., Stappers B. W., Andersson A., Bezuidenhout M. C., Driessen L. N., Heywood I., 2023, *Monthly Notices of the Royal Astronomical Society*, **525**, 3626

Rhodes L., et al., 2024, *Monthly Notices of the Royal Astronomical Society*, **533**, 4435

Richards J. L., et al., 2011a, *The Astrophysical Journal Supplement Series*, **194**, 29

Richards J. W., et al., 2011b, *The Astrophysical Journal*, **733**, 10

Rickett B. J., 1969, *Nature*, **221**, 158

Rickett B. J., 1977, *Annual Review of Astronomy and Astrophysics*, **15**, 479

Rickett B. J., 1990, *Annual Review of Astronomy and Astrophysics*, **28**, 561

Rickett B. J., Lyne A. G., 1990, *Monthly Notices of the Royal Astronomical Society*, **244**, 68

Rickett B. J., Coles W. A., Bourgois G., 1984, *Astronomy and Astrophysics*, **134**, 390

Ridder M. E., Heinke C. O., Sivakoff G. R., Hughes A. K., 2023, *Monthly Notices of the Royal Astronomical Society*, **519**, 5922

Riess A. G., et al., 1998, *The Astronomical Journal*, **116**, 1009

Riess A. G., et al., 2004, *The Astrophysical Journal*, **607**, 665

Riley J. M., 1993, *Monthly Notices of the Royal Astronomical Society*, **260**, 893

Riley J. M., Green D. A., 1995, *Monthly Notices of the Royal Astronomical Society*, **275**, 527

Riley J. M., Green D. A., 1998, *Monthly Notices of the Royal Astronomical Society*, **301**, 203

Roberts M. S. E., 2013, in van Leeuwen J., ed., *IAU Symposium Vol. 291, Neutron Stars and Pulsars: Challenges and Opportunities after 80 years*. pp 127–132, doi:10.1017/S174392131202337X, <https://ui.adsabs.harvard.edu/abs/2013IAUS..291..127R>

Rodriguez A. C., 2025, *Astronomy & Astrophysics*, **695**, L8

Rogers A., Er X., 2019, *Monthly Notices of the Royal Astronomical Society*, **485**, 5800

Rol E., et al., 2007, *The Astrophysical Journal*, **669**, 1098

Romani R. W., Blandford R. D., Cordes J. M., 1987, *Nature*, **328**, 324

Ronchi M., Rea N., Gruber V., Hurley-Walker N., 2022, *The Astrophysical Journal*, **934**, 184

Rose K., et al., 2023, *The Astrophysical Journal*, **951**, L43

Rose K., et al., 2024, *Monthly Notices of the Royal Astronomical Society*, **534**, 3853

Rouco Escorial A., et al., 2023, *The Astrophysical Journal*, **959**, 13

Route M., 2019, *The Astrophysical Journal*, **872**, 79

Route M., Wolszczan A., 2012, *The Astrophysical Journal*, **747**, L22

Route M., Wolszczan A., 2013, *The Astrophysical Journal*, **773**, 18

Route M., Wolszczan A., 2016, *The Astrophysical Journal*, **830**, 85

Rowlinson A., et al., 2016, *Monthly Notices of the Royal Astronomical Society*, **458**, 3506

Rowlinson A., et al., 2019, *Astronomy and Computing*, **27**, 111

Rowlinson A., et al., 2022, *Monthly Notices of the Royal Astronomical Society*, **517**, 2894

Rowlinson A., et al., 2024, *Monthly Notices of the Royal Astronomical Society*, **534**, 2592

Roy S., Hyman S. D., Pal S., Lazio T. J. W., Ray P. S., Kassim N. E., 2010, *The Astrophysical Journal*, **712**, L5

Russell T. D., Soria R., Miller-Jones J. C. A., Curran P. A., Markoff S., Russell D. M., Sivakoff G. R., 2014, *Monthly Notices of the Royal Astronomical Society*, **439**, 1390

Russell T. D., et al., 2016, *Monthly Notices of the Royal Astronomical Society*, **460**, 3720

Russell T. D., et al., 2020, *Monthly Notices of the Royal Astronomical Society*, **498**, 5772

Ryan G., van Eerten H., Piro L., Troja E., 2020, *The Astrophysical Journal*, **896**, 166

Ryan G., van Eerten H., Troja E., Piro L., O'Connor B., Ricci R., 2024, *The Astrophysical Journal*, **975**, 131

Rybicki G. B., Lightman A. P., 1985, *Radiative processes in astrophysics.. John Wiley & Sons, Chichester, UK*, <https://ui.adsabs.harvard.edu/abs/1985rpabook....R>

Ryle M., Elsmore B., 1951, *Nature*, **168**, 555

STScI Development Team 2013, pysynphot: Synthetic photometry software package, *Astrophysics Source Code Library*, record ascl:1303.023

Sabater J., et al., 2019, *Astronomy and Astrophysics*, **622**, A17

Sadler E. M., et al., 2006, *Monthly Notices of the Royal Astronomical Society*, **371**, 898

Saikia D. J., Salter C. J., 1988, *Annual Review of Astronomy and Astrophysics*, **26**, 93

Sarbadhicary S. K., et al., 2021, *The Astrophysical Journal*, **923**, 31

Sari R., Piran T., Narayan R., 1998, *The Astrophysical Journal*, **497**, L17

Sari R., Piran T., Halpern J. P., 1999, *The Astrophysical Journal*, **519**, L17

Scargle J. D., 1982, *The Astrophysical Journal*, **263**, 835

Scargle J. D., 1989, *The Astrophysical Journal*, **343**, 874

Scargle J. D., Norris J. P., Jackson B., Chiang J., 2013, *The Astrophysical Journal*, **764**, 167

Scheuer P. A. G., 1968, *Nature*, **218**, 920

Schilizzi R. T., Cohen M. H., Romney J. D., Shaffer D. B., Kellermann K. L., Swenson Jr. G. W., Yen J. L., Rinehart R., 1975, *The Astrophysical Journal*, **201**, 263

Schilizzi R. T., Ekers R. D., Dewdney P. E., Crosby P., 2024, The Square Kilometre Array: A Science Mega-Project in the Making, 1990–2012. Historical & Cultural Astronomy, Springer International Publishing, Cham, doi:10.1007/978-3-031-51374-9, <https://link.springer.com/10.1007/978-3-031-51374-9>

Schmidt M., 1963, *Nature*, **197**, 1040

Schroeder G., et al., 2022, *The Astrophysical Journal*, **940**, 53

Schroeder G., et al., 2024, *The Astrophysical Journal*, **970**, 139

Schroeder G., et al., 2025, *The Astrophysical Journal*, **982**, 42

Scuderi S., Panagia N., Stanghellini C., Trigilio C., Umana G., 1998, *Astronomy & Astrophysics*, **332**, 251

Seaquist E. R., Palimaka J., 1977, *The Astrophysical Journal*, **217**, 781

Seaquist E. R., Gregory P. C., Perley R. A., Becker R. H., Carlson J. B., Kundu M. R., Bignell R. C., Dickel J. R., 1974, *Nature*, **251**, 394

Seaton D. B., Partridge R. B., 2001, *Publications of the Astronomical Society of the Pacific*, **113**, 6

Seethapuram Sridhar S., Operations S., Breen S., Whitney S., Ball L., 2025, SKAO Staged Delivery, Array Assemblies And Layouts, doi:10.5281/zenodo.16951020

Sfaradi I., et al., 2024a, *Monthly Notices of the Royal Astronomical Society*, **527**, 7672

Sfaradi I., et al., 2024b, *Astronomy and Astrophysics*, **686**, A129

Sfaradi I., Horesh A., Fender R., Rhodes L., Bright J., Williams-Baldwin D., Green D. A., 2025, *The Astrophysical Journal*, **979**, 189

Shankar S., Møsta P., Barnes J., Duffell P. C., Kasen D., 2021, *Monthly Notices of the Royal Astronomical Society*, **508**, 5390

Shimwell T. W., et al., 2017, *Astronomy and Astrophysics*, **598**, A104

Shimwell T. W., et al., 2019, *Astronomy and Astrophysics*, **622**, A1

Shimwell T. W., et al., 2022, *Astronomy and Astrophysics*, **659**, A1

Shimwell T. W., et al., 2025, *Astronomy and Astrophysics*, **695**, A80

Shulyak D., Reiners A., Engeln A., Malo L., Yadav R., Morin J., Kochukhov O., 2017, *Nature Astronomy*, **1**, 0184

Sieber W., 1982, *Astronomy and Astrophysics*, **113**, 311

Sihlangu I., Oozeer N., Bassett B. A., 2022, *Journal of Astronomical Telescopes, Instruments, and Systems*, **8**, 011003

Silverman J. M., et al., 2013, *The Astrophysical Journal Supplement Series*, **207**, 3

Skinner C. J., Exter K. M., Barlow M. J., Davis R. J., Bode M. F., 1997, *Monthly Notices of the Royal Astronomical Society*, **288**, L7

Slee O. B., Siegman B. C., 1988, *Monthly Notices of the Royal Astronomical Society*, **235**, 1313

Slee O. B., Solomon L. H., Patston G. E., 1963, *Nature*, **199**, 991

Slee O. B., Wilson W., Ramsay G., 2008, *Publications of the Astronomical Society of Australia*, **25**, 94

Smirnov O. M., et al., 2025a, *Monthly Notices of the Royal Astronomical Society*, **538**, L62

Smirnov O. M., et al., 2025b, *Monthly Notices of the Royal Astronomical Society*, **538**, L89

Smith N., 2014, *Annual Review of Astronomy and Astrophysics*, **52**, 487

Snijders M. A. J., Batt T. J., Roche P. F., Seaton M. J., Morton D. C., Spoelstra T. A. T., Blades J. C., 1987, *Monthly Notices of the Royal Astronomical Society*, **228**, 329

Soderberg A. M., et al., 2004a, *The Astrophysical Journal*, **606**, 994

Soderberg A. M., Frail D. A., Wieringa M. H., 2004b, *The Astrophysical Journal*, **607**, L13

Soderberg A. M., Kulkarni S. R., Berger E., Chevalier R. A., Frail D. A., Fox D. B., Walker R. C., 2005, *The Astrophysical Journal*, **621**, 908

Soderberg A. M., et al., 2006a, *Nature*, **442**, 1014

Soderberg A. M., Nakar E., Berger E., Kulkarni S. R., 2006b, *The Astrophysical Journal*, **638**, 930

Soderberg A. M., et al., 2006c, *The Astrophysical Journal*, **650**, 261

Soderberg A. M., et al., 2010, *Nature*, **463**, 513

Sokolowski M., et al., 2021, *Publications of the Astronomical Society of Australia*, **38**, e023

Soleri P., Fender R., 2011, *Monthly Notices of the Royal Astronomical Society*, **413**, 2269

Somalwar J. J., et al., 2023, *The Astrophysical Journal*, **945**, 142

Somalwar J. J., et al., 2025a, *The Astrophysical Journal*, **982**, 163

Somalwar J. J., Ravi V., Lu W., 2025b, *The Astrophysical Journal*, **983**, 159

Sooknuman K., et al., 2021, *Monthly Notices of the Royal Astronomical Society*, **502**, 206

Spangler S. R., Shawhan S. D., Rankin J. M., 1974a, *The Astrophysical Journal*, **190**, L129

Spangler S. R., Rankin J. M., Shawhan S. D., 1974b, *The Astrophysical Journal*, **194**, L43

Spingola C., et al., 2016, *Monthly Notices of the Royal Astronomical Society*, **457**, 2263

Sridhar N., Metzger B. D., 2022, *The Astrophysical Journal*, **937**, 5

Staley T. D., et al., 2013, *Monthly Notices of the Royal Astronomical Society*, **428**, 3114

Stanway E. R., Marsh T. R., Chote P., Gänsicke B. T., Steeghs D., Wheatley P. J., 2018, *Astronomy and Astrophysics*, **611**, A66

Stappers B., Kramer M., 2016, in Taylor R., Camilo F., Leeuw L., Moodley K., eds, Vol. 277, MeerKAT Science: On the Pathway to the SKA. Proceedings of Science, p. 9, doi:10.22323/1.277.0009

Staveley-Smith L., Briggs D. S., Rowe A. C. H., Manchester R. N., Reynolds J. E., Tzioumis A. K., Kesteven M. J., 1993, *Nature*, **366**, 136

Stein R., et al., 2021, *Nature Astronomy*, **5**, 510

Stephenson F. R., Green D. A., 2002, International Series in Astronomy and Astrophysics, **5**

Stewart A. J., et al., 2016, *Monthly Notices of the Royal Astronomical Society*, **456**, 2321

Stewart A. J., Muñoz-Darias T., Fender R. P., Pietka M., 2018, *Monthly Notices of the Royal Astronomical Society*, **479**, 2481

Stirling A. M., Spencer R. E., de la Force C. J., Garrett M. A., Fender R. P., Ogle R. N., 2001, *Monthly Notices of the Royal Astronomical Society*, **327**, 1273

Stroh M. C., et al., 2021, *The Astrophysical Journal*, **923**, L24

Sukumar S., Allen R. J., 1989, *The Astrophysical Journal*, **341**, 883

Sullivan III W. T., 2009, Cosmic Noise: A History of Early Radio Astronomy. Cambridge University Press, Cambridge, UK

Surnis M. P., et al., 2023, *Monthly Notices of the Royal Astronomical Society*, **526**, L143

Suvorov A. G., Melatos A., 2023, *Monthly Notices of the Royal Astronomical Society*, **520**, 1590

Suvorov A. G., Dehman C., Pons J. A., 2025, *The Astrophysical Journal*, **991**, 134

Swinbank J. D., et al., 2015, *Astronomy and Computing*, **11**, 25

Tan C. M., et al., 2018, *The Astrophysical Journal*, **866**, 54

Tanvir N. R., et al., 2009, *Nature*, **461**, 1254

Tarter J., 2001, *Annual Review of Astronomy and Astrophysics*, **39**, 511

Taylor A. R., Seaquist E. R., Hollis J. M., Pottasch S. R., 1987, *Astronomy and Astrophysics*, **183**, 38

Taylor G. B., Frail D. A., Kulkarni S. R., Shepherd D. S., Feroci M., Frontera F., 1998, *The Astrophysical Journal*, **502**, L115

Taylor G. B., Frail D. A., Berger E., Kulkarni S. R., 2004, *The Astrophysical Journal*, **609**, L1

Taylor G. B., et al., 2012, *Journal of Astronomical Instrumentation*, **1**, 1250004

Thompson T. A., Chang P., Quataert E., 2004, *The Astrophysical Journal*, **611**, 380

Thyagarajan N., Helfand D. J., White R. L., Becker R. H., 2011, *The Astrophysical Journal*, **742**, 49

Tingay S. J., Hancock P. J., 2019, *The Astronomical Journal*, **158**, 31

Tingay S. J., et al., 2013, *Publications of the Astronomical Society of Australia*, **30**, e007

Tingay S. J., et al., 2015, *The Astronomical Journal*, **150**, 199

Tingay S. J., et al., 2018, *The Astrophysical Journal*, **857**, 11

Toet S. E. B., Vedantham H. K., Callingham J. R., Veken K. C., Shimwell T. W., Zarka P., Röttgering H. J. A., Drabent A., 2021, *Astronomy and Astrophysics*, **654**, A21

Tong H., 2023, *The Astrophysical Journal*, **943**, 3

Torne P., et al., 2015, *Monthly Notices of the Royal Astronomical Society*, **451**, L50

Totani T., 2013, *Publications of the Astronomical Society of Japan*, **65**, L12

Trasco J. D., Wood H. J., Roberts M. S., 1970, *The Astrophysical Journal*, **161**, L129

Treumann R. A., 2006, *Astronomy and Astrophysics Review*, **13**, 229

Trigilio C., Leto P., Leone F., Umana G., Buemi C., 2000, *Astronomy & Astrophysics*, **362**, 281

Trigilio C., Leto P., Umana G., Buemi C. S., Leone F., 2008, *Monthly Notices of the Royal Astronomical Society*, **384**, 1437

Trigilio C., et al., 2018, *Monthly Notices of the Royal Astronomical Society*, **481**, 217

Troja E., et al., 2016, *The Astrophysical Journal*, **827**, 102

Troja E., et al., 2017, *Nature*, **551**, 71

Troja E., et al., 2018, *Monthly Notices of the Royal Astronomical Society*, **478**, L18

Troja E., et al., 2019, *Monthly Notices of the Royal Astronomical Society*, **489**, 2104

Troja E., et al., 2022a, *Monthly Notices of the Royal Astronomical Society*, **510**, 1902

Troja E., et al., 2022b, *Nature*, **612**, 228

Turner K. C., 1985, in Hjellming R. M., Gibson D. M., eds, *Astrophysics and Space Science Library* Vol. 116, *Radio Stars*. p. 283, doi:10.1007/978-94-009-5420-5\_41

Turner J. D., et al., 2021, *Astronomy and Astrophysics*, **645**, A59

Turner J. D., et al., 2025, *Monthly Notices of the Royal Astronomical Society*, **537**, 1070

Umana G., Trigilio C., Catalano S., 1998, *Astronomy and Astrophysics*, **329**, 1010

Ung D., 2019, Ph.D. thesis, Curtin University, <https://ui.adsabs.harvard.edu/abs/2019PhDT.....11U>

Usov V. V., Katz J. I., 2000, *Astronomy and Astrophysics*, **364**, 655

Vallisneri M., van Haasteren R., 2017, *Monthly Notices of the Royal Astronomical Society*, **466**, 4954

Varghese S. S., Obenberger K. S., Dowell J., Taylor G. B., 2019, *The Astrophysical Journal*, **874**, 151

Varghese S. S., Dowell J., Obenberger K. S., Taylor G. B., Anderson M., Hallinan G., 2024, *Journal of Geophysical Research (Space Physics)*, **129**, e2023JA032272

Vaughan S., Edelson R., Warwick R. S., Uttley P., 2003, *Monthly Notices of the Royal Astronomical Society*, **345**, 1271

Vedantham H. K., 2018, in Murphy E. J., ed., Vol. 517, *Science with a Next Generation Very Large Array*. Astronomical Society of the Pacific, San Francisco, USA, p. 491, <https://ui.adsabs.harvard.edu/abs/2018ASPC..517..491V>

Vedantham H. K., et al., 2017, *The Astrophysical Journal*, **845**, 89

Vedantham H. K., et al., 2020, *Nature Astronomy*, **4**, 577

Vernardos G., et al., 2024, *Space Science Reviews*, **220**, 14

Vidotto A. A., Fares R., Jardine M., Donati J. F., Opher M., Moutou C., Catala C., Gombosi T. I., 2012, *Monthly Notices of the Royal Astronomical Society*, **423**, 3285

Villadsen J., Hallinan G., 2019, *The Astrophysical Journal*, **871**, 214

Villadsen J., Hallinan G., Bourke S., Güdel M., Rupen M., 2014, *The Astrophysical Journal*, **788**, 112

Volonteri M., 2010, *Astronomy and Astrophysics Review*, **18**, 279

Vurm I., Metzger B. D., 2021, *The Astrophysical Journal*, **917**, 77

Wagstaff K. L., et al., 2016, *Publications of the Astronomical Society of the Pacific*, **128**, 084503

Waldrum E. M., Pooley G. G., Grainge K. J. B., Jones M. E., Saunders R. D. E., Scott P. F., Taylor A. C., 2003, *Monthly Notices of the Royal Astronomical Society*, **342**, 915

Walker M. A., 2007, in Havercorn M., Goss W. M., eds, *Astronomical Society of the Pacific Conference Series* Vol. 365, *SINS - Small Ionized and Neutral Structures in the Diffuse Interstellar Medium*. Astronomical Society of the Pacific, San Francisco, USA, p. 299, doi:10.48550/arXiv.astro-ph/0610737, <https://ui.adsabs.harvard.edu/abs/2007ASPC..365..299W>

Walker M., Wardle M., 1998, *The Astrophysical Journal*, **498**, L125

Walker M. A., Tuntsov A. V., Bignall H., Reynolds C., Bannister K. W., Johnston S., Stevens J., Ravi V., 2017, *The Astrophysical Journal*, **843**, 15

Wang J.-S., Peng F.-K., Wu K., Dai Z.-G., 2018, *The Astrophysical Journal*, **868**, 19

Wang Y., Tuntsov A., Murphy T., Lenc E., Walker M., Bannister K., Kaplan D. L., Mahony E. K., 2021a, *Monthly Notices of the Royal Astronomical Society*, **502**, 3294

Wang Z., et al., 2021b, *The Astrophysical Journal*, **920**, 45

Wang Z., et al., 2022a, *Monthly Notices of the Royal Astronomical Society*, **516**, 5972

Wang Y., et al., 2022b, *The Astrophysical Journal*, **930**, 38

Wang Y., et al., 2023, *Monthly Notices of the Royal Astronomical Society*, **523**, 5661

Wang J., Norden M., Donker P., 2025a, *Journal of Astronomical Telescopes, Instruments, and Systems*, **11**, 017002

Wang Z., et al., 2025b, *Publications of the Astronomical Society of Australia*, **42**, e005

Wang Z., et al., 2025c, *Nature*, **642**, 583

Wang Y., et al., 2025d, *The Astrophysical Journal*, **982**, L53

Warwick J. W., et al., 1979, *Science*, **204**, 995

Wayth R. B., Brisken W. F., Deller A. T., Majid W. A., Thompson D. R., Tingay S. J., Wagstaff K. L., 2011, *The Astrophysical Journal*, **735**, 97

Wayth R. B., et al., 2015, *Publications of the Astronomical Society of Australia*, **32**, e025

Weiler K. W., Panagia N., Montes M. J., Sramek R. A., 2002, *Annual Review of Astronomy and Astrophysics*, **40**, 387

Welch J., et al., 2009, *IEEE Proceedings*, **97**, 1438

Wendker H. J., 1987, *Astronomy and Astrophysics Supplement Series*, **69**, 87

Wendker H. J., 1995, *Astronomy and Astrophysics Supplement Series*, **109**, 177

Wendker H. J., Baars J. W. M., Altenhoff W. J., 1973, *Nature Physical Science*, **245**, 118

Werthimer D., et al., 2001, in *The Search for Extraterrestrial Intelligence (SETI) in the Optical Spectrum III*. SPIE, pp 104–109, doi:10.1117/12.435384, <https://www.spiedigitallibrary.org/conference-proceedings-of-spie/4273/0000/Berkeley-radio-and-optical-SETI-programs--SETIhome-SERENDIP-and-10.1117/12.435384.full>

Weston J. H. S., et al., 2016a, *Monthly Notices of the Royal Astronomical Society*, **457**, 887

Weston J. H. S., et al., 2016b, *Monthly Notices of the Royal Astronomical Society*, **460**, 2687

White R. L., Becker R. H., 1995, *The Astrophysical Journal*, **451**, 352

White R. L., Becker R. H., Helfand D. J., Gregg M. D., 1997, *The Astrophysical Journal*, **475**, 479

White J. A., Aufdenberg J., Boley A. C., Hauschildt P., Hughes M., Matthews B., Wilner D., 2018, *The Astrophysical Journal*, **859**, 102

White J. A., et al., 2019, *The Astrophysical Journal*, **875**, 55

Whitehorn N., et al., 2016, *The Astrophysical Journal*, **830**, 143

Whiting M., Humphreys B., 2012, *Publications of the Astronomical Society of Australia*, **29**, 371

Wild J. P., Smerd S. F., Weiss A. A., 1963, *Annual Review of Astronomy and Astrophysics*, **1**, 291

Williams P. K. G., Bower G. C., Croft S., Keating G. K., Law C. J., Wright M. C. H., 2013, *The Astrophysical Journal*, **762**, 85

Wilms J., Pottschmidt K., Pooley G. G., Markoff S., Nowak M. A., Kreykenbohm I., Rothschild R. E., 2007, *The Astrophysical Journal*, **663**, L97

Winters J. G., et al., 2019, *The Astronomical Journal*, **157**, 216

Wołowska A., Kunert-Bajraszewska M., Mooley K., Hallinan G., 2017, *Frontiers in Astronomy and Space Sciences*, **4**, 38

Wołowska A., et al., 2021, *The Astrophysical Journal*, **914**, 22

Wolszczan A., Frail D. A., 1992, *Nature*, **355**, 145

Wood C. M., et al., 2021, *Monthly Notices of the Royal Astronomical Society*, **505**, 3393

Woosley S. E., 1993, *The Astrophysical Journal*, **405**, 273

Woosley S. E., Bloom J. S., 2006, *Annual Review of Astronomy and Astrophysics*, **44**, 507

Wootten A., Thompson A. R., 2009, *IEEE Proceedings*, **97**, 1463

Worden S. P., et al., 2017, *Acta Astronautica*, **139**, 98

Wozniak P. R., 2000, *Acta Astronomica*, **50**, 421

Wright A. E., Barlow M. J., 1975, *Monthly Notices of the Royal Astronomical Society*, **170**, 41

Wright J. T., Haqq-Misra J., Frank A., Kopparapu R., Lingam M., Sheikh S. Z., 2022, *The Astrophysical Journal*, **927**, L30

Wrobel J. M., Walker R. C., 1999, in, Vol. 180, *Synthesis Imaging in Radio Astronomy II, A Collection of Lectures from the Sixth NRAO/NMIMT Synthesis Imaging Summer School*. Astronomical Society of the Pacific, San Francisco, USA, p. 171, <https://ui.adsabs.harvard.edu/abs/1999ASPC.180.171W>

Xiao X., Shen R.-F., 2024, *The Astrophysical Journal*, **972**, 60

Xu H., et al., 2023, *Research in Astronomy and Astrophysics*, **23**, 075024

Yamasaki S., Totani T., Kiuchi K., 2018, *Publications of the Astronomical Society of Japan*, **70**, 39

Yang Y.-P., Li Q.-C., Zhang B., 2020, *The Astrophysical Journal*, **895**, 7

Yao J. M., Manchester R. N., Wang N., 2017, *The Astrophysical Journal*, **835**, 29

Yao Y., et al., 2022, *The Astrophysical Journal*, **934**, 104

Zackay B., Ofek E. O., Gal-Yam A., 2016, *The Astrophysical Journal*, **830**, 27

Zarka P., 1998, *Journal of Geophysical Research*, **103**, 20159

Zarka P., 2007, *Planetary and Space Science*, **55**, 598

Zarka P., Lazio J., Hallinan G., 2015, in *Advancing Astrophysics with the Square Kilometre Array*. SKA Organization, p. 120, doi:10.22323/1.215.0120

Zauderer B. A., et al., 2011, *Nature*, **476**, 425

Zauderer B. A., Berger E., Margutti R., Pooley G. G., Sari R., Soderberg A. M., Brunthaler A., Bietenholz M. F., 2013, *The Astrophysical Journal*, **767**, 152

Zevin M., et al., 2017, *Classical and Quantum Gravity*, **34**, 064003

Zevin M., Nugent A. E., Adhikari S., Fong W.-f., Holz D. E., Kelley L. Z., 2022, *The Astrophysical Journal*, **940**, L18

Zhang B., 2020a, *Nature*, **587**, 45

Zhang B., 2020b, *The Astrophysical Journal*, **890**, L24

Zhang B., 2023, *Reviews of Modern Physics*, **95**, 035005

Zhang B., Gil J., 2005, *The Astrophysical Journal*, **631**, L143

Zhang R., Yuan H., 2023, *The Astrophysical Journal Supplement Series*, **264**, 14

Zhang X., et al., 2023, *The Astrophysical Journal*, **959**, 89

Zhao J.-H., et al., 1992, *Science*, **255**, 1538

Zhou B., Li X., Wang T., Fan Y.-Z., Wei D.-M., 2014, *Physical Review D*, **89**, 107303

Zhou X., Huang H.-T., Cheng Q., Zheng X.-P., 2024, *Monthly Notices of the Royal Astronomical Society*, **530**, 1636

Zhou X., Kurban A., Liu W.-T., Wang N., Yuan Y.-J., 2025, *The Astrophysical Journal*, **986**, 98

Zhu H., Baker D., Pen U.-L., Stinebring D. R., van Kerkwijk M. H., 2023, *The Astrophysical Journal*, **950**, 109

Zic A., et al., 2019, *Monthly Notices of the Royal Astronomical Society*, **488**, 559

Zic A., et al., 2020, *The Astrophysical Journal*, **905**, 23

Zic A., et al., 2024, *Monthly Notices of the Royal Astronomical Society*, **528**, 5730

de Gouveia Dal Pino E. M., 2005, *Advances in Space Research*, **35**, 908

de Ruiter H. R., Willis A. G., Arp H. C., 1977, *Astronomy and Astrophysics Supplement Series*, **28**, 211

de Ruiter I., Meyers Z. S., Rowlinson A., Shimwell T. W., Ruhe D., Wijers R. A. M. J., 2024, *Monthly Notices of the Royal Astronomical Society*, **531**, 4805

de Ruiter I., et al., 2025, *Nature Astronomy*, **9**, 672

de Vries W. H., Becker R. H., White R. L., Helfand D. J., 2004, *The Astronomical Journal*, **127**, 2565

van Haarlem M. P., et al., 2013, *Astronomy & Astrophysics*, **556**, A2

van Loo S., Blomme R., Dougherty S. M., Runacres M. C., 2008, *Astronomy and Astrophysics*, **483**, 585

van Paradijs J., et al., 1997, *Nature*, **386**, 686

van Paradijs J., Kouveliotou C., Wijers R. A. M. J., 2000, *Annual Review of Astronomy and Astrophysics*, **38**, 379

van Velzen S., Körding E., Falcke H., 2011, *Monthly Notices of the Royal Astronomical Society*, **417**, L51

van den Eijnden J., et al., 2021, *Monthly Notices of the Royal Astronomical Society*, **507**, 3899

van der Horst A. J., Rol E., Wijers R. A. M. J., Strom R., Kaper L., Kouveliotou C., 2005, *The Astrophysical Journal*, **634**, 1166

van der Horst A. J., et al., 2008, *Astronomy and Astrophysics*, **480**, 35